UNIVERSITÀ DELLA CALABRIA

UNIVERSITY OF CALABRIA

Department of Pharmacy, Health and Nutritional Science

Department of Chemistry and Chemical Tecnologies

Ph.D. in

Translational Medicine

CYCLE

XXX

THESIS TITLE

Advanced Mass Spectrometric Approaches for the Determination of Food Quality and Development of New Methodologies for Enrichment of Nutraceuticals in Functional Foods

SSD CHIM06

Coordinator: Ch.mo Prof. Sebastiano Andò

Signature

Supervisor/Tutor: Prof. Leonardo Di Donna

Signature

Ph.D. student: Lucia Bartella

Signature

ABSTRACT

The research works presented in this Ph.D. thesis are based on the nutraceuticals and functional foods research.

The first part of the thesis deals with three main topics:

1. **Structural characterization of new HMG-flavonoids in bergamot juice**

   Two unknown 3-hydroxy-3-methylglutaryl flavanone glycosides were identified and characterized by the combination of liquid chromatography and tandem mass spectrometry experiments.

2. **Preparation of extracts enriched in HMG-flavonoids**

   A novel food-grade procedure to obtain HMG-flavonoids enriched extracts with an high purity grade was developed. The purification procedure was tested on different citrus fruits, i.e. bergamot, sour orange and chinotto.

3. **Development of a new procedure for the enrichment of foodstuffs in hydroxytyrosol**

   New functional foods are presented. They were obtained by the enrichment of foodstuffs generally used in daily diet, i.e. flour, whole wheat flour and sugar, with the nutraceutical compound hydroxytyrosol.

The second part concerns the development of advanced mass spectrometric analytical procedure for quality assessment of foods, through the quantification of nutraceutical compounds and the determination of target quality molecules.

The works presented in this field are the following:

1. **Determination of Hydroxytyrosol and Tyrosol derivatives compounds in Extra Virgin olive oil by Microwave Hydrolysis and LC-MS/MS analysis**

   A novel method to determine the absolute amount of hydroxytyrosol and tyrosol derivatives in EVOO samples was developed. The procedure consists in a simple and fast microwave assisted acidic hydrolysis reaction, combined with the use of liquid chromatography- tandem mass spectrometry analysis.

2. **Absolute Evaluation of Hydroxytyrosol in Extra Virgin Olive Oil by Paper Sray Tandem Mass Spectrometry**

A novel and fast methodology for the evaluation of the absolute amount of Hydroxytyrosol in extra virgin olive oil was set up. The method is based on the exploitation of paper spray ionization (PS) tandem mass spectrometry (MS/MS).

3. **Discriminant Analysis of Vegetables Oils by Paper Spray Mass Spectrometry and Statistical Approach**

An innovative approach for the characterization of triacylglycerols profile of different vegetable oils was developed. The method employs the paper spray ionization technique that in combination with chemometric analysis has allowed to discriminate the extra virgin olive oil from the others vegetable oils commonly used as adulterants.

4. **Quantitative Evaluation of Caffeine in beverages and drugs by Paper spray tandem Mass Spectrometry**

A simple and fast method for the quantification of caffeine in beverages and drugs is presented. Also this analytical procedure is based on the use of paper spray tandem mass spectrometry.

CORSO DI DOTTORATO IN MEDICINA TRASLAZIONALE XXX CICLO
CANDIDATA Dott.ssa Lucia Bartella
RELAZIONE SULLE ATTIVITA' SVOLTE

BREVETTI DEPOSITATI

1. Di Donna, L., Sindona, G., **Bartella, L.**, Gallucci, G., Cappello A. ESTRATTI DI FRUTTO DI BERGAMOTTO, FOGLIE DI BERGAMOTTO, ARANCIO AMARO E CHINOTTO Deposito brevetto n. CS102015000006781 24/02/2015

PUBBLICAZIONI

1. Domenico Taverna, Leonardo Di Donna, **Lucia Bartella**, Anna Napoli, Giovanni Sindona, Fabio Mazzotti*. ***Fast analysis of caffeine in beverages and drugs by paper spray mass spectrometry***. Analytical and Bioanalytical chemistry, May 2016, Volume 408, Issue 14, pp 3783-3787.

2. **Lucia Bartella**, Emilia Furia*, Leonardo Di Donna. ***Mass spectrometry and potentiometry studies of Al(III)-naringin complexes.*** RSC Adv., 2017, 7, 55264 DOI: 10.1039/C7RA12281K

3. **Lucia Bartella**, Fabio Mazzotti, Anna Napoli, Giovanni Sindona, Leonardo Di Donna*. ***A comprehensive evaluation of tyrosol and hydroxytyrosol derivatives in extra virgin olive oil by microwave assisted hydrolysis and HPLC-MSMS***. Analytical and Bioanalytical Chemistry (2018) DOI: 10.1007/s00216-018-0885-1 *Article In Press*

Submitted:

1. Marco Fiorillo, Maria Peiris-Pagè, Rosa Sanchez-Alvarez, **Lucia Bartella**, Leonardo Di Donna, Vincenza Dolce, Giovanni Sindona, Federica Sotgia*, Anna Rita Cappello* and Michael P. Lisanti*. ***Bergamot natural products eradicate cancer stem cells (CSCs) by targeting mevalonate, Rho-GDI-signalling and mitochondrial metabolism.***

PARTECIPAZIONE A SCUOLE INTERNAZIONALI

1. NATO School, NATO SPS ASI 984915, 9-16 Aprile 2016 , Hotel La Principessa, Campora San Giovanni – CS

2. 20° Corso di Spettrometria di Massa 2016. Siena, Certosa di Pontignano, 12-18 Marzo 2016

CONTRIBUTI A CONGRESSI NAZIONALI E INTERNAZIONALI

(autore che ha presentato)

1. **Lucia Bartella**, Fabio Mazzotti, Antonio Tagarelli , Anna Napoli,Giovanni Sindona, Leonardo Di Donna. ***Discriminant analysis of vegetable oils by paper spray mass spectrometry and statistical approach.*** Book of Abstract Quinta edizione MS Food Day 11-13 Ottobre 2017 Bologna, pagina 174, ISBN 9788890738838 **POSTER**

2. Fabio Mazzotti, Leonardo Di Donna, **Lucia Bartella**, Anna Napoli, Giovanni Sindona. ***Assay of lovastatin in dietary supplement by LC MS/MS under MRM condition.*** Book of Abstract Quinta edizione MS Food Day 11-13 Ottobre 2017 Bologna, pagina 206, ISBN 9788890738838 **POSTER**

3. **Lucia Bartella**, Fabio Mazzotti, Anna Napoli,Giovanni Sindona, Leonardo Di Donna. ***Comprehensive determination of tyrosol and hydroxytyrosol derivatives in extra virgin olive oil by microwave chemistry and tandem mass spectrometry.*** Book of Abstract Quinta edizione MS Food Day 11-13 Ottobre 2017 Bologna, Book of Abstract pagina 37, ISBN 9788890738838 **ORALE**

4. **Lucia Bartella**, Fabio Mazzotti, Giuseppina De Luca, Anna Napoli,Giovanni Sindona, Leonardo Di Donna. ***Structural characterization of Peripolin, a new 3-hydroxy-3-methylglutaryl flavonoid glycoside from bergamot juice.*** XXV° Congresso Nazionale della Società Chimica Italiana. Paestum (SA) 10/09/2017 –

14/09/2017, Book of Abstract Volume IV pagina 244 (ORG-PO06) ISBN 9788886208802 **POSTER**

5. Furia Emilia; **Bartella Lucia**; Presta Marco; Di Donna Leonardo; Marini Federico. ***Thermodynamic study of naringin under physiological conditions.*** XXV° Congresso Nazionale della Società Chimica Italiana. Paestum (SA) 10/09/2017 – 14/09/2017, Book of Abstract Volume II pagina 266 (ANA-PO29) **POSTER**

6. **Lucia Bartella**, Domenico Taverna, Leonardo Di Donna, Anna Napoli,Giovanni Sindona, Fabio Mazzotti. ***Quantitative assay of caffeine in beverages and drugs by paper spray mass spectrometry and isotope dilution method.*** NATO School, NATO SPS ASI 984915, 9-16 Aprile 2016 , Hotel La Principessa, Campora San Giovanni – CS, **POSTER** e **ORALE** ***su invito del comitato Scientifico della scuola.***

7. **Lucia Bartella**, Domenico Taverna, Fabio Mazzotti, Anna Napoli,Giovanni Sindona, Leonardo Di Donna. ***Determinazione assoluta dell'idrossitirosolo libero e totale in olio extravergine di oliva in accordo alla direttiva CE 432/2012.*** ExpoChimica, San Lazzaro – Bologna, 25-27 Novembre 2015, **POSTER**

8. **Lucia Bartella**, Domenico Taverna, Fabio Mazzotti, Anna Napoli,Giovanni Sindona, Leonardo Di Donna. ***Rapid quality assessment of food by paper spray mass spectrometry and isotope dilution methods.*** Book of Abstract Quarta edizione MS Food Day P.37 Pagina 293, ISBN 9788890932861 7-9 Ottobre 2015 Università di Foggia, **POSTER**

9. Leonardo Di Donna**, Lucia Bartella**, Fabio Mazzotti, Domenico Taverna, Giovanni Sindona. ***Preparation of HMG flavonoids extracts from bergamot fruit and their identification by mass spectrometry.*** Book of Abstract Quarta edizione MS Food Day P.51 Pagina 293, ISBN 9788890932861 7-9 Ottobre 2015 Università di Foggia, **POSTER**

PARTECIPAZIONE A CONGRESSI

1. "La chimica scienza della sicurezza e dello sviluppo sostenibile" Università della Calabria- 22-23 giugno 2015

2. "IV MS FOOD DAY" Foggia- 7-9 ottobre 2015

3. "FAO WORLD FOOD DAY" Università della Calabria- 23 ottobre 2015

4. "ExpoChimica" Bologna- 25-27 novembre 2015

5. V° MS Food Day. Bologna 11/10/2017 -13/10/2017

6. XXVI° Congresso Nazionale della Società Chimica Italiana. Paestum (SA) 10/09/2017 – 14/09/2017

SEMINARI

1. *Recent Advances in Computational Proteomics"* 11 dicembre 2014 Prof. Pedro A. Fernandes

2. *"Rational design of glycomimetic compounds targeting fungal transglycosylases"* – Prof. Merino 3 febbraio 2015

3. *"Epigenetic alteration and microRNA dysregulation in human cancers"* – Dott. Domenico Zito 14 aprile 2015

4. *"Interaction of VIIiquidVIIi with biological and biomimetic membranes"* – Dr. Aravind Vijayaraghavan - 15 giugno 2015

5. *"Accreditamento dei laboratori e sicurezza degli alimenti"* – Dott.ssa Silvia Tramontin e Dott. Federico Pecoraro – 17 giugno 2015

6. *"Quantum Chemistry Applied to Asymmetric Homogeneous and Enzymatic Catalysis"* Prof. Fahmi Himo - 11 settembre 2015

7. *"Atomistic View of Human Diseases"* Dott.ssa Alessandra Magistrato – 10 dicembre 2015

8. *"Effective models for complex materials"*Prof. Miche Pavone- Dipartimento di Chimica e Tecnologie Chimiche – 1 marzo 2016

9. *"The Pt(IV) derivatives as antitumor prodrugs. Comparison with cisplatin"* Prof. Domenico Osella- Dipartimento di Chimica e Tecnologie Chimiche – 3 marzo 2016

10. *"Photochemical* VIII *iquid* VIII *i of [FeFe]-hydrogenases: from photophysical properties to H2 photo-production"* Dr. Luca Bertini – Dipartimento di Chimica e Tecnologie Chimiche – 9 marzo 2016

11. *"Salute e sicurezza sui luoghi di lavoro"* Ing. Pompeo Franco Bruno- Centro Sanitario UNICAL- 6-9 settembre 2016

12. *"Recent advances towards personalyzed chemotherapy"* Prof Tamer Shoeib- Dipartimento di Chimica e Tecnologie Chimiche – 4 maggio 2017

13. *"Capacità sequestrante di leganti naturali nei confronti di metalli biodisponibili"* Dott.ssa E. Furia Dipartimento di Chimica e Tecnologie Chimiche – 12/14 luglio 2017

14. *"Metabonomica"* Dott. A. Beneduci Dipartimento di Chimica e Tecnologie Chimiche –11/13 luglio 2017

CORSI

1. *"NMR for organic and biological chemistry: Old experiments for new applications. Theoretical and practical overview"* – 2 CFU – Dott. Ignacio Delso Hernàdez 24 novembre-3 dicembre 2015

2. Corso specialistico : Crystal Structure, Periodicity and energy bands, Structure and VIIIliquidVIIIic of clean surfaces, Adsorption on surfaces – 1CFU – Dipartimento di Chimica e Tecnologie Chimiche- 9-12 febbraio 2016

3. *"PhD 3.0-La terza missione dell'Università nel Terzo livello di formazione: Valorizzazione della Ricerca e Innovazione"* 40 ore di attività- Liason Office UNICAL- 5-28 luglio 2016

4. *"Applicazione degli Studi di Fotodegradazione in Quality Assurance e Drug Design".* 1CFU Dott.ssa Giuseppina Ioele – Dipartimento di Farmacia e Scienza della Salute e della Nutrizione- 20-21 settembre 2016

5. *"Principles and applications of photodynamic therapy".* 1CFU Dott.ssa Marta E. Alberto – Dipartimento di Chimica e Tecnologie Chimiche- 23-24 novembre 2016

6. *"Farmaci liquido-cristallini"* 3CFU Prof. P. F. Nicoletta Dipartimento di Farmacia e Scienza della Salute e della Nutrizione- 19 gennaio 14 ebbraio 2017

7. *"Advanced English"* 2 CFU Dott.ssa A.F. Plastina Dipartimento di Farmacia e Scienza della Salute e della Nutrizione-22 febbraio 11 marzo 2017

8. *"Analisi dei Dati-Informatica"* 2CFU Ing. A. Tagarelli Dipartimento di Farmacia e Scienza della Salute e della Nutrizione- 18 aprile 23 maggio 2017

ATTIVITA' DI TUTORAGGIO

1. Tutor didattico per il corso di "Chimica" per il primo anno del corso di laurea triennale in Scienze Geologiche. Giugno – Luglio 2017

2. Tutor didattico per il corso di "Chimica Analitica Quantitativa" per il corso di laurea triennale in Chimica. Marzo - Settembre 2017

3. Tutor didattico per il corso di "Chimica Bioorganica" per il corso di laurea magistrale in Chimica. Marzo - Settembre 2017

4. Tutor didattico per il corso di "Chimica Generale ed Inorganica" per il corso di laurea triennale in Biologia/ S.T. Biologiche. Marzo - Settembre 2017

5. Tutor didattico per il corso di "Chimica – Attività affine" / Esami critici per il corso di laurea triennale in Scienze Geologiche. Ottobre - Novembre 2015

ACKNOWLEDGMENTS

I want to thank my supervisor, Professor Leonardo Di Donna. Thanks for the time he has devoted to me and for his scientific ideas that have make my Ph.D. course an experience very productive and stimulating. He was for me a great example of chemist and professor.

CONTENTS

III. Discriminant Analysis of Vegetables Oils by Paper Spray Mass Spectrometry and Statistical Approach

IV. Quantitative Evaluation of Caffeine in beverages and drugs by Paper spray tandem Mass Spectrometry

CHAPTER 1

Introduction

1. NUTRACEUTICALS AND FUNCTIONAL FOODS

In the last decades, there has been a great deal of attention toward the field of food chemistry, because many research studies have highlighted the existence of a strong relationship between daily diet and human health. Current scientific knowledge supports the hypothesis that diet may modulate various functions in the body and play a key role in the prevention of some diseases. (1)

Nutraceutical is the hybrid term of nutrition and pharmaceutical. It was used for the first time in 1989 by De Felice and the Foundation for Innovation in Medicine. (2) Its definition was clarified in 1994 as "*any substance that may be considered a food or part of a food and provides medical or health benefits, including the prevention and treatment of disease. Such products may range from isolated nutrients, dietary, supplements and diets to genetically engineered 'designer' foods, herbal products, and processed foods such as cereals, soups, and beverages.*" (3)

Today, foods are not considered necessary only to satisfy hunger but also to make available same active principles that improve physical and mental well-being of the consumers and prevent different diseases. (4,5) In this regard, functional foods play a specific role.

The term "functional food" is related to nutraceuticals. It was introduced for the first time in Japan in 1984 and defines a food product fortified with nutraceutical compounds that produces positive effects on the general body condition decreasing the risk of some diseases. (6,7)

In the 1990s, it was given a formal legislative category called FOSHU (FOod for Specified Health Uses). (8-10) Generally, a "functional food" must contain an ingredient with specific health properties (11), but there is not a single definition for this food category.

In Europe, there is not a formal legislative definition for "functional foods". According to the European Commission Concerted Action on Functional Food Science in Europe (FuFoSE), the food product can be considered functional, if it has the basic nutritional properties and beneficial effects on one or more functions of the human organism, improving the general and physical conditions or/and decreasing the risk of the diseases. (12) The government agencies in USA, FDA (Food and Drugs Administration) and USDA (United States Department of Agriculture) have proposed a different definition of this food category.

Today, the accepted definition is the following: "*Natural or processed foods that contain known or unknown biologically-active compounds; which, in defined, effective non-toxic amounts, provide a clinically proven and documented health benefit for the prevention, management, or treatment of chronic disease*". (13)

The Mediterranean diet is rich in nutraceutical components which have functional features with positive effects on health and wellness. Mediterranean diet is mostly characterized by the consumption of cereals, legumes, vegetables, fruits and olive oil; it also includes fish or seafood, white meat and eggs, small amount of poultry and dairy products. Therefore, the importance of this diet resides not only in the nutritional values of the constituents but also in their content of pharmacologically active principles. These discoveries have increased the consumer awareness of the potential benefits of compounds naturally present in foods and plants for human health promotion and maintenance. Today, research studies in nutraceuticals, functional foods and natural products are hot topics. (14-17)

Natural products, such as plants extract or pure compounds, provide unlimited opportunities for new active principles discoveries because of the unmatched availability of chemical diversity. The compounds present in natural products are called phytochemicals ("*phyto*" means "plant") because they are produced by plants, fruits, vegetables, spices and traditional herbal medicinal plants. In recent years, many studies have shown that many foodstuffs in our diet contain a high content of phytochemicals, and can provide protection against various diseases. Foodstuffs such as fruits, citrus fruits and vegetables are considered functional foods. The protective effects of these diet components were found for cancer and also for chronic diseases such as cardiovascular diseases. (18-22) Antioxidants such as Vitamins C and E are essential for the protection against ROS, but the majority of the antioxidant activity of foodstuffs such as fruit or vegetable, may be from polyhydroxylated phenolic compounds. Intake of controlled diets rich in fruits and vegetables significantly increased the antioxidant capacity of plasma. (23-26)

As already mentioned, among the constituents of Mediterranean diet, olive oil is considered another essential functional food, because of its constant intake may provide potential health benefits to humans, lowering the incidence of cardiovascular disease. (27-29) It was suggested that this effect is due primarily to the antioxidant properties of polyhydroxylated aromatic molecules present in the oil as minor compounds.

Antioxidant compounds such as phenolic molecules are therefore the focus of many recent studies. Their antioxidant activity is predominantly determined by their structures, in particular by the electron delocalization over an aromatic nucleus. When these compounds react with a free radical, the delocalization of the electron over the aromatic nucleus allows the formation of a stable radical which prevents the continuation of the free radical chain reaction.

Today, the research in the functional foods field is continuously increasing.
Isolation and structural characterization of unknown active principles from daily foodstuffs have became very interesting in order to understand how diet can affect human health, and how these pharmacologically active principles can be used as an alternative to the classical and commercial drugs. *In vitro* and *in vivo* experiment, followed by clinical trials are necessary to demonstrate the effectiveness of bioactive compounds. Clinical trials directed towards understanding the pharmacokinetics, bioavailability, efficacy, safety and drug interactions of newly developed bioactive compounds and their formulations (extracts) require a careful evaluation. They must be carefully planned to safeguard the health of participants and to evaluate their positive and side effects both immediate and long-term.
Therefore, research studies are focused on the development of advanced analytical procedure to determine the quality and the safety of food, through the accurate quantification of nutraceutical molecules.

1.1 FLAVONOIDS IN PLANT SOURCES

Flavonoids are very common and widespread secondary metabolites of plants with a variable phenolic structure and are formed by a series of condensation reactions between hydroxycinnamic acid and malonyl residues, giving rise to a chemical structure of 15 carbons. The carbon skeleton consists in two benzene rings (A and B ring) linked by a three carbon chain, and their structure is also referred to as C6—C3—C6. The three-carbon bridge between the phenyl rings is commonly cyclized to form a third ring (C-ring). According to the cyclization and the degree of unsaturation and oxidation of the three-carbon segment, they can be classified into several groups. The basic structures of the main classes of flavonoids are shown in Figure 1.

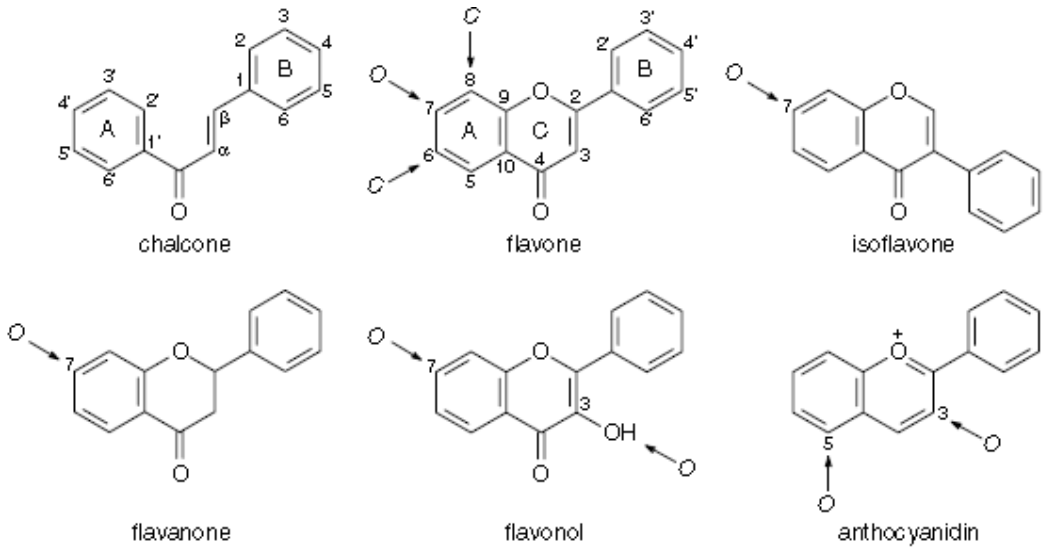

Figure 1 Basic structure of the main classes of flavonoids. Common C- and O- glycosylation positions are indicated with an arrow

In plants, flavonoids may occur in various modified forms corresponding to additional hydroxylation, methylation and, most importantly, glycosylation. Flavonoids commonly occur as flavonoid *O*-glycosides, in which one or more hydroxyl groups of the aglycone are bound to a sugar with formation of a glycosidic O—C bond, which is an acid-labile hemiacetal bond. The glycosylation makes the flavonoid less reactive and more water soluble, It can be seen as an essential form of protection in plants to prevent cytoplasmic damage and to store the flavonoids safely in the cell vacuole.(30) In principle, any of the hydroxyl groups can be glycosylated but certain positions are favored: for example, the 7-hydroxyl group in flavones, flavanones and isoflavones, the 3- and 7-hydroxyls in

flavonols and the 3- and 5-hydroxyls in anthocyanidins are common glycosylation sites (Fig. 1). Glucose, galactose and rhamnose are the most common sugars, while arabinose, mannose, fructose, and the glucuronic and galacturonic acids are less frequent. Disaccharides are often found in association with flavonoids, the most commons are rutinose (rhamnosyl-(α1→6)-glucose) and neohesperidose (rhamnosyl-(α1→2)-glucose); occasionally tri- and even tetrasaccharides may be found as conjugates with flavonoids. Acylated glycosides, in which one or more sugars hydroxyls are esterified with an acid, also occur. Glycosylation may also take place by direct linkage of the sugar to the flavonoid's basic nucleus, via an acid-resistant C—C bond, to form flavonoid *C*-glycosides. Flavonoid *C*-glycosides are commonly further divided into mono-*C*-glycosylflavonoids, di-*C*-glycosylflavonoids and *C*-glycosylflavonoid-*O*-glycosides. (31) In the last category, a hydrolyzable sugar is linked either to a phenolic hydroxyl group or a hydroxyl group of the *C*-glycosyl residue. To date, *C*-glycosylation has only been found at the C-6 and/or C-8 position of the flavonoid nucleus (Fig. 1). (30,31)

Flavonoids are an integral part of human and animal diet. Being phytochemical compound, flavonoids cannot be synthesized by humans and animals. Flavonoids in food are generally responsible for color, taste, prevention of fat oxidation, and protection of vitamins and enzymes.

Available reports tend to show that flavonoids are responsible for a variety of pharmacological activities. Their activities are structure dependent. The chemical nature of flavonoids depends on their structural class, degree of hydroxylation, other substitutions and conjugations, and degree of polymerization. (32)

Recent interest in these substances has been stimulated by the potential health benefits arising from their antioxidant activities. Functional hydroxyl groups in flavonoids mediate their antioxidant effects by scavenging free radicals and/or by chelating metal ions. The chelation of metals could be crucial in the prevention of radical generation, which damage target biomolecules. As dietary components, flavonoids are thought to have health-promoting properties due to their high antioxidant capacity demonstrated both in vivo and in vitro systems. Several studies have suggested protective effects of flavonoids against many infectious (bacterial and viral diseases) and degenerative diseases such as cardiovascular diseases, cancers, and other age-related diseases. (26, 32-37)

1.2 HMG-FLAVONOIDS IN CITRUS FRUITS

In 2009 two new flavonoids were isolated and characterized from bergamot juice (Fig. 2), as HMG conjugates of neohesperidin and naringin namely, Melitidin (naringin 7-(2”-α-rhamnosyl-6”-(3””-hydroxy-3””-methylglutaryl)-β-D-glucopyranoside) and Brutieridin (neohesperidin 7-(2”-α-rhamnosyl-6”-(3””-hydroxy-3””-methylglutaryl)-β-D-glucopyranoside). (38)

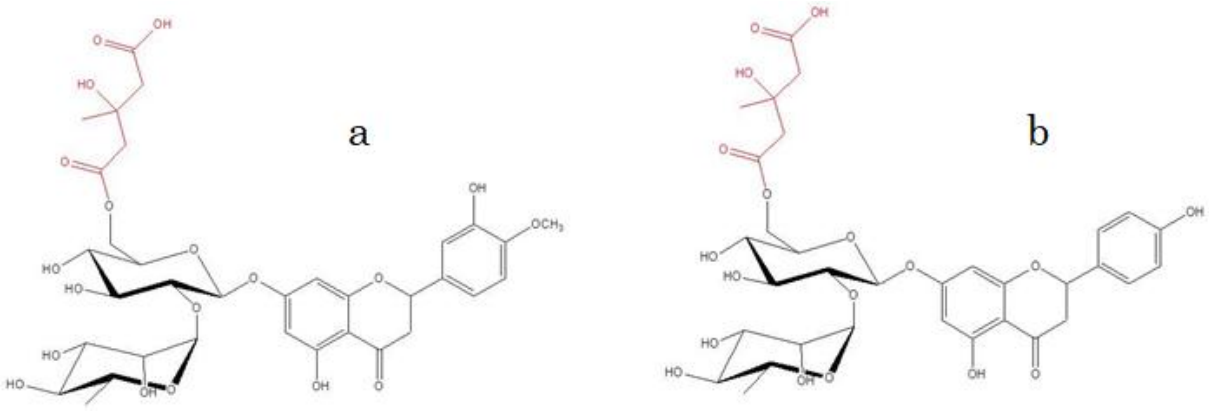

Figure 2 Chemical structure of a- *Brutieridin* and b- *Melitidin*

Bergamot, *Citrus Bergamia Risso*, belongs to the family Rutaceae, subfamily Esperidea, and is widespread in the Mediterranean area. The natural habitat of this tree is restricted to the coastal region of the Ionian Sea in the southern Calabrian region of Italy. (39)

Its volatile fraction is still used in the cosmetic and perfumery industries, and for many years, bergamot juice was considered a secondary product and waste from the essential oil extraction. Furthermore, because of its organoleptic properties and its bitter taste, it did not reach the popularity of other citrus juices, but it was used to fortify other fruit juice or beverages instead of synthetic additives.

The true peculiarity of this fruit is the abundance and variety of flavonoid glycosides present. Naringin, neohesperidin, neoeriocitrin, melitidin and brutieridin are present in juice and in other compartments of fruit, in the order of several hundreds of ppm Other flavonoids, as rhoifolin, neodiosmin and poncirin are present at lower concentration. (40-42)

Melitidin and brutieridin are considered two statin-like flavonoids able to inhibit the HMG-CoA reductase, the rate-limiting enzyme which catalyzes the conversion of HMG-CoA into mevalonate, the cholesterol precursor. (43,44)

To evaluate the potential effects of these new flavonoids bearing the 3 hydroxy-3-methyl-glutaric acid (HMG) moiety, a series of studies were performed. It was performed an in vitro study in which their inhibitory effect on HMG-CoA reductase, was compared, against commercial statin drugs with excellent results. (45)

Results obtained by a recent in vivo study on animals, have demonstrated that the effect of bergamot extract containing HMG- flavonoids is similar to that obtained by simvastatin on the lipid profile and, more important, increase the HDL levels. At last, the extract is cytitoxic only at very high doses and no genotoxic effects have been found. (46) Moreover, computational studies based on density functional theory have demonstrated that both molecules, Melitidin and Brutierdin, bind efficiently to the catalytic site of HMG-CoA reductase. (47) 3-hydroxy-3-methyl glutaryl flavanone glycosides were also found in other citrus fruit like bitter orange and chinotto. (48,49)

1.3 PHENOLIC COMPOUNDS IN OLIVE OIL

Olive oil is a product of the mechanical extraction from the fruit of *Olea europeae L*. (Oleaceae family). It is composed by a triacylglycerol fraction, constituting approximately 98–99 %, and by an unsaponifiable fraction (0,4–5 %).

Olive oil is an important constituent of the Mediterranean diet; it is considered a functional food for its beneficial effects as regards breast and colon cancer, diabetes accompanied by hypertriacylglycerolaemia, inflammatory, and autoimmune diseases such as rheumatoid arthritis. (50,51)

The beneficial effects can be attributed not only to the high ratio between unsaturated and saturated fatty acids of olive oil, but also to the antioxidant property of its phenolic compounds. The pulp of olives contains these hydrophilic compounds at high concentration, but they are also transferred to the oil during the production.

The phenols present in olive oil includes numerous substances: simple phenolic compounds such as vanillic, gallic, coumaric and caffeic acids, tyrosol and hydroxytyrosol and more complex compounds like the secoiridoids (oleuropein and ligstroside), and the lignans (1-acetoxypinoresinol and pinoresinol). Other phenolic compounds are flavonoids.

The secoiridoids oleuropein and ligstroside, the main complex phenols in virgin olive oil, are secondary metabolites characterized by the presence of elenolic acid in its glucosidic form. Oleuropein is the ester between 2-(3,4-dihydroxyphenyl) ethanol (hydroxytyrosol) and the oleosidic skeleton common to the glycosidic secoiridoids of the Oleaceae, while ligstroside is the ester between 2-(p-hydroxyphenyl) ethanol (tyrosol) and the oleosidic skeleton. (52)

Moreover, the ligstroside and the oleuropein aglycone, and their deacetoxylated homologues such as oleocanthal and oleacin can be found in the olive oil.

Hydroxytyrosol and tyrosol, the main simple phenolic compounds, can be present as a free or esterified phenols with elenolic acid, forming oleuropein and its derivatives, or ligstroside and its derivative compounds (Figure 3).

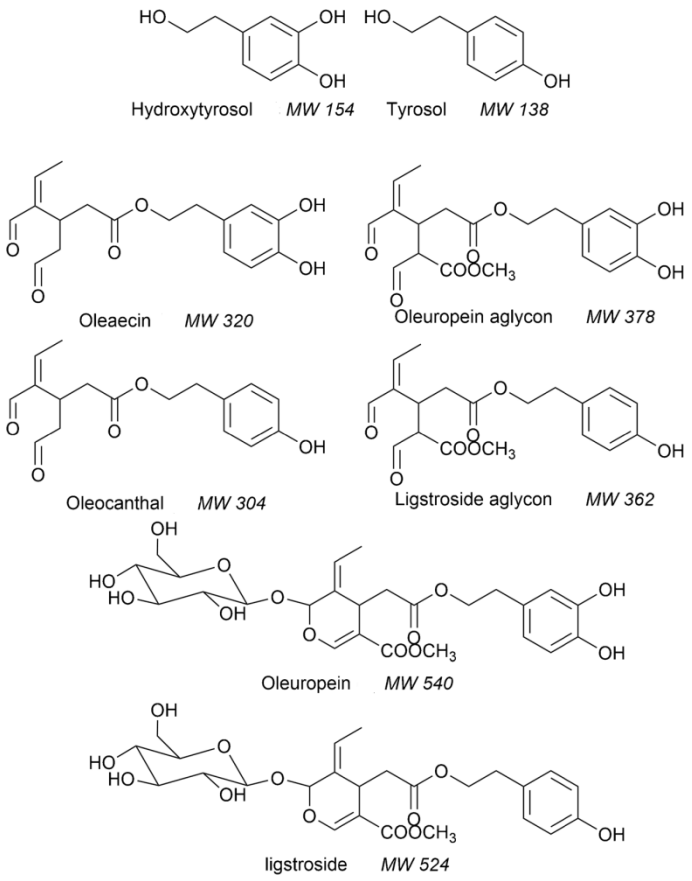

Figure 3 Chemical structure of the main phenolic compounds present in olive oil

Hydroxytyrosol [3,4-dihydroxyphenylethanol (Htyr)] is one of the main phenolic compounds in olives, virgin oil and waste water obtained during the production of olive

oil. In fresh virgin oil, hydroxytyrosol mostly occurs as ester, even if with the aging the non-esterified form prevails due to hydrolytic reactions. (53,54)

Hydroxytyrosol is the only phenol that has been recognized by the European Food Safety Authority (EFSA) as a protector of blood lipids from oxidative damage. (55) In order to support this health claim, 5 mg of hydroxytyrosol and its derivatives (e.g. oleuropein complex and tyrosol) in olive oil should be consumed daily. These amounts can be easily consumed in the context of a balanced diet (EFSA Panel on Dietetic Products Nutrition and Allergies 2011). (56)

Besides the cardio-protective effects (57,58), numerous studies, mostly performed in vitro or using animal models, have shown the potential of HT for preventing additional diseases. These include protection against metabolic diseases (59-61), anti-carcinogenic activity (62-66), anti-inflammatory activity (67), protection against digestive disorders (68) and antimicrobial activity (69).

The accumulating disease-preventing evidence and the fact that hydroxytyrosol has no known toxic effects (70) emphasize the potential of this compound as a nutraceutical in functional foods, food supplements and even medicine.

2. MASS SPECTROMETRY IN NUTRACEUTICALS RESEARCH

Today, nutraceutical compounds are considered quality markers of food, and the development of advanced analytical procedures to quantify these marker compounds has became indispensable in nutraceutical research. It includes the identification of new nutraceuticals, chemical structure characterization, and quality control of foods through their quantification. Due to the complexity of these natural matrices, the use of advanced analytical techniques is necessary.

Mass spectrometry technique is one of the most important tools within this field because it is now recognized as an extremely specific and sensitive technique for the analysis of food products with superior accuracy and higher throughput.

In the last few years, the role of mass spectrometry (MS) and related techniques is increased as an enabling tool in food analysis and quality control. Improvement in instrumentations, online separations techniques and data processing have contributed to determine the great expansion of MS in food-related analysis. A large variety of analytical approaches are used in food chemistry, with different aims and using complementary methodologies.

The chromatography combined with mass spectrometry (MS) is considered one of the most sensitive and selective analytical techniques. Among hyphenated methodologies, today HPLC-MS procedure is most widely used for food analysis. Liquid chromatography coupled with mass spectrometry (MS) offers a powerful tool due to its specificity, which also allows the identification of even co-eluting compounds. The use of tandem mass spectrometry (MS/MS) provides a wealth of structural information, and at the same time it increases selectivity allowing an excellent quantification. (71-79)

Different mass spectrometer can be used in combination with liquid chromatography.

For quantitative purposes, the analyzers able to perform tandem mass spectrometric analysis (MS/MS) in time (ion trap) or in space (quadrupole) are the most employed.

To determine the molecular accurate mass and the elemental formulas of unknown compounds high-resolution analyzers are used.

The most employed analyzers in this field are the following:

Quadrupole: this mass analyzer (Q) is considered a "mass filter". Combined DC and RF potentials on the quadrupole rods can be set to pass only a selected mass-to-charge ratio. All other ions do not have a stable trajectory through the quadrupole mass analyzer and will collide with the quadrupole rods, never reaching the detector. Quadrupole can have other functions besides its use as a mass filter. An RF-only quadrupole acts as an ion guide for ions within a broad mass range. While, a DC-only quadrupole is used as a lens element in some ion optic designs.

Triple quadrupole (QqQ) is a tandem MS analyzer in which the first and third quadrupoles work as mass filters and the second works as collision cell in RF-only mode, causing fragmentations of the analyte through interaction with a collision gas. Triple quadrupole (QqQ) allows to work in different scan mode: 1- full scan, 2 – product ion scan, 3 – precursor ion scan, 4- neutral loss scan and 5 – selected ion monitoring (SRM) or multiple reaction monitoring (MRM). The Figure 4 shows the scan modes in tandem mass spectrometry with QqQ instrument.

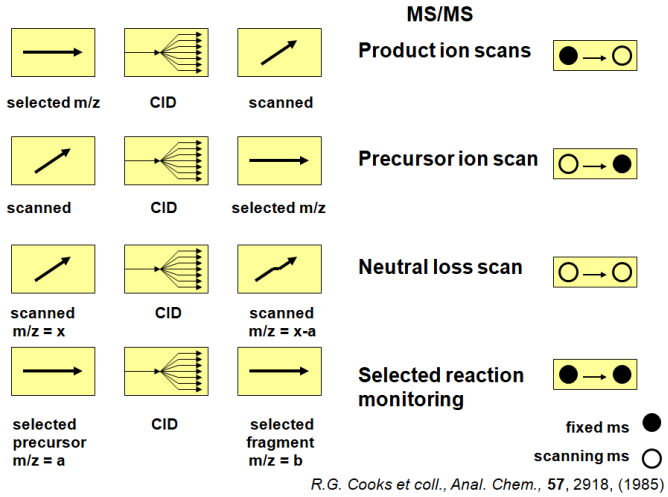

Figure 4 Scan modes of triple quadrupole

Triple quadrupole (QqQ) is simple, robust and often used for quantitative purposes when higher sensitivity and specificity is required. This instrument, together with other multi-stage analyzers, is capable of multiple reaction monitoring (MRM), which improves selectivity and sensitivity of the determination if compared to single stage MS. This scanning mode has unique capability for simultaneous monitoring of large number of compounds in complex mixtures. (80)

Ion Trap: two types of ion trap instrument exist, quadrupole ion trap and linear ion trap. The first consists in three electrodes, two end-cap electrodes that normally are at ground potential and between them a ring electrode to which a radio frequency (RF) is applied to generate a quadrupole electric field. In the linear ion trap (LIT) ions are confined radially by a two-dimensional (2D) radio frequency (RF) field, and axially by stopping potentials applied to end electrodes. The ion trap analyzers are employed to store ions and characterize their properties in the isolated state. They allow to perform MS/MS experiments through three sequential steps: isolation of the parent ion, its dissociation to give characteristic products, and their identification using a second stage of mass analysis. (80,81)

Ion trap and quadrupole analyzer are used specially for quantitative purpose, because their high selectivity.

The most used analyzers for high resolution mass spectrometry analysis are the following:

Time-of-flight TOF analyser measures the mass-dependent time it takes ions of different masses to move from the ion source to the detector. This requires that the starting time (the time at which the ions leave the ion source) is well-defined. Therefore, ions are either formed by a pulsed ionization method (usually MALDI), or various kinds of rapid electric field switching are used as a 'gate' to release the ions from the ion source in a very short time. The ions leaving the ion source of a time-of-flight mass spectrometer have neither exactly the same starting times nor exactly the same kinetic energies. To compensate for these differences, various time-of-flight mass spectrometer designs were developed. The most TOF analyzer used is TOF-Reflectron which has an ion optic device (reflectron). Ions in a time-of-flight mass spectrometer pass through a "mirror" or "reflectron" and their flight is reversed. This process allows ions with greater kinetic energies to penetrate deeper into the reflectron than ions with smaller kinetic energies. The ions that penetrate deeper will take longer to return to the detector. If a packet of ions of a given mass-to-charge ratio contains ions with varying kinetic energies, then the reflectron will decrease the spread in the ion flight times, and therefore improve the resolution of the time-of-flight mass spectrometer. Time of flight (TOF) mass spectrometer has the advantage of high mass resolution. It allows to determine the elemental formulas of unknown compounds through their accurate mass. (80)

FT-ICR Fourier transforms ion cyclotron resonance (FT ICR) mass spectrometer, introduced by Comisarow & Marshall (1974a) is based on the measurement of the frequency of ion rotation in the magnetic field – cyclotron frequency. Ion mass to charge (m/q) ratio is inversely proportional to the cyclotron frequency and it is possible to determine the m/q ratio if its frequency and the magnetic field strength B are known. The main part of the FT ICR spectrometer is a measuring cell in which ions get trapped by electric field in the direction along magnetic field vector and by magnetic field in perpendicular direction. By applying RF electric field containing resonant frequency in the plane of ion cyclotron motion we are exciting their synchronous cyclotron motion. Rotating ions induce image current which is digitized and converted using Fourier transform into the frequency domain and then in mass spectra. This analyser offers highest resolving power and mass measurement accuracy among all types of mass spectrometers. (80)

Orbitrap: The Orbitrap mass analyzer consists essentially of two outer electrodes and a central electrode, which enable it to work as both an analyzer and detector. When voltage is applied between the outer and the central electrodes, the resulting electric field is strictly linear along the axis and thus oscillations along this direction will be purely harmonic. At the same time, the radial component of the field strongly attracts ions to the central electrode. Ions are injected into the volume between the central and outer electrodes. With voltage applied between the central and outer electrodes, a radial electric field bends the ion trajectory toward the central electrode while tangential velocity creates an opposing centrifugal force. With a correct choice of parameters, the ions remain on a nearly circular spiral inside the trap. At the same time, the axial electric field caused by the special conical shape of electrodes pushes ions toward the widest part of the trap initiating harmonic axial oscillations. Outer electrodes are then used as receiver plates for image current detection of these axial oscillations. The digitized image current in the time domain is Fourier-transformed into the frequency domain in the same way as in FTICR and then converted into a mass spectrum. (80,82)
Often, hybrid analyzer are used; for example QqTOF or LTQ – Orbitrap, which provide high mass resolution, sensibility and selectivity thanks to the physic of mass analyser and its capability to perform tandem mass spectrometric experiments.

Among the various ionization techniques, electrospray source (ESI) and atmospheric pressure chemical ionization (APCI) are the most used in combination with liquid chromatography. ESI source works in negative and positive ionization mode, and it is excellent for analysis of polar, ionized and ionizable molecule. Sensitivity depends on the molecular structure, in fact, ESI ionization is not efficient for compounds of low polarity. For these compounds APCI and APPI (atmospheric pressure photo-ionization) techniques may be used. (80)

ESI: It is a soft ionization technique which produces very little fragmentation. The ESI interface is recommended for use with highly polar and is suitable for thermolabile analytes and macromolecules. In the ESI source, the HPLC eluent passes through a heated capillary tube. A potential difference (typically 3–5 kV) is applied to the nebulizer spray-tip, adding a charge to analytes in the mobile phase. The mobile phase is sprayed out of the end of the tube and into the heated interface, where the solvent evaporates, leaving ions in

the gaseous state. These ions are generated by 'coulomb explosion' of electrically charged droplets and may be of various charge states. In some models the charged capillary is surrounded by another capillary containing a nebulizing inert gas to aid in final evaporation by reducing surface tension. (74-78,80)

APCI: The APCI ionization technique is typically used for compounds that do not ionize well with ESI, often more stable, with lower molecular weight compounds and also non-polar molecules. Chemical ionization is the first ionization mechanism in APCI, the mobile phase is evaporated and the ions are generated by corona discharge. In particular, the electrons ionize the auxiliary gas which reacts with the solvent molecules. Charged solvent species are formed through a series of gas-phase reactions. In positive ion mode, analyte is protonated by solvent ions. While in negative ion mode the abstraction of a proton from analyte occurs. This technique is typically not suitable for thermo-labile analytes, because APCI source operates at high temperature (350-550°C), leading to increased risk of analyte degradation. (74-78, 80)

Today, the development of novel ionization techniques allows to perform mass spectrometric analysis without a chromatographic separation step. This new class of ionization methods belong to the ambient ionization technique family requiring no sample preparation or a minimal preparation step. This ionization process is advancing the analytical sciences, because it allows the analysis of complex systems without previously chemical separations or purification.

The most used ambient ionization techniques are DESI – desorption electrospray ionization, and DART – direct analysis in real time, together other complementary techniques. Ambient ionization methods are characterized by operating in the open air, at atmospheric pressure and temperature conditions. Whereas the conventional atmospheric pressure ionization methods (ESI, APCI or MALDI) require a sample preparation step, ambient MS allows the analysis of sample in its native state or without laborious purification procedure. (83-87)

The capabilities of ambient ionization mass spectrometry have been demonstrated with the direct analysis of natural and pharmaceutical drug compounds, monitoring of illicit chemicals ,characterization of biological molecules, and sampling of complex matrices on surfaces, food, urine, blood, and tissue. (88-94)

Paper Spray ionization Among ambient ionization tecniques, paper spray ionization represents a solution to fast qualitative and quantitative analysis at extremely low cost of consumables. It was recognized previously that paper can be used for electrospray. (95) In this kind of ionization process, a sample is loaded onto a piece of paper and ions are generated directly for MS analysis by applying a high voltage to the wetted paper.

Paper, typically made from cellulose, is a hydrophilic porous material that can hold a certain amount of liquid. Wetted paper is conductive, and the network of cellulose offers micro-channels for liquid (including dissolved analyte) transport. Presumably, the high electric potential applied between the paper triangle and MS inlet generates an electric field that induces a charge that accumulates at the apex of the paper triangle. Similar to electrospray, the Coulombic force breaks the liquid to form charged droplets, which undergo subsequent desolvation processes to generate dry ions.

Paper spray ionization does not require sheath gas, and it works well even when the MS inlet capillary temperature is set to room temperature. When few microlitres of a polar solvent are applied to the paper triangle as spray solvent, a Taylor cone is observed at the tip when examined under a microscope. The mist of fine droplets formed is clearly visible under strong illumination. The Taylor cone and the spray typically disappear after about 1 min, presumably because of the loss of solution via the spray as well as the evaporation of solvent. (96)

In comparison with traditional ESI or nano-ectrospray ionization sources, a distinct advantage of using paper for spray ionization is the potential for making disposable sample cartridges for MS analysis. Although some other porous materials potentially could also be used for spray ionization, the commercial availability at low cost and the ease of fabrication and chemical modification of paper make it a superior candidate for producing sample cartridges that have multiple functions for simple sample treatment and ionization.

REFERENCES

1. R.E.C. Wildman, M. Kelley (2007). Handbook of Nutraceuticals and Functional foods; In: Nutraceuticals and Functional Foods, Taylor & Francis, New York,1,9.

2. E.K. Kalra, *AAPS Pharm Sci*, 5,25.

3. http://www.fimdefelice.org

4. Menrad, K. (2003). Market and Marketing of functional food in Europe. *Journal of Food Engineering*, 56, 181-188.

5. Roberfroid, M. B. (2000). Concept and strategy of functional food science: The European perspective. *The American Journal of Clinical Nutrition*, 71, S1660-S1664.
6. Hardy, G. (2000). Nutraceuticals and functional foods: Introduction and meaning. *Nutrition*, 16, 688-697.

7. Stanton, C., Ross, R. P., Fitzgerald, G. F. and Van Sinderen, D. (2005). Fermented functional foods based on probiotics and their biogenic metabolites. *Current opinion in Biotechnology*, 16, 198-203

8. Roberfroid, M. B. (2000b). Concept and strategy of functional food science: The European perspective. An European consensus of scientific concepts of functional foods. *Nutrition*, 16, 689-691.

9. Kwak, N. S., and Jukes, D. J. (2001). Functional foods. Part 1. The development of a regulatory concept. *Food Control*, 12, 99-107.

10. Menrad, K. (2003). Market and Marketing of functional food in Europe. *Journal of Food Engineering*, 56, 181-188.

11. Niva, M.(2007). All foods effect health: Understandings of functional foods and healthy eating among health-oriented Finns. *Appetite*, 48, 384-393.

12. Diplock. A. T., Aggett, P. J., Anshwell, M., Bornet, F., Fern, E. B., and Roberfroid, M. B. (1999). Scientific concepts of functional foods in Europe: Concensus document. British Journal of Nutrition, 81(suppl. 1), S1-S27.

13. Marthirosyan, D. M. and Singh, J. (2015). A new definition of functional food by FFC: what makes a new definition unique? *Functional Foods in Health and Disease*, 5(6), 209-223

14. Estruch, R.; Salas-Salvado, J. (2013.) Towards an even healthier Mediterranean diet. *Nutr. Metab. Cardiovasc. Dis. 23*, 1163–1166.

15. Lairon, D. (2007). Intervention studies on Mediterranean diet and cardiovascular risk. *Mol. Nutr.Food Res. 51*, 1209–1214.

16. Ortega, R.M.; Palencia, A.; Lopez-Sobaler, A.M. (2006). Improvement of cholesterol levels and reduction of cardiovascular risk via the consumption of phytosterols. *Br. J. Nutr. 96*, S89–S93.

17. Ninfali, P.; Mea, G.; Giorgini, S.; Rocchi, M.; Bacchiocca, M. (2005) Antioxidant capacity of vegetables, spices and dressings relevant to nutrition. *Br. J. Nutr. 93*, 257–266.

18. Cosa, P, Vlietinck, A.J., Berghe, D.V., Maes, L. (2006). Anti-infective potential of natural products: How to develop a stronger in vitro 'proof-of-concept'. *J. Ethnopharmacol.* 106: 290-302

19. Vasanthi H.R., ShriShriMal N., Das D.K. (2012) Phytochemicals from Plants to Combat Cardiovascular Disease *Current Medicinal Chemistry*, 19, 2242-2251

20. Wanga H., Khorb T.O., Shub L., Sub Z., Fuentesb F., Leeb J.H., Ah-Ng Tony Kong. (2012). Plants Against Cancer: A Review on Natural Phytochemicals in Preventing and Treating Cancers and Their Druggability. *Anticancer Agents Med Chem*. 12(10): 1281–1305.

21. B.M. Ames, M.K. Shigenaga, T.M. Hagen. (1993). Oxdidants, Antioxidants, and degenerative diseases of aging. *Proc. Natl. Acad. Sci*. U.S.A. 1;90 (17) 7915. 22.

22. J.B. German, C.J. Dillard, in: W.R. Bidlack, S.T. Omaye, M.S. Meskin, D. Johner (Eds.). (1998). Phytochemicals—A New Paradigm, Technomic Publishing Company Inc., Lancaster, Pennsylvania, USA, pp. 13–32.

23. Shahidi, F. and Naczk, M. (1995). *Food phenolics, sources, chemistry, effects, applications*. Lancaster, PA, Technomic Publishing Co. Inc.

24. Rice-Evans, C.A., Miller, N.J., Bolwell, P.G., Bramley, P.M., and Pridham, J.B. (1995). The relative antioxidant activities of plant-derived polyphenolic flavonoids. *Free Radical Res.*, 22:375–383.

25. Scalbert, A. and Williamson, G. (2000). Dietary intake and bioavailability of polyphenols. *J. Nutr.*, 130:2073S–2085S.

26. Manach, C., Scalbert, A., Morand, C., Rémésy, C., and Jimenez, L. (2004). Polyphenols-Food sources and bioavailability. *Am. J. Clin. Nutr.*, 79: 727-47

27. Willett, W. C.; Sacks, F.; Trichopoulou, A.; Drescher, G.; Ferro-Luzzi, A.; Helsing, E.; Trichopoulos, D. (1995). Mediterranean diet pyramid: a cultural model for healthy eating. *Am. J. Clin. Nutr*. 61, 1402S–1406S.

28. Visioli, F.; Galli, C. (1998) . Olive oil phenols and their potential effects on human health. *J. Agric. Food Chem*. 46, 4292–4296.

29. Estruch, R.; Martnez-Gonz_alez, M. A.; Corella, D.; Salas-Salvado, J.; Ruiz-Guti_errez, J.; Covas, M. I.; Fiol, M.; G_omez-Gracia, E.; L_opez- Sabater, V. E.; Ar_os, F.; Conde, M.; Lahoz, C.; Lapetra, J.; S_aez, G.; Ros, E. (2006). Effects of a Mediterranean-style diet on cardiovascular risk factors: a randomized trial. *Ann. Intern. Med*. 145, 1–11.

30. Harborne JB, Mabry TJ. (1982). The Flavonoids: Advances in Research. Chapman and Hall: London, 1982.

31. Markham KR. Techniques of Flavonoid Identification. Academic Press: London, 1982.

32. Iwashina T. The structure and distribution of the flavonoids in plants. (2000) *J. Plant Res.* 113: 287.

33. Di Carlo G, Mascolo N, Izzo AA, Capasso F. (1999) Flavonoids: old and new aspects of a class of natural therapeutic drugs. *Life Sci.* 65: 337.

34. Nijveldt RJ, van Nood E, van Hoorn DEC, Boelens PG, van Norren K, van Leeuwen PAM. (2001) Flavonoids: a review of probable mechanisms of actions and potential applications. *Am. J. Clin. Nutr*. 74: 418.

35. Pietta PG. Flavonoids as antioxidants. (2000) *J. Nat. Prod.* 63:1035.

36. Mojzisova G, Kuchta M. Dietary flavonoids and risk ofcoronary heart disease. (2001) *Physiol. Res.* 50: 529.

37. Pelzer LE, Guardia T, Juarez AO, Guerreiro E. Acute and chronic antiinflammatory effects of plant flavonoids. (1998) *Farmaco* 53: 421.

38. Di Donna, L., De Luca, G., Mazzotti, F., Napoli, A., Salerno, R., Taverna, D., et al. (2009). Statin-like principles of Bergamot Fruit (Citrus Bergamia): isolation of 3-hydroxymethylglutaryl flavonoid glycosides. *Journal of Natural Products*, 72(7), 1352–1354.

39. Hodgson, R. W. (1967). History, World Distribution, Botany and Varieties; Reuther, W., Webber, H. J., Batchelor, L. D., Eds.; University of California: Berkeley, CA, *The Citrus Industry*, Vol 1. 494-496.

40. Gattuso, G.; Caristi, C.; Gargiulli, C.; Bellocco, E.; Toscano, G.; Leuzzi, U. *J.* (2006) Flavonoid glycosides in bergamot juice (Citrus bergamia Risso). *Agric. Food Chem. 54*, 3929–3935.

41. Gattuso, G.; Barreca, D.; Caristi, C.; Gargiulli, C.; Leuzzi, U. J. (2007) Distribution of Flavonoids and Furocoumarins in Juices from Cultivars of Citrus bergamia Risso. *Agric. Food Chem*. 55, 9921–9927.

42. Dugo, P.; Lo Presti, M.; Ohman, M.; Fazio, A.; Dugo, G.; Mondello, L. (2005). Determination of flavonoids in citrus juices by micro-HPLC-ESI/MS *J. Sep. Sci. 28*, 1149–1156.

43. Goldstaein J.L., Brown M.S. (1990). Regulation of the mevalonate pathway. *Nature* 1;343(6257):425-30

44. Ross, S. D., Allen, I. E., Connelly, J. E., Korenblat, B. M., Smith, M. E., Bishop, D., et al. (1999). Clinical outcomes in statin treatment trials: A meta-analysis. *Archives of Internal Medicine*, 159(15), 1793–1802.

45. Patent ITCS20080019 (A1) — 2010-04-10. Di Donna Leonardo; Dolce Vincenza; Sindona Giovanni

46. Di Donna L., Iacopetta D., Cappello A.R., Gallucci G., Martello E., Fiorillo M., Dolce V., Sindona G. (2014). Hypocholesterolaemic activity of 3-hydroxy-3-methyl-glutaryl flavanones enriched fraction from bergamot fruit (Citrus bergamia): ‘‘In vivo’’ studies. *Journal of Functional Food*, 7(1), pp 558-568

47. Leopoldini M, Malaj N., Toscano M., Sindona G., Russo N. (2010). On the inhibitor effects of bergamot juice flavonoids binding to the 3-hydroxy-3-methylglutaryl-CoA reductase (HMGR) enzyme. *J. Agric. Food Chem*. 58, 10768–10773

48. Mencherini T., Campone L., Lisa Piccinelli A., Mesa M.G., Sánchez D.M., Aquino R.P., Rastrelli L. (2013) HPLC-PDA-MS and NMR Characterization of a Hydroalcoholic Extract of Citrus aurantium L. var. amara Peel with Antiedematogenic Activity. *J. Agric. Food Chem*. 61, 1686−1693

49. Scordino M., Sabatino L., Belligno A., Gagliano G. (2011) Flavonoids and furocoumarins distribution of unripe chinotto (*Citrus×myrtifolia Rafinesque*) fruit:

beverage processinghomogenate and juice characterization. *Eur Food Res Technol* 233:759–767

50. Owen RW, Giacosa A, Hull WE, Haubner R, Wurtele G, Spiegelhalder B & Bartsch H (2000). Olive-oil consumption and health: the possible role of antioxidants. *Lancet Oncology* 1, 107–112.

51. Alarcon de la Lastra C, Barranco MD, Motilova V & Herrerias JM (2001) Mediterranean diet and health: biological importance of olive oil. *Current Pharmaceutical Design* 7, 933–950.

52. Bianco A & Uccella N (2000) Biophenolic components of olives. *Food Research International* 33, 475–485.

53. Mazzotti F., Benabdelkamel H., Di Donna L., Maiuolo L., Napoli A., Sindona G. (2012). Assay of tyrosol and hydroxytyrosol in olive oil by tandem mass spectrometry and isotope dilution method. *Food Chemistry* 135, 1006–1010

54. Cinquanta L, Esti M & La Notte E (1997) Evolution of phenolic compounds in virgin olive oil during storage. *Journal of the American Oil Chemists Society* 74, 1259–1264.

55. Visioli F (2012) Olive oil phenolics: where do we stand? Where should we go? *J Sci Food Agric* 92(10):2017–2019

56. EFSA Panel on Dietetic Products Nutrition and Allergies (2011) Scientific opinion on the substantiation of health claims related to polyphenols in olive. EFSA J 9(4):2033–2058

57. Cabrerizo S, La Cruz D, Pedro J, López-Villodres JA, Muñoz-Marín J,Guerrero A, Reyes JJ, Labajos MT, González-Correa JA (2013) Role of the inhibition of oxidative stress and inflammatory mediators in the neuroprotective effects of hydroxytyrosol in rat brain slices subjected to hypoxia reoxygenation. *J Nutr Biochem* 24(12):2152–2157

58. Merra E, Calzaretti G, Bobba A, Storelli MM, Casalino E (2014) Antioxidant role of hydroxytyrosol on oxidative stress in cadmium-intoxicated rats: different effect in spleen and testes. *Drug Chem Toxicol* 37(4):420–426

59. Cao G, Sofic E & Prior RL (1997) Antioxidant and prooxidant behavior of flavonoids: structure-activity relationships. *Free Radical Biology and Medicine* 22, 749–760.

60. Bali EB, Ergin V, Rackova L, Bayraktar O, Kucukboyaci N, Karasu C. (2014) Olive leaf extracts protect cardiomyocytes against 4-hydroxynonenal-induced toxicity in vitro: comparison with oleuropein, hydroxytyrosol, and quercetin. *Planta Med* 80(12):984–992

61. Bulotta S, CelanoM, Lepore SM, Montalcini T, Pujia A, Russo D (2014) Beneficial effects of the olive oil phenolic components oleuropein and hydroxytyrosol: focus on protection against cardiovascular and metabolic diseases. *J Transl Med* 12(1):219

62. Anter J, Tasset I, Demyda-Peyras S, Ranchal I, Moreno-Millán M, Romero-Jimenez M, Muntané J, Castro MDL, Muñoz-Serrano A, Alonso-Moraga Á (2014) Evaluation of potential antigenotoxic, cytotoxic and proapoptotic effects of the olive oil by-product “alperujo”, hydroxytyrosol, tyrosol and verbascoside. *Mut Res Genet Toxicol Environ Mutagen* 772:25–33

63. Burattini S, Salucci S, Baldassarri V, Accorsi A, Piatti E, Madrona A, Espartero JL, Candiracci M, Zappia G, Falcieri E (2013) Antiapoptotic activity of hydroxytyrosol and hydroxytyrosyl laurate. *Food Chem Toxicol* 55:248–256

64. Carrera-González M, Ramírez-Expósito M,MayasM,Martínez-Martos J (2013) Protective role of oleuropein and its metabolita hydroxytyrosol on cancer. *Trends Food Sci Technol* 31(2):92–99

65. Sun L, Luo C, Liu J (2014) Hydroxytyrosol induces apoptosis in human colon cancer cells through ROS generation. *Food Func* 5:1909–1914

66. Zhao B, Ma Y, Xu Z,Wang J,Wang F,Wang D, Pan S,Wu Y, Pan H, Xu D (2014) Hydroxytyrosol, a natural molecule from olive oil, suppresses the growth of human hepatocellular carcinoma cells via inactivating AKT and nuclear factor-kappa B pathways. *Cancer Lett* 347(1):79–87

67. Takeda Y, Bui VN, Iwasaki K, Kobayashi T, Ogawa H, Imai K(2014) Influence of olive-derived hydroxytyrosol on the toll like receptor 4-dependent inflammatory response of mouse peritoneal macrophages. *Biochem Biophys Res Commun* 446(4):1225–1230

68. Sánchez-Fidalgo S, de Ibargüen LS, Cárdeno A, de la Lastra CA (2012) Influence of extra virgin olive oil diet enriched with hydroxytyrosol in a chronic DSS colitis model. *Eur J Nutr* 51(4):497–506

69. Bisignano C, Filocamo A, Ginestra G, Giofre SV, Navarra M, Romeo R, Mandalari G (2014) 3, 4-DHPEA-EA from Olea Europaea L. is effective against standard and clinical isolates of Staphylococcus sp. *Ann Clin Microbiol Antimicrob* 13(1):24–28

70. Auñon-Calles D, Canut L, Visioli F (2013) Toxicological evaluation of pure hydroxytyrosol. *Food Chem Toxicol* 55:498–504

71. Yeboah K.F. , Konishi Y. (2003). Mass Spectrometry of Biomolecules: Functional Foods, Nutraceuticals, and Natural Health Products. *Analytical Letters* 36, 15, 3271 -3307

72. Careri M., Bianci F., Corradini C. (2002). Recent advances in the applications of mass spectrometry in food-related analysis. *Journal of Chromatography A*, 970, 3–64

73. R.E. Ardrey, Liquid Chromatography–Mass Spectrometry: An Introduction, John Wiley & Sons, Ltd., West Sussex, 2003.

74. Snyder, L.R., Kirkland, J.J. & Glajch, J.L. (1997). Practical HPLC Method Development. Second Edition. New York, USA: John Wiley & Sons, Inc.

75. Snyder, L.R., Kirkland, J.J. & Dolan, J.W. (Editors). (2010). Introduction to Modern Liquid Chromatography. Third edition. New Jersey, USA: John Wiley & Sons, Inc.

76. McMaster, M.C. (2005). LC/MS. A Practical User's Guide. Hoboken, New Jersey, USA: John Wiley & Sons, Inc.

77. Niessen, W.M.A. (2006). Liquid Chromatography-Mass Spectrometry. Third edition. New York, USA: CRC Press.

78. Meyer, V.R. (2010). Practical High-Performance Liquid Chromatography. Fifth edition. Padstow, Cornwall, Great Britain: John Wiley & Sons, Inc.

79. Aiello D., De Luca D., Gionfriddo M., Naccarato A., Napoli A., Romano E., Russo A., Sindona G., Tagarelli A. (2011). Multistage mass spectrometry in quality, safety and origino of foods. *Eur. J. Mass Spectrom*. 17, 1-31

80. Gross J.H. Mass Spectrometry. A textbook - 2nd Edition

81. Cooks R.G., Glish G.L., McLuckey S.A., Kaiser R.E. (1991). Ion Trap Mass Spectrometry. *Chem. Eng. News*, *69* (12), 26–41

82. Zubarev R.A., Makarov A. (2013). Orbitrap Mass Spectrometry. Anal. Chem. 85, 5288−5296

83. Wang H, Liu J, Cooks RG, Ouyang Z. (2010). Paper spray for direct analysis of complex mixtures using mass spectrometry. *Angew Chem Int Ed Engl*, 49(5):877-80

84. Wang H., Manicke N.E., Yang Q., Zheng L., Shi R., Cooks R.G., Ouyang Z. (2011). Direct Analysis of Biological Tissue by Paper Spray Mass Spectrometry. *Anal Chem*., 83(4): 1197–1201.

85. Takáts Z, Wiseman JM, Gologan B, Cooks RG. (2004). Mass spectrometry sampling under ambient conditions with desorption electrospray ionization. *Science.* 2004;306: 471–3. 2

86. Cody RB, Laramee JA, Durst HD. (2005). Versatile new ion source for the analysis of materials in open air under ambient conditions. *Anal Chem.* 77:2297–302. 30.

87. Monge ME, Harris GA, Dwivedi P, Fernández FM. Chem Rev. 2013;113:2269–308. 31. Cooks RG, Ouyang Z, Takats Z, Wiseman JM. (2006). Detection technologies. Ambient mass spectrometry. *Science*, 311: 1566–70.

88. Wiseman JM, Ifa DR, Zhu Y, Kissinger CB, Manicke NE, Kissinger PT, Cooks RG (2008). Desorption electrospray ionization mass spectrometry: Imaging drugs and metabolites in tissues. *Proc Natl Acad Sci U S A.* 25;105(47):18120-5.

89. Weston DJ, Bateman R, Wilson ID, Wood TR, Creaser CS. (2005). Direct analysis of pharmaceutical drug formulations using ion mobility spectrometry/quadrupole-time-of-flight mass spectrometry combined with desorption electrospray ionization. *Anal Chem*. 1;77(23):7572-80.

90. Takáts Z[1], Cotte-Rodriguez I, Talaty N, Chen H, Cooks RG. (2005) Direct, trace level detection of explosives on ambient surfaces by desorption electrospray ionization mass spectrometry. *Chem Commun (Camb)*. 21;(15):1950-2.

91. Huang G, Chen H, Zhang X, Cooks RG, Ouyang Z. (2007). Rapid screening of anabolic steroids in urine by reactive desorption electrospray ionization. *Anal Chem.* 17(21): 8327-32

92. Di Donna, L.; Taverna, D.; Indelicato, S.; Napoli, A.; Sindona, G.; Mazzotti, F. (2017) Rapid assay of resveratrol in red wine by paper spray tandem mass spectrometry and isotope dilution. *Food Chem.* 229, 354-357

93. Taverna, D.; Di Donna, L.; Mazzotti, F.; Policicchio B.; Sindona, G.; (2013) High-throughput determination of Sudan Azo-dyes within powdered chili pepper by paper spray mass spectrometry. *J. Mass Spectrom.* 48, 544–547

94. Mazzotti, F.; Di Donna, L.; Taverna D.; Nardi M.; Aiello D.; Napoli, A.; Sindona, G. (2013). Evaluation of dialdehydic anti-inflammatory active principles inextra-virgin olive oil by reactive paper spray mass spectrometry. *International Journal of Mass Spectrometry* 352, 87– 91

95. Fenn, J. B. U.S. Patent 6,297,499, 2001.

96. H. Wang, J. Liu, R. G. Cooks, Z. Ouyang. (2010). Paper spray for direct analysis of complex mixtures using mass spectrometry. *Angew. Chem.* 122, 889-892

CHAPTER 2

Nutraceuticals and Functional Foods

I. STRUCTURAL CHARACTERIZATION OF NEW HMG-FLAVONOIDS IN BERGAMOT JUICE

1. INTRODUCTION

Analytical separation and structural characterization of flavonoids: an overview

Liquid chromatography based methods are the most used analytical techniques in the flavonoids determination. HPLC analysis of flavonoids is usually performed in reverse-phase (RP) mode, using C8- or C18-bonded silica columns, with an i.d. ranging from 3 to 4.6 mm. In some cases, also other stationary phases, such as silica, Sephadex and polyamide are used. The choice of the RP stationary phase is more important for the quality of the analysis. Generally, a C18-RP column that is well end-capped is preferred, because residual silanol groups could cause worsening of the flavonoid separation. Gradient elution is generally performed with binary solvent systems, composed by water containing acetate or formate buffer, and methanol or acetonitrile as organic solvent. Phosphate buffers is not preferred, especially in LC-MS analysis. LC analysis is usually performed at room temperature. Run time range from 30 min to 1hour is sufficient to separate the flavonoids from an extract, but in case of extreme complexity of the flavonoids fraction, run time until 2 hours could be required. (1-5)

Moreover, comprehensive two dimensional liquid chromatography (LC×LC) is very used because this technique offers much higher peak capacities than separations in a single dimension. Gas chromatography is not widely used in flavonoid analysis because of the limited volatility of flavonoid glycosides. (6,7)

The UV spectrophotometry is a popular technique to detect and quantify flavonoid glycosides and aglycones, as, generally, the concentration of the flavonoids is rather high, in the order of hundreds mg/L. Multiple-wavelength or diode-array UV detection is a full satisfactory tool in screening and quantification studies. (8) The first maximum of absorbance is within 240–285 nm range, and it is due to the A-ring; while the second maximum, in the 300–550 nm range, is due to the substitution pattern and conjugation of the C-ring. The presence of sostituents such as methyl, methoxy and hydroxyl group, does not significantly alter the maximum of absorbance.

Mass spectrometry is the most used detection technique in LC analysis of flavonoids. Generally, flavonoids are part of a complex mixture within a plant extract, and in most cases, to identify them, single stage MS is used in combination with UV detection. (9) LC-

UV/MS analysis, with the aid of standard and reference data, facilitates the confirmation and identification of flavonoids in a sample because provides the molecular mass of the different constituents. In this type of analysis, therefore, the UV signal is also employed for quantitative analysis. For the identification of unknowns flavonoids tandem mass spectrometry (MS/MS and MS^n) is used.

The interfaces used in LC-MS analysis of flavonoids are the atmospheric pressure ionization techniques, i.e. atmospheric pressure chemical ionization (APCI) and electrospray ionization (ESI). Both positive and negative ionization are used. ESI is more frequently used in this type of analysis, but APCI is gaining in popularity. According to most studies, for both APCI and ESI, the negative ion mode provides best sensitivity. Generally, positive ionization is used for complementary information to identify unknown compounds. Negative ionization provides the highest sensitivity, and it is most suited to infer the molecular mass of separated flavonoids, especially in cases of low concentration. The most used analyzers are quadrupole, ion trap and the TOF analyzer used to perform high resolution experiments. The mass spectra obtained from quadrupole and ion trap are very similar in the fragmentation pattern, even if relative abundances of fragment ions and adducts can show differences. Obviously, the main advantage of the ion-trap instrument is the possibility to perform MS^n experiments to confirm the flavonoid structure. As well ESI and APCI ionization techniques, chemical ionization, fast atom bombardment (FAB), and matrix-assisted laser desorption ionization (MALDI) are also used. (10-14)

Structural characterization of flavonoid glycosides

As mentioned above, LC-UV/MS analysis is the most employed technique in flavonoid studies, but this type of experiments provide solely information on the molecular mass and retention time of the sample constituents. For the full structural characterization of flavonoids, tandem mass spectrometry experiments in low and high resolution mode (LC-MS/MS and MS/MS, HR MS and HR MS/MS), must be performed.

The fragmentation of flavonoid glycosides is generally described according to the nomenclature proposed by Domon & Costello (1988) for glycoconjugates (Figure 1). (12)

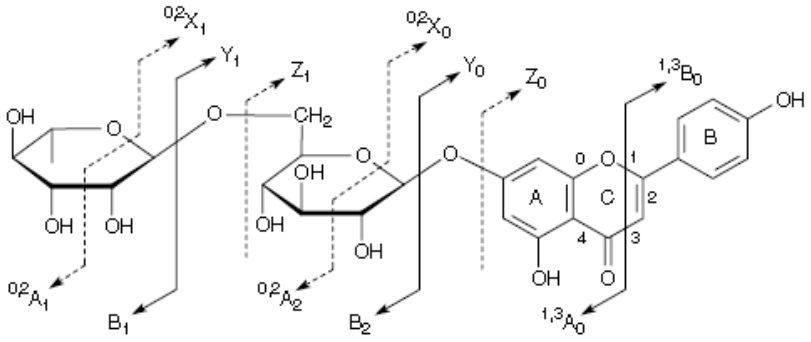

Figure 1 Fragmentation nomenclature used for MS analysis of flavonoid glycosides. the figure shows the apigenin-7-O-rutinosede (12)

Ions containing the aglycone are labeled $^{k,l}X_j$, Y_j and Z_j. The subscript *j* denote the number of the interglycosydic bond cleaved, counting from the aglycone, while the superscripts *k* and *l* indicate cleavages within the carbohydrate rings. The glycosydic bond linking the glycan part to the aglycone is numbered 0. Ions containing the carbohydrate residue are designed by $^{k,l}A_i$, B_i and C_i where *i* valuerepresents the number of the glycosydic bond cleaved, counting from the non-reducing end. When more than one glycosylation position are involved, an additional superscript *m*, which denotes aglycone substitution, is used for ions $^{k,l}X^m_j$, Y^m_j.

- *Flavonoid O-glycosides*

For flavonoid O-glycosides, ESI (+) MS/MS is usually performed in low collision energy mode. The fragmentation obtained by cleavage of the glycosidic *O*-linkage with concomitant H-rearrangement, leads to the elimination of the monosaccharide residue, *i.e.* loss of 162 amu (hexose), 146 amu (deoxyhexose) or 132 amu (pentose), and to the formation of corresponding Y_0^+ aglycone ion. (13,14) In negative ionization mode, the fragmentation pattern shows in addition to the aglycone ion $[Y_0]^-$, an abundant radical aglycone $[Y_0\text{-H}]^{-\bullet}$. This radical ion was observed in the high-energy CID spectra of quercetin *O*-glycosides (14), and it is formed by a homolytic cleavage of the glycosidic bond between the aglycone and the glycan residue. (15)

Flavonoid *O*-diglycosides are also frequently encountered. The most common disaccharides include rutinose [rhamnosyl-(α1→6)-glucose] and neohesperidose [rhamnosyl-(α1→2)-glucose]. These flavonoids are characterized by the presence of the interglycosidic linkage between the glucose and rhamnose units. ESI (+) MS/MS provides Y_1^+ and Y_0^+ fragment ions which correspond to losses of the terminal rhamnose unit and

the rhamnosylglucose residue, respectively. MS/MS with higher collision energies promote the formation of the aglycone fragment ion Y_0^+. In some cases, the complementary monosaccharide ions $[B_1]^+$ (*m/z* 147) and$[B_2]^+$ (*m/z* 309) can also be detected. (13,14) A [Y*]+ ion, corresponding to the loss of the inner glucose residue ($[M+H-162]^+$), is formed by the migration of a hydrogen from the hydroxyl group at C5 of the aglycone to the terminal rhamnose and a rearrangement reaction. The rearrangement entails migration of the glucose acetalic oxygen to the terminal rhamnose anomeric carbon, losing the internal glycoside residue. Formation of the $[Y^*]^+$ ion is favored at low collision energies and this ion can reach very high relative abundances. (16)

Flavonoid di-*O*-glycosides are flavonoids containing two monosaccharides linked to different hydroxyl groups of the aglycone. ESI (+) MS/MS experiment provides the ions $[Y^{3'}{}_0]^+$ and/or $[Y^7{}_0]^+$, and also the $[Y^{3'}{}_0Y^7{}_0]^+$, formed by the cleavage of both sugar-aglycone linkages at C3′ and C7 of flavone ring. The position of glycan substituents of different mass can easily be located in flavonol-3,7-di-*O* glycosides because the protonated molecules more readily lose a glycan substituent at the C3 position compared to the C7 position. (19) The susceptibility of the sugar-aglycone bond to acid hydrolysis certainly depends on the position of the sugar, while, the nature of the sugar only has a negligible effect on the strength of the sugar-aglycone bond. (14)

- *Flavonoid C-glycosides*

In flavonoid *C*-glycosides, glycosylation occurs by direct linkage of the sugar to the basic flavonoid nucleus with the formation of a *C*-*C* bond. These flavonoids are divided in three classes mono-*C*-glycosyl-, di-*C*-glycosyl- and *O*,*C*-diglycosyl-flavonoids. It is necessary an higher collision Energy than O-glycosides to fragment C-glycosides, because of the absence of the acid-labile bond. (13) The main fragmentations of mono-C-glycoseides concern cross-ring cleavages of the saccharide residue and the loss of water molecules. (13,14) Other fragment ions are shown in the figure 2.

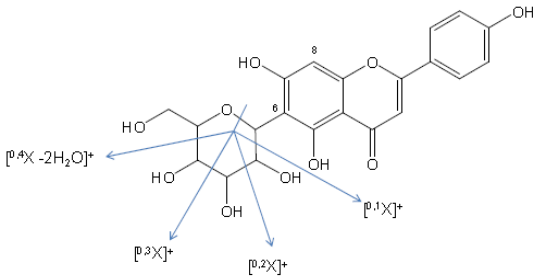

Figure 2 characteristic fragmentation of C-glycosides. Cross-ring cleavage of glucose moiety (12,13,14)

The *O,C*-diglycosyl flavonoids present UV-vis spectra identical to their equivalent *O*- and *C*-glycosides, but they can be distinguished through ESI(+)-MS/MS spectra. Protonated *O*-diglycosides produces Y_1^+ and Y_0^+ ions, whereas *C*-glycosides only yield [M + H]+ ions together with cross-ring cleavages of the sugar residue and loss of water molecules. At low collision energies protonated *O,C*-diglycosides only produces Y_1^+ ions, formed by fragmentation at the interglycosydic linkage. At higher collision energies, however, protonated *O,C*-diglycosides exhibit both types of fragmentations. (13)

2. MATERIALS AND METHODS

2.1 Chemicals

HPLC grade solvents were purchased from Carlo Erba (Milan, Italy). Standard flavonoids were purchased from Extrasynthese (Gnay, France) and other chemicals were from Sigma-Aldrich (St. Louis, MO).

2.2 Plant materials

Bergamot fruits (*Citrus Bergamia*) were collected by Unionberg Association, located at Condofuri Marina (RC, Italy), and stored at -20°C.

2.3 Isolation of flavonoids by HPLC-UV/MS

After fruit squeezing, the juice was centrifuged at 6000 rpm, filtered on a Buchner funnel, and passed through a C_{18} cartridge (Supelclean LC-18, 60 mL, 10 g; Supelco, St. Louis, MO), previously activated with MeOH and washed with water. After loading, the cartridge was washed with 15 ml water and then eluted with 2 × 15 ml of MeOH. The eluate was evaporated under vacuum to dryness, recovered in water and finally lyophilized. For the screening of flavonoids fraction, a solution of 1000 mg/l of the extract was injected in HPLC system and analyzed in analytical mode. LC-UV/MS analysis was performed using a Waters Fraction-Lynx system (Milford, MA) composed by an autosampler/collector Waters 2767 Sample Manager, a 600E pump working in analytical mode, a 486 UV detector and a ZMD quadrupole mass spectrometer equipped with an electrospray ionization (ESI) source.

The chromatographic separation was carried out using a C_{18} reversed-phase column, Luna (250 × 4.6 mm, 5 μm, Phenomenex), injecting a volume of 20 μl. The run time was 70 min, the flow rate was 1 ml/min, and the gradient was built using 0.1% HCOOH in H_2O (solvent A) and MeOH (solvent B) as mobile phase. The elution gradient was composed of the following step: isocratic elution 80% A for 7 min; linear gradient from 80% A to 40% A in 33 min; isocratic elution 40% A for 5 min; linear gradient from 40% A to 20% A in 5 min; isocratic elution 20% A for 7 min; linear gradient from 20% A to 80% A in 5 min; equilibration of the column for 8 min.

The MS conditions were the following: capillary voltage -3.15 kV, cone voltage -3 V, extractor -2 V, RF lens -0.34 V, source block and desolvation temperature 120, 250 °C respectively, ion energy 0.5 V, LM resolution 14.5, HM resolution 15.0 and multiplier 650 V. The nebulizer gas was set to 650 L/h

To isolate the unknown flavonoids, 400 mg of the purified juice containing flavonoid fraction were dissolved in 1 ml of water and submitted to a first step of purification by semipreparative chromatography, with a C_{18} reversed-phase column, Synergy Fusion-RP 80 A (100 × 21.20 mm, 5 μm, Phenomenex). Semipreparative run was performed at 21 ml/min flow rate, using 0.1% HCOOH in H_2O (solvent A) and MeOH (solvent B). It consisted in an isocratic run of 17 min (60%A, 40% B). In order to verify the separation, each collected fraction was injected in the HPLC system. The fractions of interest were mixed, lyophilized and dissolved again (50 mg in 30% of EtOH) for the second purification step, which was carried out to obtain the pure compounds. Second semipreparative chromatography consisted in an isocratic run of 4.5 min, using 30% of EtOH, at 21 ml/min using the same C_{18} reverse-phase column. In the two steps of the semipreparative purification, fractions were collected every 18s. All the fractions corresponding to the same UV and mass signal were mixed and the solvent was evaporated under vacuum. The residual water was lyophilized to obtain the powdered compounds. The semipreparative purifications were repeated until an appropriate amount was reached to perform the other experiments for characterization.

2.4 High resolution mass spectrometry

High resolution mass spectrometry experiments were carried out with an hybrid Q-Star Pulsar-i (MDS Sciex Applied Biosystems, Toronto, Canada) mass spectrometer equipped with an electrospray ion source. Solution samples containing the purified flavonoids were

introduced into MS instrument by direct infusion (5µl/min) at the optimum ion spray voltage of 4800 V (-4800 in negative ionization mode). The HR (+) ESI-MS and the HR (-) ESI-MS spectra were acquired by the time-of-flight analyser. The molecular formula was retrieved by Analyst™ QS software (MDS-Sciex, Applied Biosystems, Toronto, Canada).
The MS/MS experiments were performed in the collision cell *q* on the selected precursor ion by keeping the first quadrupole analyser at unit resolution, and scanning the time-of-flight (TOF) analyser. The experiments were conducted in a range of collision energy from 20 to 40 eV for positive mode, and from -20 to -40 eV for negative mode, using N_2 as collision gas.

2.5 Enzymatic and chemical hydrolysis

Basic hydrolysis were performed by treating the pure compound with sodium hydroxide. Enzymatic hydrolysis were carried out using hesperidinase; in particular 1 mg of purified compound and 1 mg of enzyme were dissolved in 1 ml of McIlvaine's buffer at pH 3.5. During the reaction the temperature was maintained at 37°C. Both hydrolysis reactions were monitored by HPLC-UV/MS analysis.

2.6 NMR measurements

NMR spectra were recorded at 25 °C on a Bruker Avance 500 MHz (11.74 T) instrument (Rheinstetten, Germany), dissolving purified samples in CD_3OD.

3. RESULTS AND DISCUSSION

In the present work, the structure of two unknown HMG-flavonoids present in bergamot juice was elucidated.
The screening of flavonoid fraction in bergamot juice by HPLC-UV/MS analysis was the first step of the study. The UV chromatogram showed the presence of two peaks corresponding to unknown flavonoids; their molecular mass were obtained by the mass peaks in total ion current chromatogram (TIC) (Figure 3).

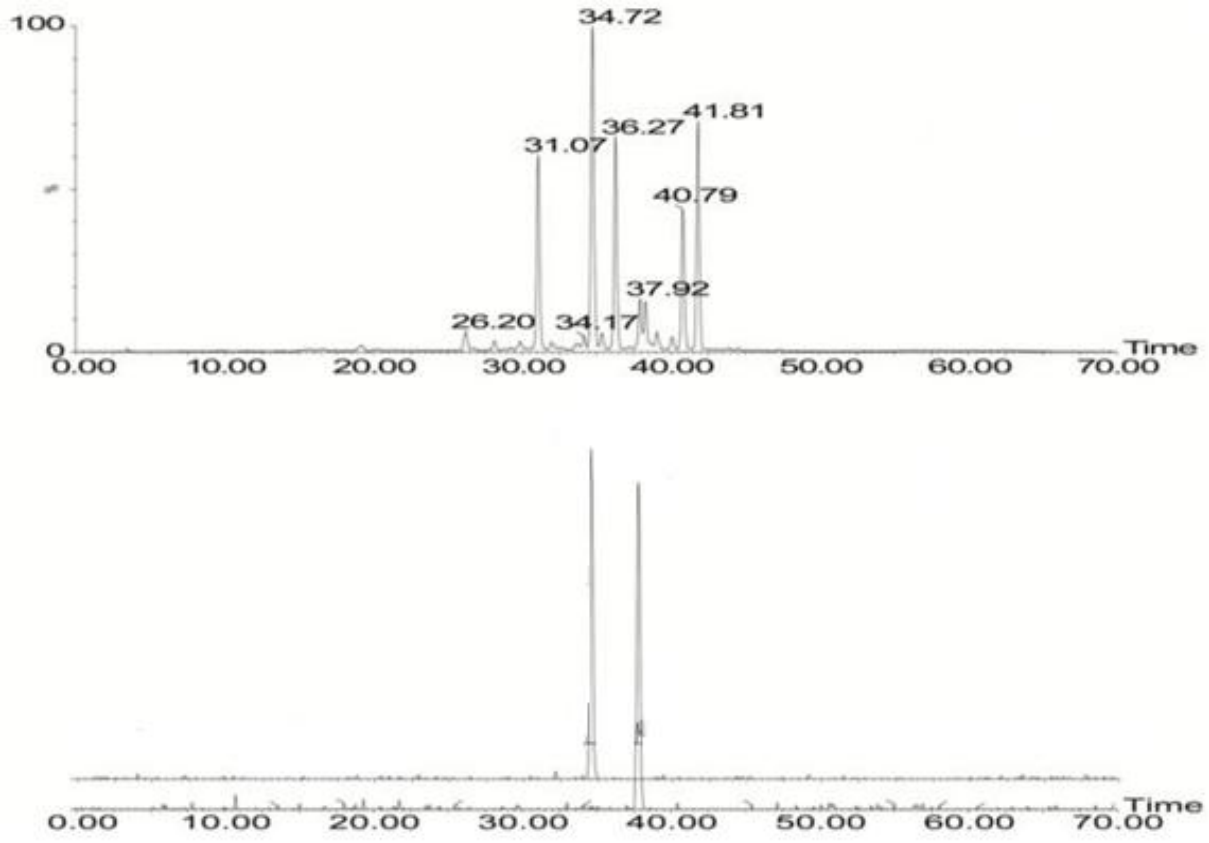

Figure 3 UV profile obtained by LC-UV/MS analysis of bergamot juice and the chromatogram of the extracted ion current of unknown compounds

The total ion current chromatogram was acquired in negative ion mode; compound **1**, rt 37.92 min, showed the deprotonated molecule $[M-H]^-$ at m/z 739, while for the compound **2** at rt 34.17 min, the deprotonated molecule was at m/z 885.

The others main peaks in the UV-chromatogram are relative to neoeriocitrin (rt 31.07 min), neohesperidin (rt 34.72 min), naringin (rt 36.27 min), melitidin (rt 40.79 min) and brutieridin (rt 41.81 min), identified by the pseudomolecular $[M-H]^-$ ions and by the comparison with the retention time of standards.

In order to gather information about their accurate molecular mass and their elemental composition, the solutions of the unknown compounds, collected from chromatographic analysis, were submitted to high-resolution mass spectrometry experiments using a ESI/QTOF instrument. The full MS spectra in positive ionization mode showed the following ions: m/z 904.3097, which corresponds to the elemental composition $C_{39}H_{54}NO_{23}$ with 1.7534 ppm accuracy; m/z 741.2245 with the elemental composition $C_{33}H_{41}O_{19}$ and an accuracy of 1.1383 ppm (Table 1).

Table 1 Accurate mass and elemental composition of unknown compounds

	rt (min)	Accurate mass	Accuracy (ppm)	Elemental composition
Compound 1	37.92	741.2245	1.1383	$C_{33}H_{41}O_{19}$
Compound 2	35.02	904.3097	1.7534	$C_{39}H_{54}NO_{23}$

A semi-preparative chromatography was performed to obtained an appropriate amount of pure compounds for further experiments of structural characterization.

The molecular structures were confirmed by high-resolution MS/MS experiments both in positive and negative ionization mode.

Structural characterization of compound 1: Peripolin

For the unknown compound **1**, the hypothesized structure is shown in figure 4:

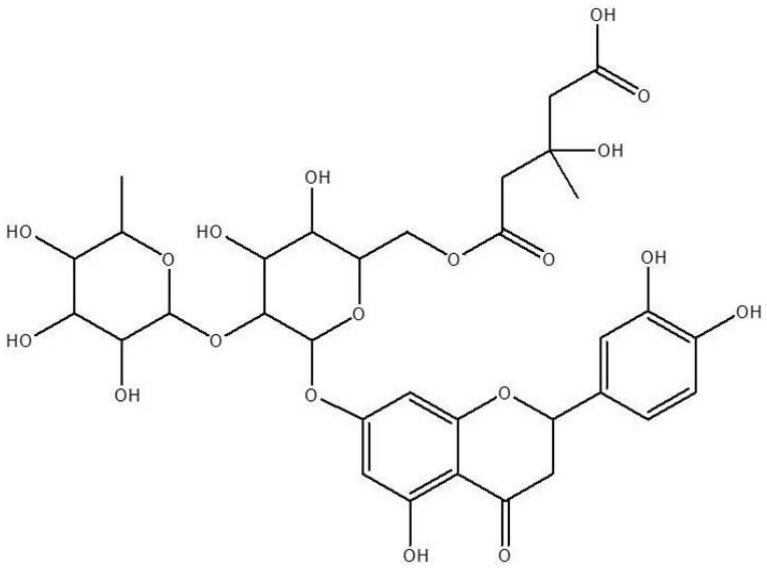

Figure 4 proposed structure of peripolin

The new flavonoid may be the 3-hydroxy-3-methylglutaryl conjugates of the already known neoeriocitrin flavanone.

The Figure 5 displays the mass spectrum obtained by HR ESI (+) MS/MS experiment recorded with a CE of 30 eV.

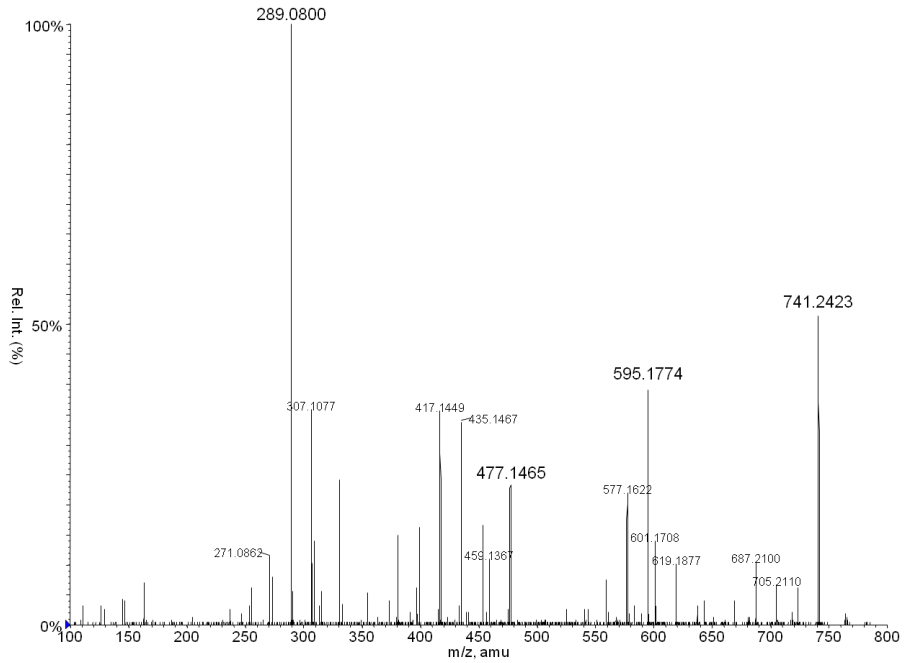

Figure 5 Low energy CID-QqTof-MS/MS (CE 30 eV) of the precursor protonated molecule obtained from compound 1

The CID-MS/MS of the precursor protonated molecule at m/z 741 showed the presence of the following product ions: the formation of aglycone moiety ion Y_0^+ at m/z 289.0800 (base peak) that corresponds to $[(M\text{-}Rha\text{-}Glc\text{-}HMG)+H]^+$, which is a characteristic fragment ion of flavonoid O-glycosides. The elemental composition gathered from the signal at m/z 289.0800 is $C_{15}H_{13}O_6$, which corresponds to the molecular formula of the protonated eriodictiol. The product ion at m/z 271.0862 comes from a consecutive reaction, which eliminates a formal water molecule from m/z 289. In addition, the product ion at m/z 595.1774 corresponds to the fragment Y_1^+ ion, assigned as ($[(M\text{-}Rha)+H]^+$), formed by the loss of the terminal rhamnose unit from the precursor ion at m/z 741 (Figure 6). This product ion suggests that the HMG moiety may be located on the glucosyl moiety.

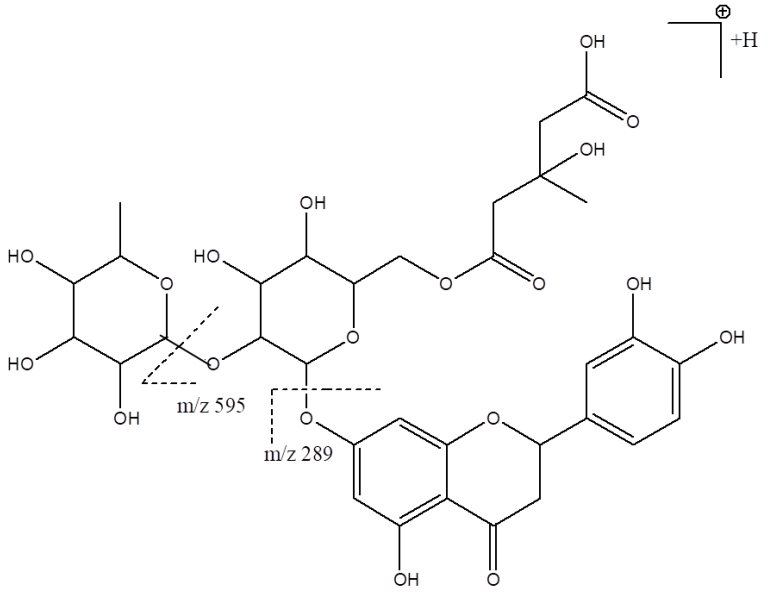

Figure 6 Main product ions in positive ion mode MS/MS experiment for compound 1

The figure 7 shows the major fragmentation routes.

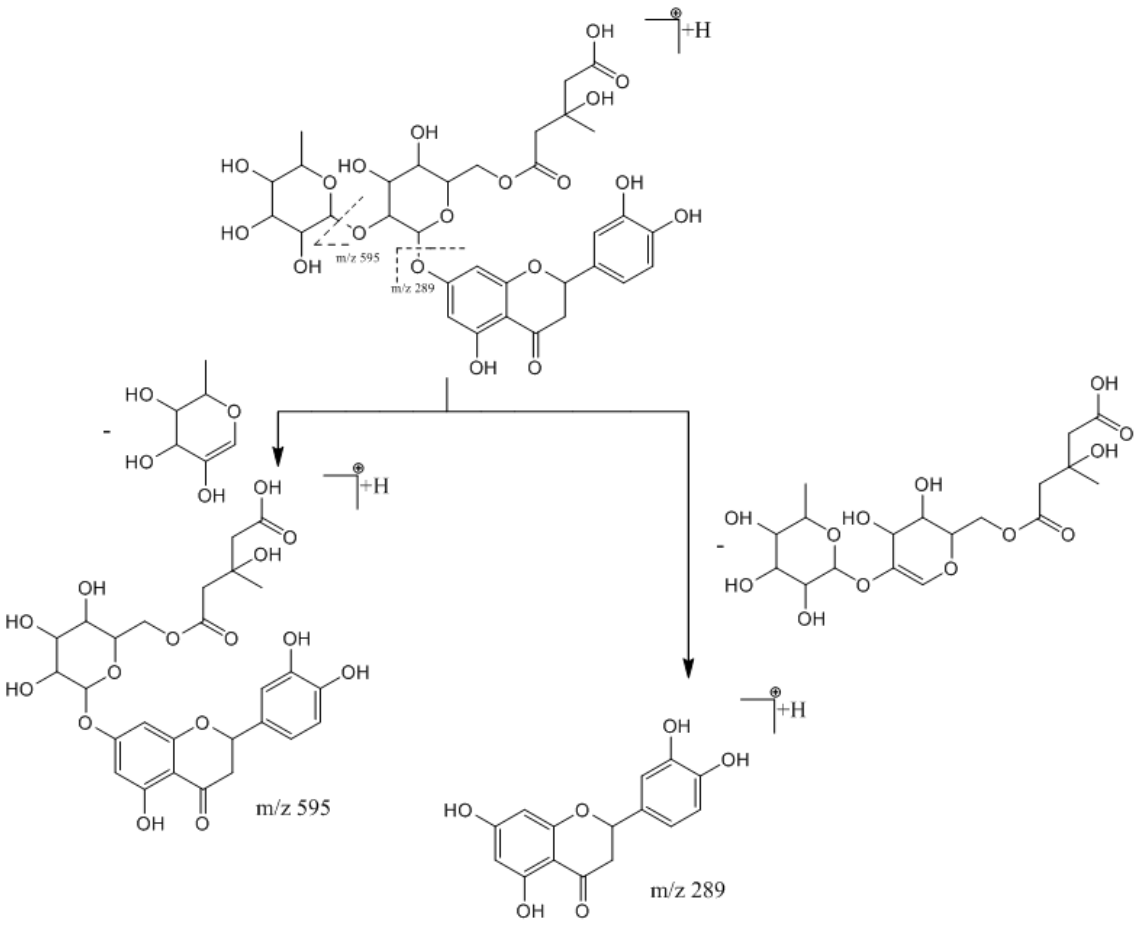

Figure 7 Proposed fragmentation pathways observed for the MS/MS spectrum of the selected protonated compound 1 at m/z 741

The peak at m/z 477.1465 corresponds to the ion $[(M\text{-}C_{10}H_{16}O_8)+H]^+$, which results by cross-ring cleavages of the glucose residue (Figure 8).

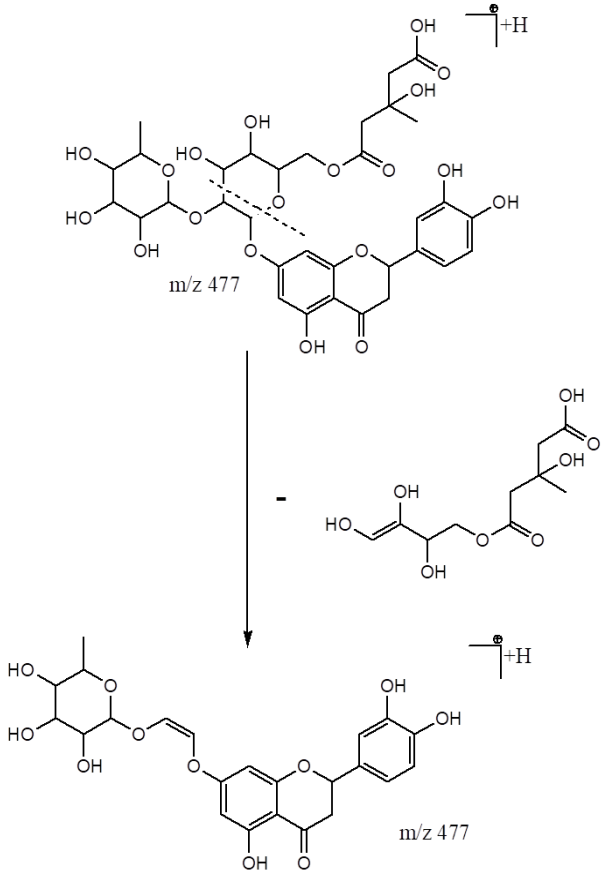

Figure 8 Proposed fragmentation pathway for the formation of the fragment ion at m/z 477

The Figure 9 displays the HR ESI (-) MS/MS spectrum of the deprotonated compound **1**, acquired with a collision energy of 30 eV**.**

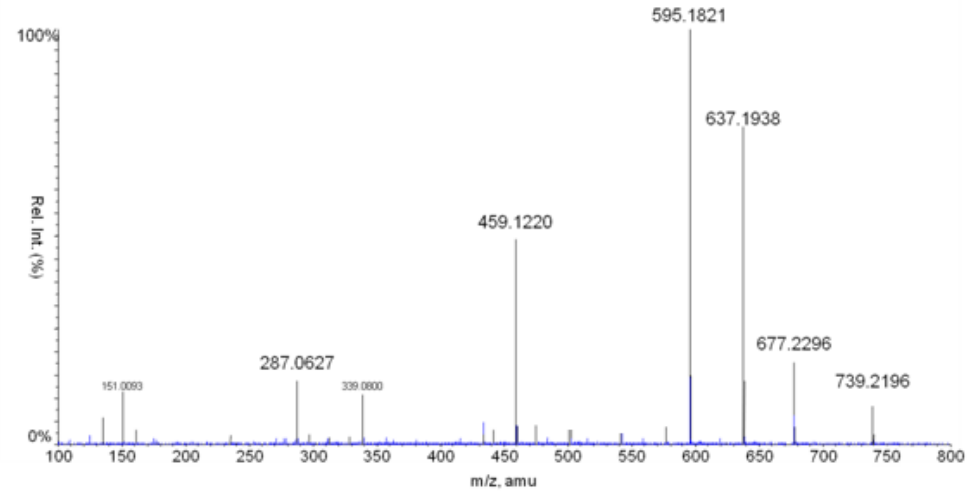

Figure 9 Low energy CID-QqTof-MS/MS (CE 30 eV) of the precursor deprotonated molecule obtained from compound 1

The product ion observed at m/z 595.1821, was formed by the elimination of 3-hydroxy-3-methyl glutaryl moiety from the precursor deprotonated molecule $[(M-C_6H_8O_4)-H]^-$. The product ion at m/z 595 corresponds to the deprotonated molecular mass of neoeriocitrin; this may confirm that the compound **1** is its HMG-conjugate.

The product ion at m/z 677.2296 is related to the formal loss of CO_2 and water from the deprotonated molecule $[(M-CO_2-H_2O)-H]^-$; the product ion at m/z 637.1938 corresponds to $[(M-C_4H_6O_3)-H]^-$; and the product ion at m/z 287.0627 was assigned as ($[(M-Rha-Glc-HMG)-H]^-$), which was the aglycone ion moiety Y_0^- (Figure 10).

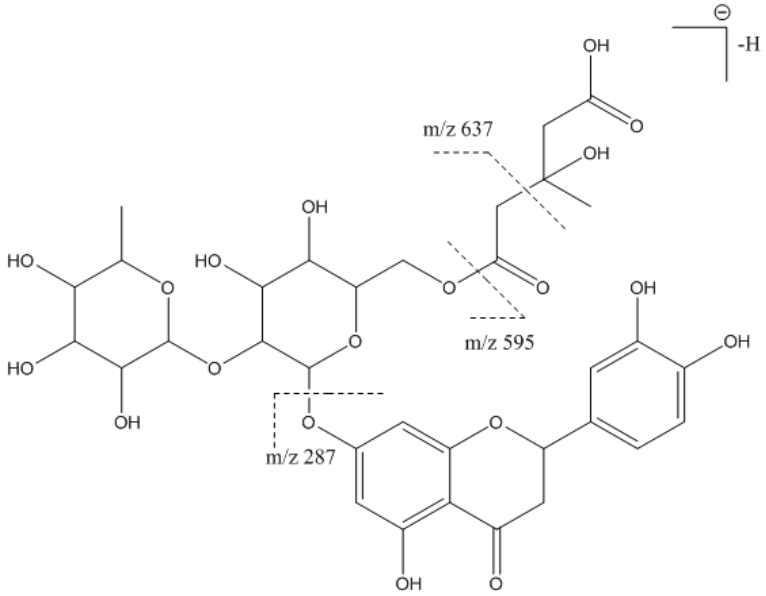

Figure 10 Main product ions formed by the product ion scan (- ion mode) of the precursor deprotonated molecule obtained from compound 1

Compound **1** showed a fragmentation pattern similar to that already known flavanones HMG-conjugates. The figure 11 displays the major fragmentation pathways.

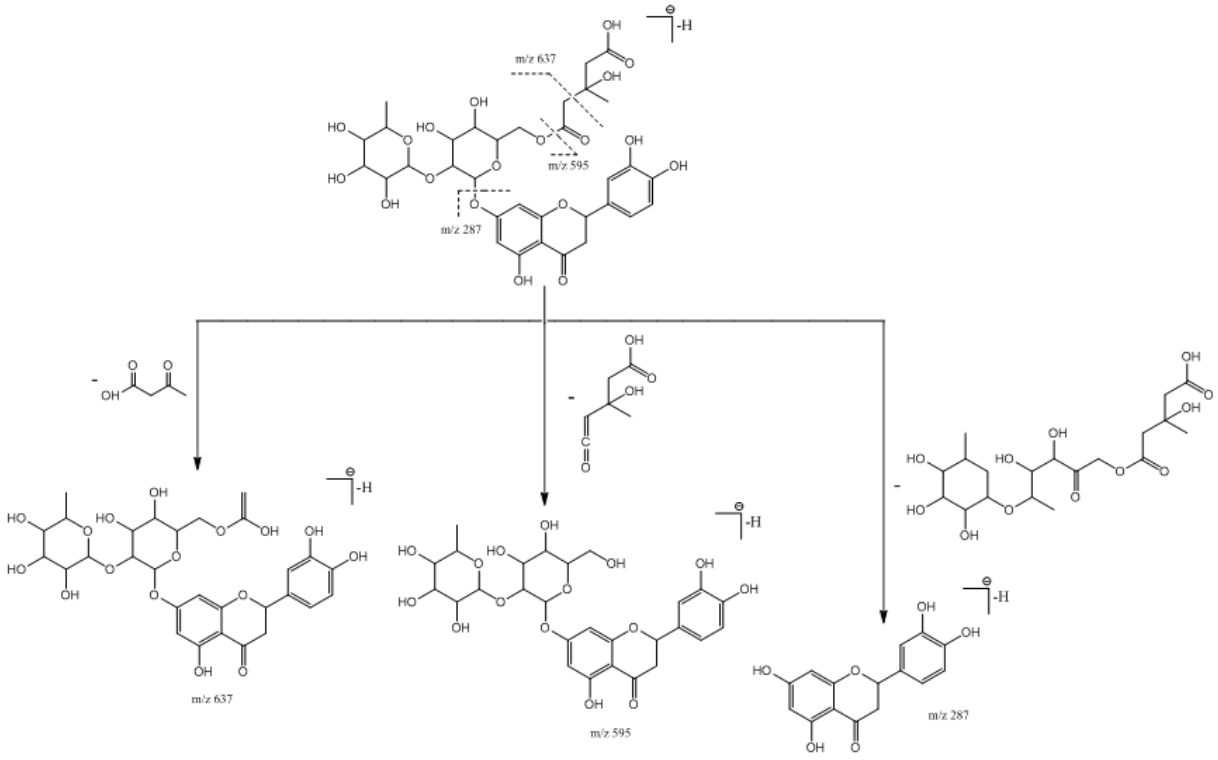

Figure 11 Proposed fragmentation pathways observed for the MS/MS spectrum of the selected deprotonated compound 1 at m/z 739

In order to confirm the proposed structure of this new HMG flavanone glycoside, hydrolysis reactions were conducted. Pure compound were submitted to basic hydrolysis to confirm the glutaric ester linkage. The compound was treated at ambient temperature with a 0.1 M sodium hydroxide solution. Reaction products were identified by HPLC-UV/MS analysis (Figure 12).

After one hour, LC-UV chromatogram displayed the almost complete disappearance of HMG-flavonoid signal and the formation of a product with deprotonated molecular ion at m/z 595. Its retention time is the same of the neoeriocitrin standard.

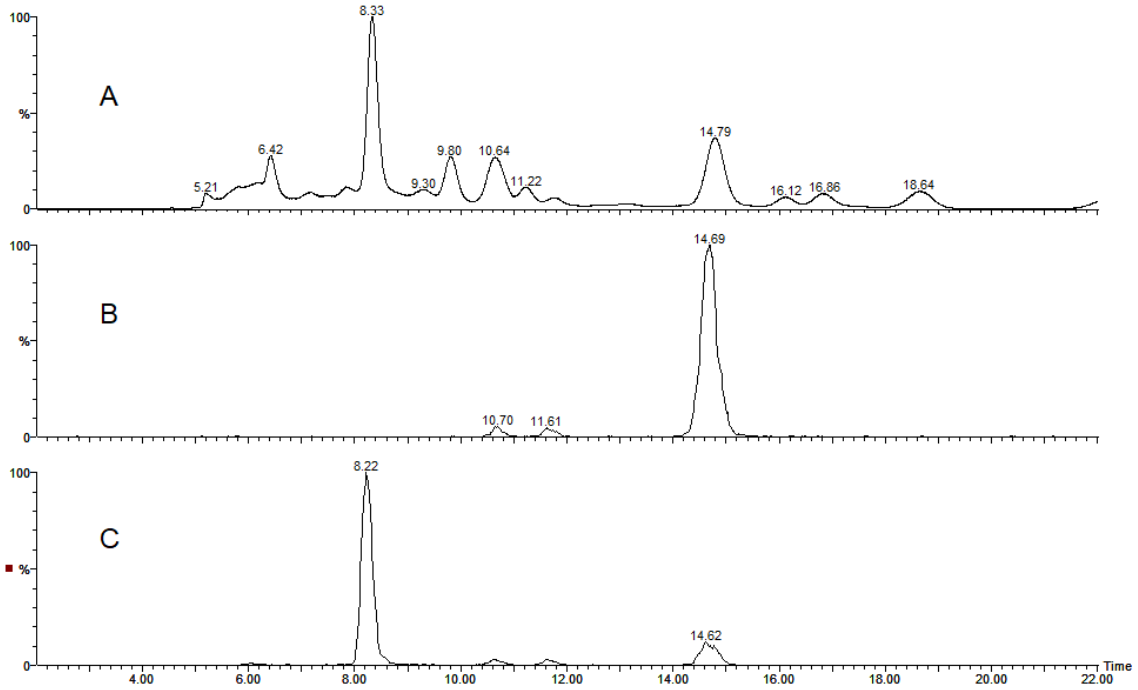

Figure 12 A-LC-UV chromatogram of reaction products after 1 hour; B-extracted ion chromatogram of the ion at m/z 739; C-extracted ion chromatogram of the ion at m/z 595

The presence of neoeriocitrin aglycone in the molecule was also confirmed by enzymatic hydrolysis. This reaction was carried out on the unknown flavonoid solution in the presence of *hesperidinase* and monitored by HPLC-UV/MS analysis at the same condition of the first experiment. LC-UV/MS chromatogram (Figure 13) highlighted the deprotonated molecular ion at m/z 593 (first peak), which corresponds to the starting molecule deprived by the rhamnose sugar, after the hydrolysis of glycosidic bond Rha-Glu.

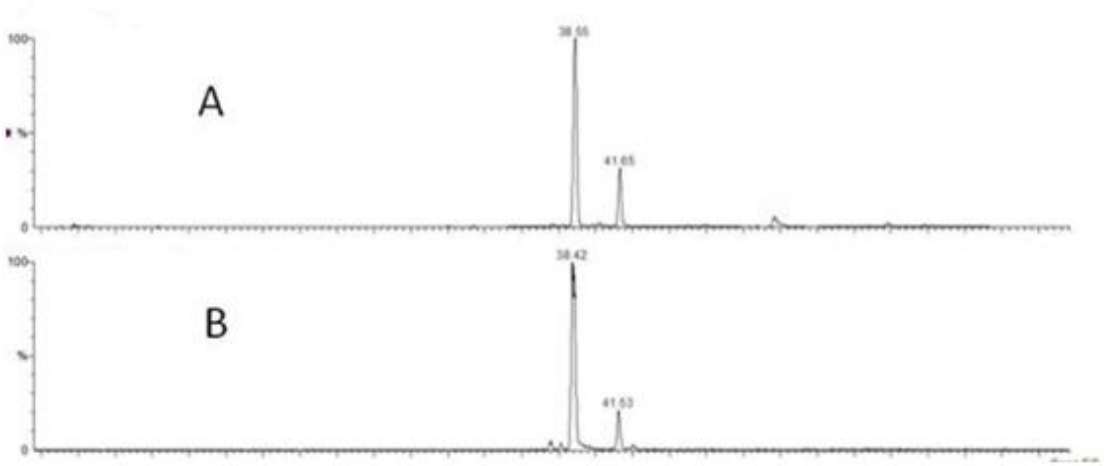

Figure 13 A-UV-chromatogram of hydrolysis products; B-extracted ion current of the ion at m/z 593

After 24 hours of reaction, the predominant product is the aglycone, shown by the presence of the peak of its deprotonated ion at m/z 287.

Since the HPLC semipreparative procedure allowed to obtain a high amount of the pure compound, it was possible to perform high resolution NMR experiments. NMR data provided evidence of the existence of two stereoisomers of the peripolin in bergamot juice. As all the flavanones, peripolin presents the unique characteristic of possessing a chiral center at the C-2 position (Figure 14), which potentially leads to the existence of two stereoisomeric forms. The existence of stereoisomeric form of flavanones was observed also in other natural compounds. (17)

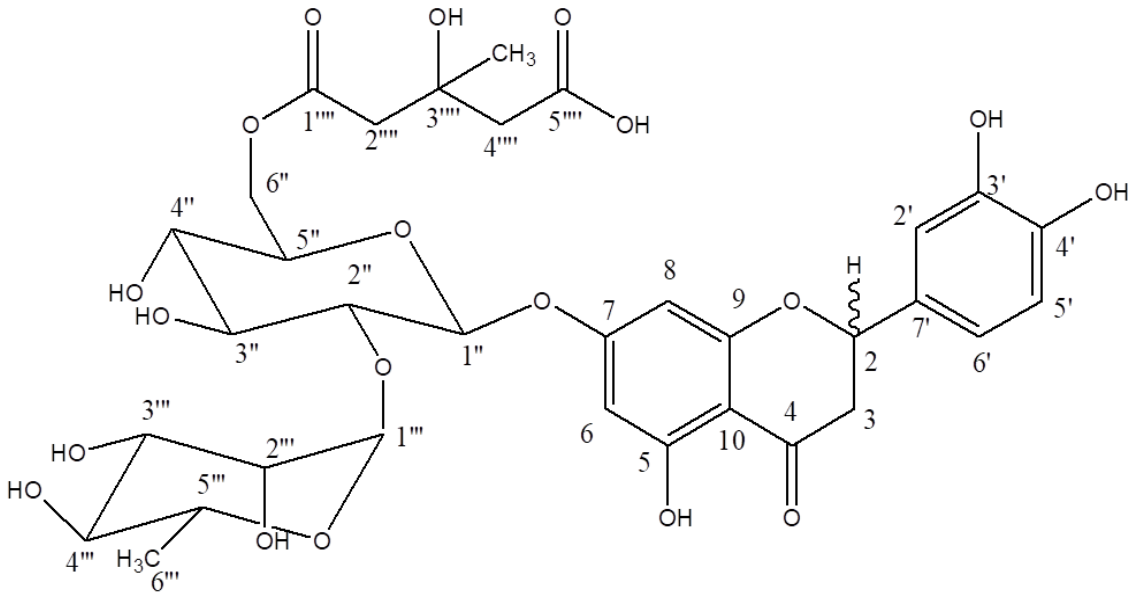

Figure 14 Molecular structure of peripolin highlighting the chiral center at the C-2 position

^{1}H NMR experiment has provided a spectrum (Figure 15) in which it can be observed the splitting of particular signal. The splitting highlights the presence of the two diastereoisomers, which probably are two epimers, differing in the configuration of the stereogenic center, at C-2.

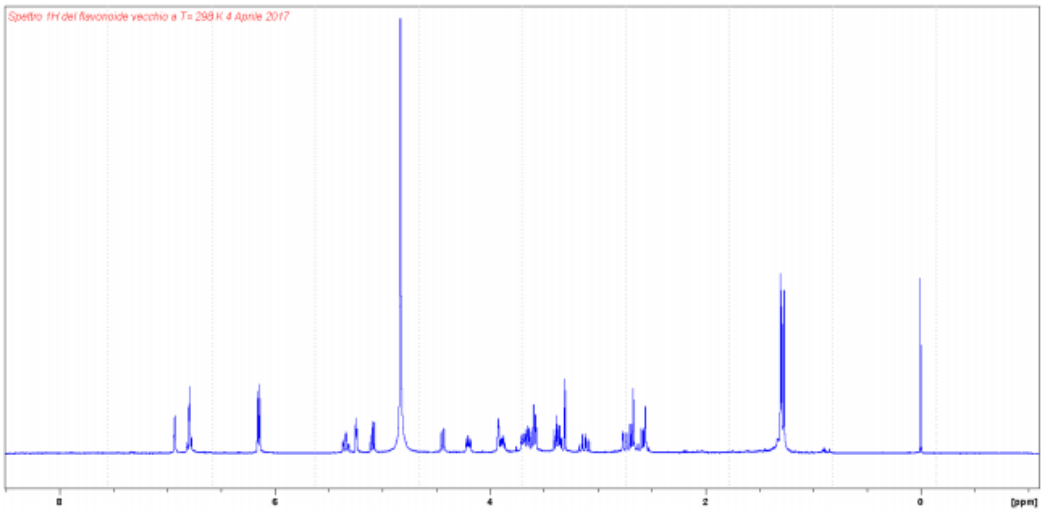

Figure 15 ^{1}H NMR spectrum of peripolin

The figures 16 shows a particular of the NMR spectrum in the chemical shift range δ_H 3.35- 3.40, in which it can be observed the signals of the protons H-4'' and H-4'''. Each signal shows the splitting pattern, which can be detected also for the protons H-3'' and H-3''', H-2'' and H-2'''.

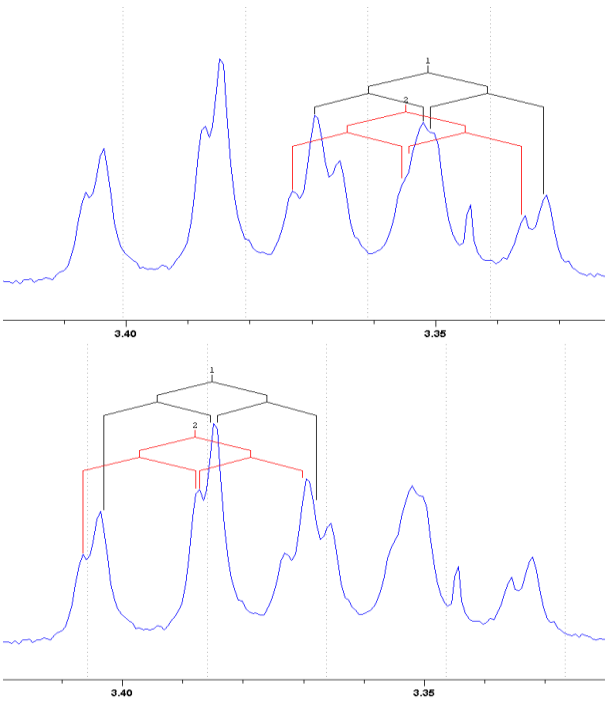

Figure 16 Signals of protons H-4'' and H-4'''

The protons of the sugar rings were assigned by 2D NMR experiments.

The ^{1}H and ^{13}C NMR data were summarized in the table 2.

Table 2 ^{1}H and ^{13}C NMR spectroscopic data for peripolin

Position	δ_H (J_{H-H} in Hz)	δ_C (J_{C-H} in Hz)
6’’’’	1.26 s	27.81, CH3, q (126.98)
6’’’	1.29 d (6.50)	18.24, CH3, q (126.28)
4’’’’	2.52-2.60 m	46.37, CH2, t (123.65)
2’’’’	2.63- 2.71 m	44.37, CH2, t (124.17)
3b	2.74 dd (17.3, 2.60)	44.11, CH2, t (131.01)
3a	3.13 dd (17.56, 12.90)	
4’’	3.35 dd (9.80, 8.00)	71.70, CH, d (142.93)
4’’’	3.40 dd (9.80, 9.65)	73.95, CH, d (144.16)
3’’	3.58 dd (9.48, 8.00)	72.20, CH, d (146.26)
3’’’	3.59 dd (3.20, 9.65)	
2’’	3.64 dd (7.63, 9.48)	78.86, CH, d (142.06)
5’’	3.68 ddd (9.80, 2.07, 7.09)	75.43, CH, d (142.05)
5’’’	3.87 qd (6.52, 9.80)	70.02, CH, d (145.22)
2’’’	3.92 dd (1.60, 3.20)	78.95, CH, d (147.72)
6b’’	4.20 dd (11.90, 7.09)	64.55, CH2, t (148.38)
6a’’	4.43 dd (11.90, 2.07)	
1’’	5.09 d (7.63)	99.29, CH, d (158.27)
1’’’	5.24 d (1.60)	102.54, CH, d (171.70)
2	5.34 dd (12.80, 2,80)	80.76, CH, d (147.32)
6	6.14 d (2.08)	97.97, CH, d (137.17)
8	6.15 d (2.08)	96.82, CH, d (142.93)
5’	6.76-6.84 m	116.34, CH, d (158.27)
6’		119.35, CH, d (160.19)
2’	6.93 d (1.80)	114.79, CH, d (155.40)

Structural characterization of compound 2: glucosyl-melitidin

Structural characterization of the second unknown flavonoid was carried out by the same procedure used for compound **1**. The proposed structure is reported in figure 17.

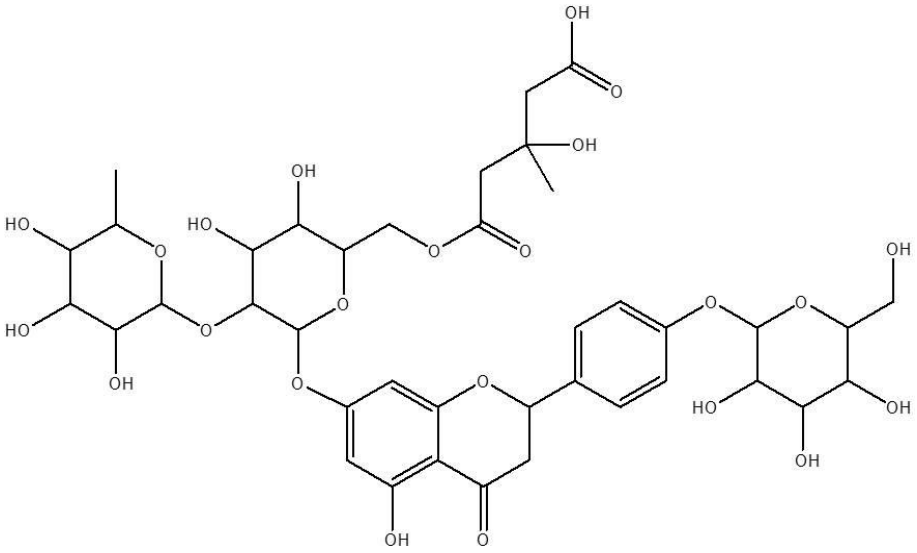

Figure 17 Proposed structure of compound 2

The figure 18 shows the ESI-QqTOF (+ ion mode) which indicate the presence of $[M+NH_4^+]$ adduct ion and the protonated molecule $[M+H^+]$, at m/z 904 and m/z 887, respectively.

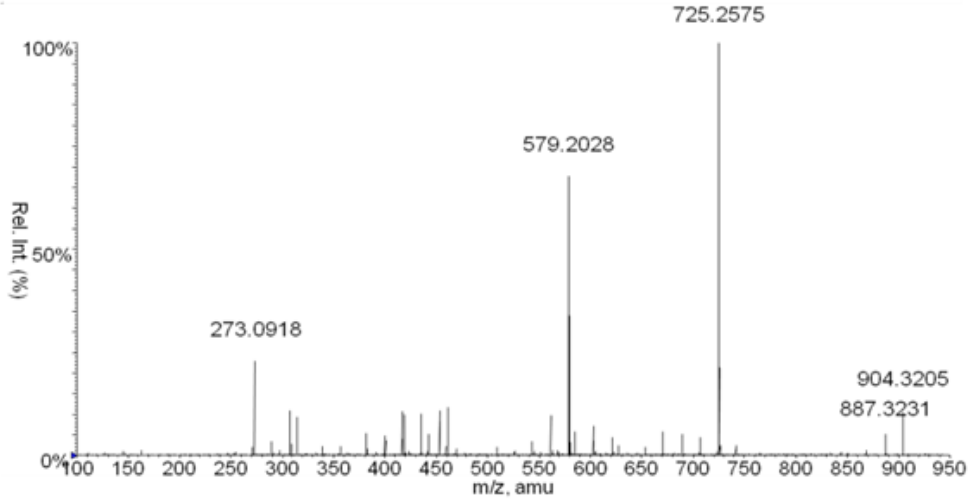

Figure 18 ESI-QqTOF-MS/MS (+ ion mode) of compound 2

The product ion at m/z 725.2575 is originated by the loss of glucose moiety $[(M-Glu)+H]^+$ and, formally, corresponds to the protonated molecule of the already known HMG – flavonoid melitidin. The product ion at m/z 579.2028 represents the ion resulting from the subsequent loss of rhamnose moiety. These product ions confirm that the glucose and rhamnose moieties are linked to the external part of molecule. The Figure 19 displays the proposed fragmentation routes for the formation of the ions at m/z 725 and m/z 579.

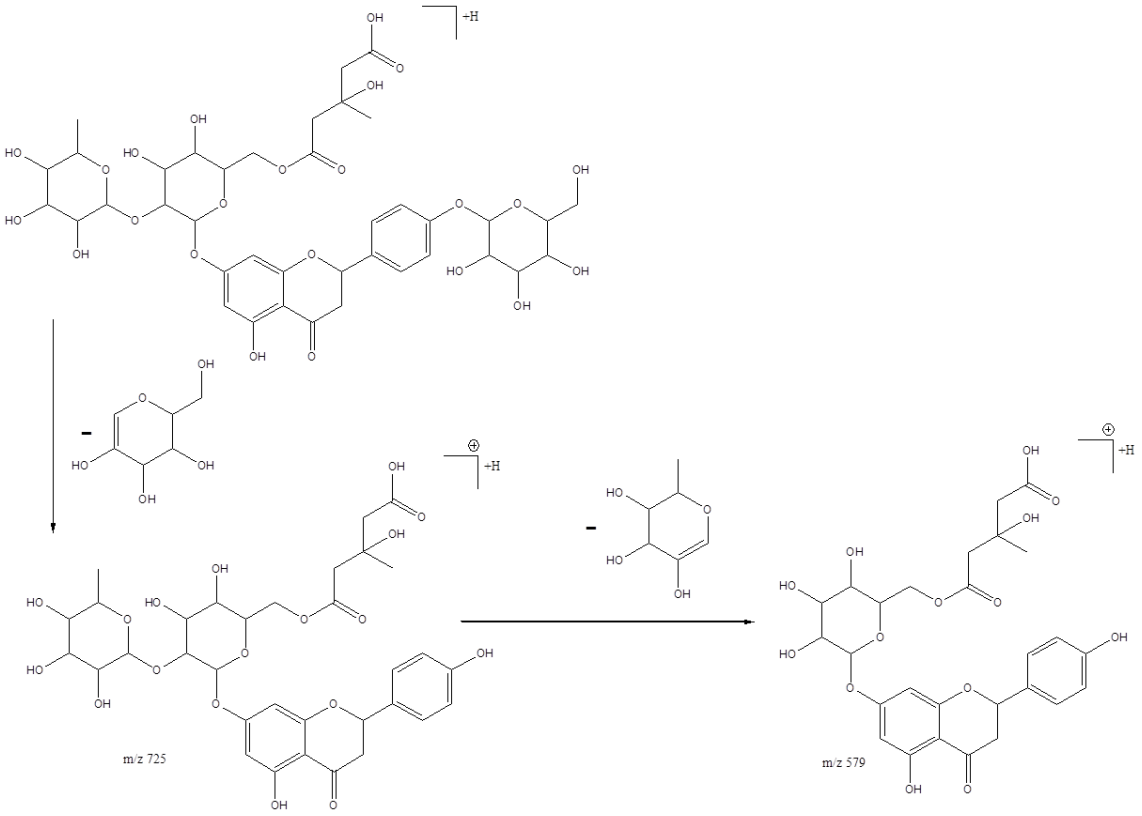

Figure 19 Proposed fragmentation pathways observed for the ESI (+) MS/MS spectrum of the compound 2

Finally, the mass spectrum showed the protonated ion of the aglycone moiety Y_0^+ at m/z 273.0918.

The low-energy CID-MS/MS of the deprotonated molecule at m/z 885 shows a similar fragmentation pattern of Melitidin (Figure 20).

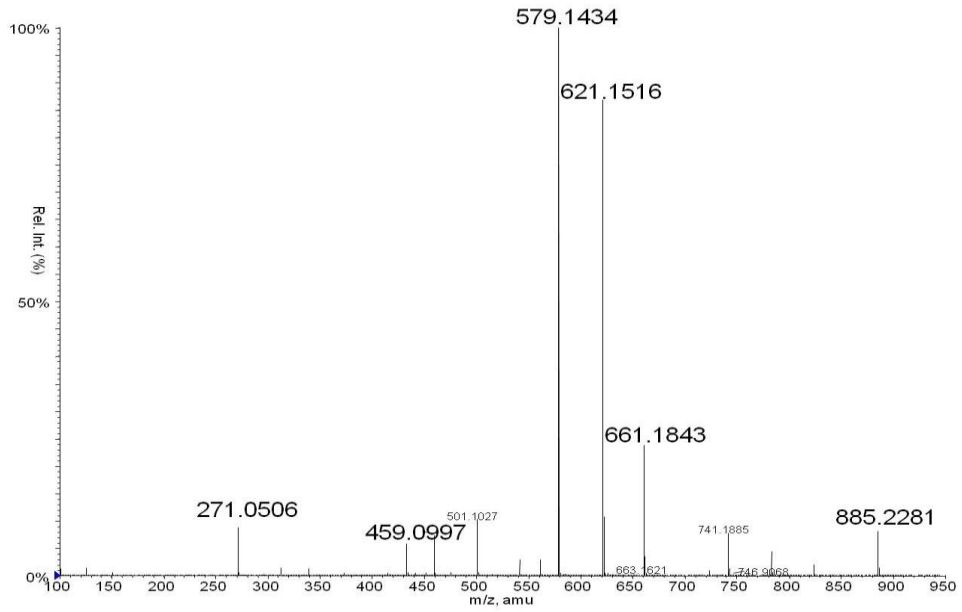

Figure 20 ESI-QqTOF-MS/MS (- ion mode) of compound 2

The product ion at m/z 621.1516 is assigned to $[(M-C_{10}H_{16}O_8)-H]^-$ and arises from the cross-ring cleavage of the glucose and the loss of 3-hydroxy-3-methyl glutaryl moieties; the base peak at m/z 579.1434 results from the loss of the terminal glucose moiety and from the cleavege of Glu-HMG bond $[(M-C_{12}H_{18}O_9)-H]^-$; the product ion at m/z 459.0997 is generated by the loss of terminal glucose unit and from the cross-ring cleavage of internal glucose moiety. Finally the product ion at m/z 271.0595 is related to the deprotonated molecule of naringin, the aglycone moiety.

In figure 21, the structure of product ions in negative ion mode MS/MS experiment are shown.

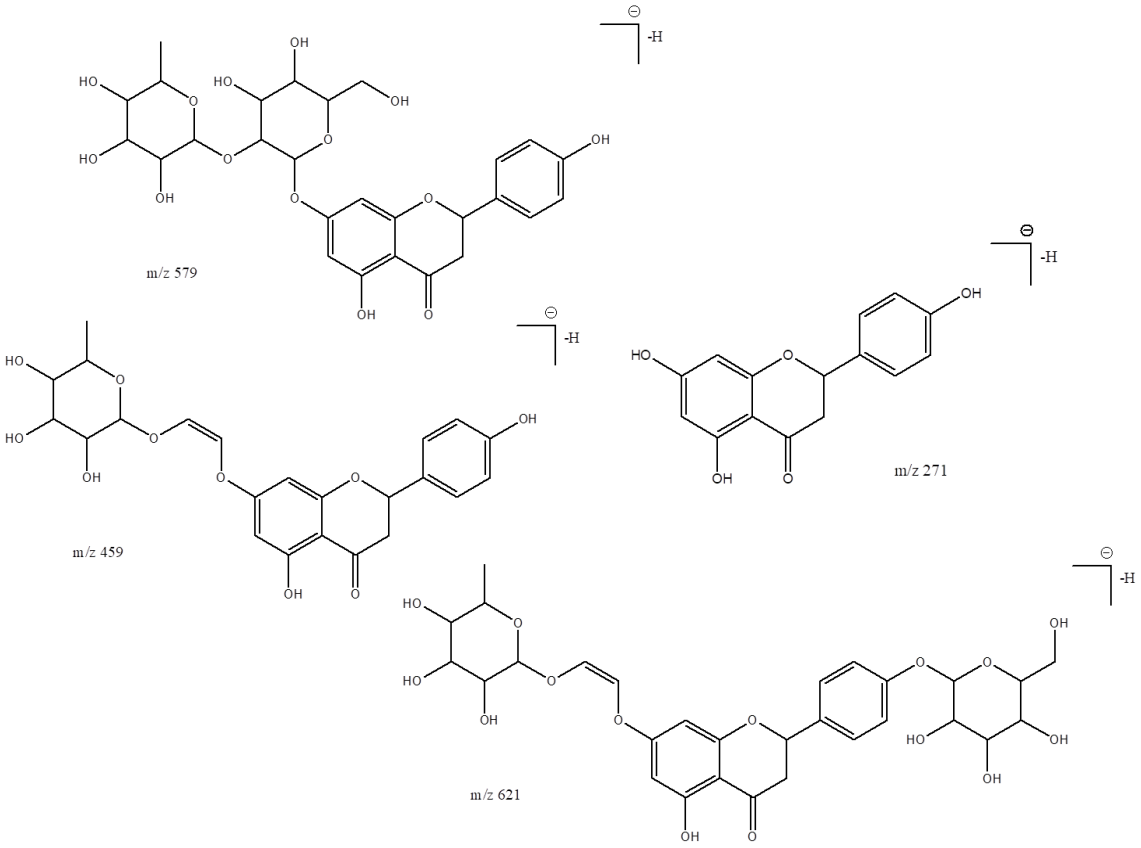

Figure 21 structure of the product ions observed in the ESI (-) MS/MS spectrum of the compound 2

Molecular structure of compound **2** is similar to that of Melitidin, except for the presence of one more glucose moiety.

In order to confirm the structure and especially the position of glucose in the molecule, the pure compound was submitted to enzymatic hydrolysis with β-glucosidase, which catalyzed the hydrolysis of glycosidic bonds to terminal residues in beta-D-glucosides and oligosaccharides.

After 2 hours, LC-UV/MS chromatogram highlighted the formation of the hydrolytic product, identified by the ion at m/z 723 corresponding to the deprotonated molecule of Melitidin. This product confirmed that the glucose moiety is linked externally to the molecule (Figure 22).

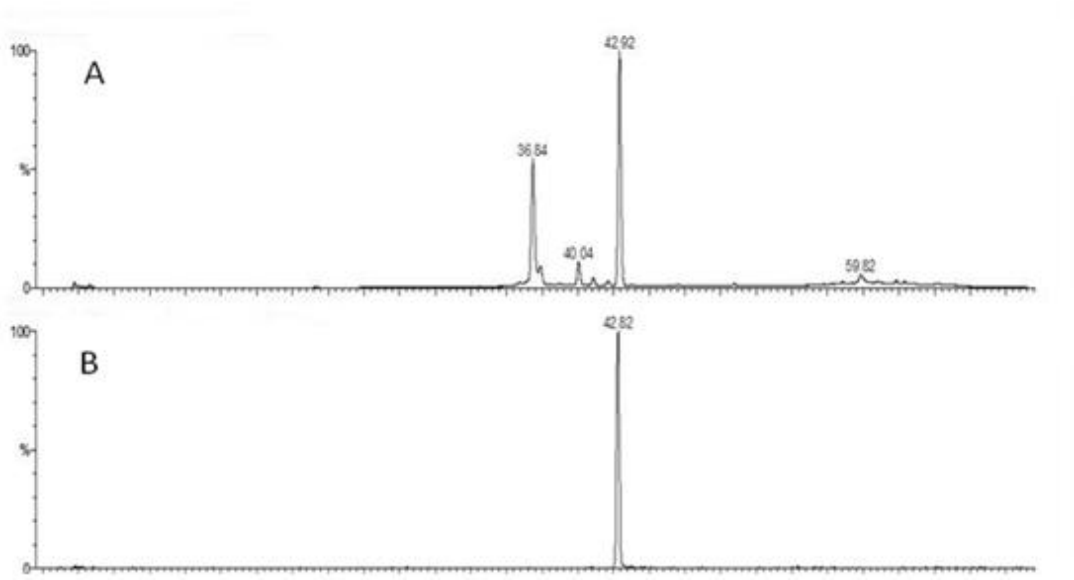

Figure 22 A- LC-UV chromatogram of hydrolysis product, B- extracted ion current of the ion at m/z 723 (rt 42.82)

The Figure 23 displays the hydrolysis products obtained by the experiment with *hesperidinase*.

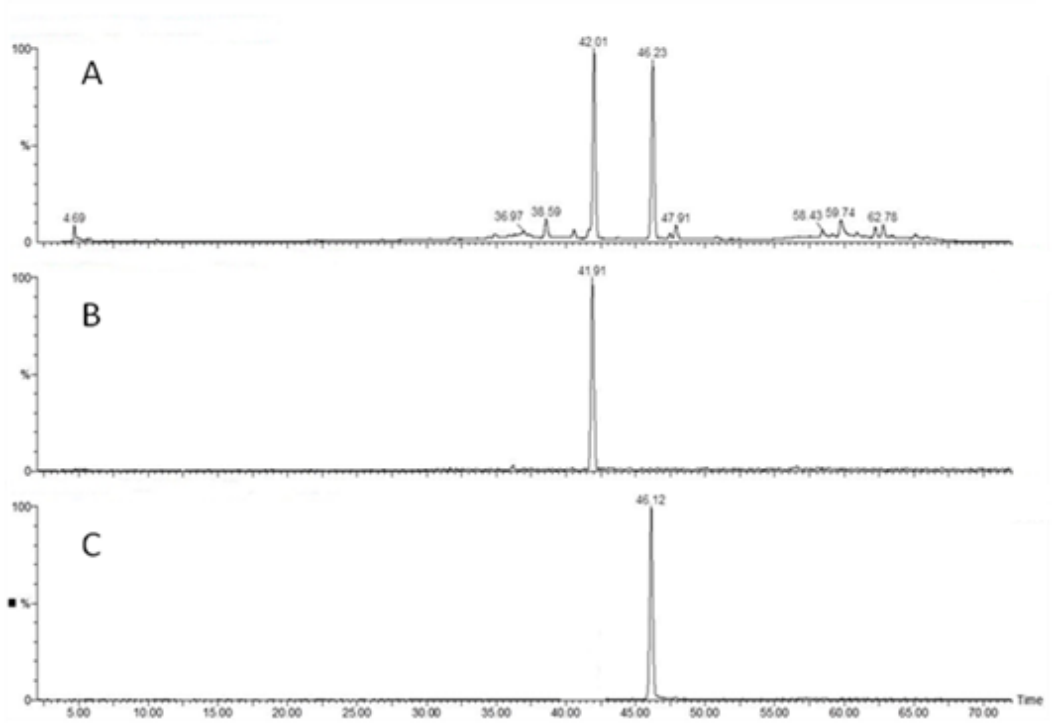

Figure 23 LC-UV chromatogram of reaction products; ion at m/z 577 (XIC rt 42.91) and ion at m/z 271 (XIC rt 46.12)

After 4 hours two chromatographic peaks were observed, corresponding to compounds with a deprotonated molecular ion of 577 amu and 271 amu. The first peak was related to

the starting molecule less a rhamnose and glucose moiety; the second to naringenin aglycon moiety. After 24 h of reaction, the predominant product was the aglycone (rt 46.12).

In this case, it was not possible to perform NMR experiments because the amount of this flavonoid collected from bergamot juice was very low, due to the difficulty of the purification procedure.

4. CONCLUSIONS

The combined use of HLPC separation, assisted by simultaneous UV and mass spectrometric detection has allowed the identification and isolation of two new 3-hydroxy-3-methylglutaril flavanone glycosides from bergamot juice. The structural characterization was performed by high-resolution tandem mass spectrometry experiments in combination with hydrolysis reactions.

REFERENCES

1. R. Tsao, Z. Deng. (2004). Separation procedures for natyrally occurring antioxidant phytochemicals. *J Chromatog B*, 1-2, 85-99

2. Berhow M.A. (2002). Modern analytical techniques for flavonoid determination. *Flavonoids in Cell Function* 61-62

3. L. Z. Lin , J. M. Harnly (2007). A Screening Method for the Identification of Glycosylated Flavonoids and Other Phenolic Compounds Using a Standard Analytical Approach for All Plant Materials. *J. Agric. Food Chem.*, 55 (4), pp 1084–1096

4. Stalikas C.D. (2007). Extraction, separation and detection method for phenolic acids and flavonoids *J. Sep. Sci*. 30, 3268 – 3295

5. de Rijke E., Out P., Niessen W.M.A., Ariese F., Gooijer C., Brinkman U. A. Th. (2006). Analytical separation and detection methods for flavonoids. *J Chromatog A*, 1112 31–6

6. Dugo, P., Cacciola, F., Kumm, T., Dugo, G. & Mondello, L. (2008). Review. Comprehensive multidimensional liquid chromatography: Theory and applications. *J Chromatog A*,**1184**, 353-368.

7. Dugo, P., Cacciola, F., Herrero, M., Donato, P. & Mondello, L. (2008). Use of partially porous column as second dimension in comprehensive two-dimensional system for analysis of polyphenolic antioxidants. *Journal of Separarion Science*, **31**, 3297-3308

8. T.J. Mabry, K.R. Markham, M.B. Thomas (Eds.), The Systematic Identification of Flavonoids, Springer-Verlag, New York, NY, USA, 1970.

9. Cuyckens, F. & Claeys, M. (2002). Optimization of a liquid chromatography method based on simultaneous electrospray ionization mass spectrometric and ultraviolet photodiode array detection for analysis of flavonoid glycosides. *Rapid Communications in Mass Spectrometry,* 16, 2341-2348.

10. De Rijke, E., Out, P., Niessen, W.M.A., Ariese, F., Gooijer, C. & Brinkman, U.A.Th. (2006). Review –Analytical separation and detection methods for flavonoids. *J of Chromatog A*, 1112, 31-63.

11. Harnly, J.M., Bhagwat, S. & Lin, L.-Z. (2007). Profiling methods for the determination of phenolic compounds in foods and dietary supplements. *Analytical and Bioanalytical Chemistry*, **389**, 47-61.

12. Domon, B. & Costello, C.E. (1988). A systematic nomenclature for carbohydrate fragmentations in FAB MS/MS spectra of glycoconjugates. *Glycoconjugate Journal*, 5, 397-409.

13. Abad-Garcia, B., Berreuta, L.A., Garmon-Lobato, S., Gallo, B. & Vicente, F. (2009). A general strategy for the characterization of phenolic compounds in fruit juices by high-performance liquid chromatography with diode array detection coupled to electrospray ionization and triple quadrupole mass spectrometry. *Journal of Chromatography A*, **1216**, 5398-5415.

14. Cuyckens, F. & Claeys, M. (2004). Mass spectrometry in the structural analysis of flavonoids. *Journal of Mass Spectrometry,* **39**, 1-15.

15. Hvattum, E. & Ekeberg, D. (2003). Study of the collision-induced radical cleavage of flavonoid glycosides using negative electrospray ionization tandem quadrupole mass spectrometry. *Journal of Mass Spectrometry*, **38**, 43-49.

16. Ma, Y.L., Vedernikova, I., Van den Heuvel, H. & Claeys, M. (2000). Internal glucose residue loss in protonated *O*-diglycosyl flavonoids upon low-energy collision-induced dissociation. *Journal of the American Society for Mass Spectrometry,* 11, 136-144.

17. F. Maltese, C. Erkelens, F. van der Kooy, Y. H. Choi, R. Verpoorte. (2009) Identification of natural epimeric flavanone glycosides by NMR spectroscopy. *Food Chemistry* 116, 575-579

II. PREPARATION OF EXTRACTS ENRICHED IN HMG-FLAVONOIDS

1. INTRODUCTION

The use of bioactive compounds in different commercial sectors such as pharmaceutical and food industries denotes the need to develop an appropriate method to extract these active components from plant materials, or to prepare extracts enriched with different active principals. (1,2) Isolation of compounds from natural sources is considered the most important, difficult and time-consuming step in natural product research and development. However, to evaluate the activity of a single natural compound or phytocomplex containing different compounds, it is necessary to perform in vitro and in vivo studies and, possibly, clinical trials. For these purpose, it is important to develop a green methodology to purify the active principles. Three major solutions were identified to design and demonstrate green process on laboratory and industrial scale to approach an optimal consumption of raw materials, solvents and energy: improving and optimization of existing processes; using non-dedicated equipment; and innovation in processes and procedures but also in discovering alternative solvents. Extraction and purification procedure, according to the principles of green chemistry, are new concepts to protect both the environment and consumers, and in the meantime enhance competition of industries to more ecologic, economic and innovative processes. (1-4)

This section of the thesis deals with development of a new food-grade methodology to prepare enriched extracts containing 3-hydroxy-3-methyl glutaryl flavanones (HMG-flavonoids) from bergamot fruit (Citrus bergamia Risso) and leaves, or bitter orange leaves (Citrus aurantium L.), or chinotto leaves (Citrus Myrtifolia). The methodology allows to obtain HMG-flavonoids phytocomplexes with different purity degrees. It’s based on the absorption/desorption of flavonoid fraction on two polymer resins, both food grade, using green solvents, as ethanol 96% and water. The developed method can be seen as a filtration process through the resins, being different respect to a classic separation procedure. Thanks to the chemical properties of polymer materials, the extract obtained by the absorption on the first resin, contains up to 40% HMG-flavonoids, while the second polymer resin allows to purify up to 95%.
The following procedure will be not described in details, due to non-disclosure restrictions.

2. MATERIALS AND METHODS

2.1 Chemicals

HPLC grade solvents were purchased from Carlo Erba (Milan, Italy). Standard flavonoids were purchased from Extrasynthese (Gnay, France) and other chemicals were from Sigma-Aldrich (St. Louis, MO).

2.2 Plant materials

Bergamot fruits and leaves were furnished by Unionberg Association, Condofuri Marina (RC, Italy), and stored at ambient temperature. Sour orange and chinotto leaves were collected in Cosenza (Italy).

2.3 Purification process

2.3.1 Preparation of starting materials

Bergamot, sour orange and chinotto leaves were dried and stored at -20°C. After grinding of the dried leaf material, an appropriate amount was extracted for 1h with distilled water or drinking water. Water extracts were freeze-dried by lyophilization process.

Bergamot juice was obtained by squeezing the fruit, filtered and stored at -20°C; while the pulp and the squeezing residues were extracted with water in the same condition of leaves, and after lyophilization the final extracts were stored at -20°C.

2.3.2 Developed methodology

The process consisted of two steps of purification. In the first step, an macroporous resin was used. The starting materials (bergamot juice, or a water extract of bergamot fruit, or a water extract of bergamot leaves, or sour orange leaves, or chinotto leaves) was absorbed through contact by the resin. The time of contact can ranged from 30 min to 1h. After absorption, the resin was filtered to eliminate the solution containing non-absorbed constituents, and then washed with water. Finally, the adsorbed compounds (glycosilated flavonoids) were eluted by food-grade ethanol (95-96% ethanol). The solution was evaporated under vacuum and lyophilized to obtained a dried extract.

The next purification step was characterized by the use of a second resin as absorbent material. The extract obtained by the first resin was dissolved in acid water, and through

the contact with the resin, flavonoids fraction was absorbed. The resin was washed by water to remove flavonoids non-HMG conjugates, and finally washed with a mixture of basic ethanol. The figure 1 shows the workflow of the purification procedure.

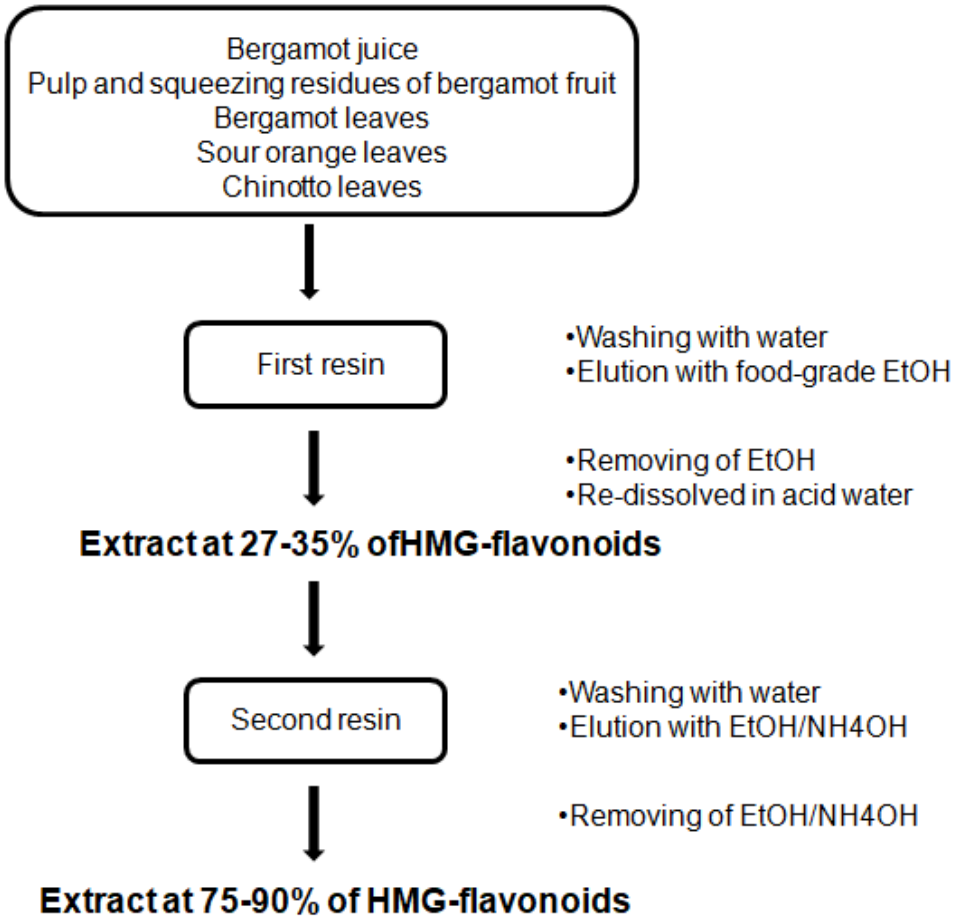

Figure 1 Layout of purification process

2.4 HPLC-UV/MS analysis

Analysis of extracts and purification products were performed by HPLC-UV/MS system, using a Waters Fraction-Lynx instrument (Milford, MA) equipped with a ZMD mass spectrometer and a 486 UV detector. The chromatographic separation was carried out using a 250x4.6 mm 5µm reversed-phase C_{18} Luna – Phenomenex column at a flow rate of 1 ml/min. The run time was 70 min and the gradient was performed using HCOOH 0.1% in water (solvent A) and MeOH (solvent B) as eluting phase. The solvent run was the following: isocratic elution 80% A for 7 min; linear gradient from 80% A to 40% A in 33 min; isocratic elution 40% A for 5 min; linear gradient from 40% A to 20% A in 5 min; isocratic elution 20% A for 7 min; linear gradient from 20% A to 80% A in 5 min;

equilibration of the column for 8 min. For each analysis, a solution of 1000 mg/L of extracts and purification products was prepared.

3. RESULTS AND DISCUSSION

The aim of this work was to develop a new process to obtain phytocomplex containing 3-hydroxy-3-methyl glutaryl flavanones, for applications in clinical studies. For this purpose, a *food-grade* methodology was set up. The purification procedure was based on the use of polymeric resins. Several research studies has demonstrated their efficiency in purification of different pharmacologically- natural active principles from plant source. (5) The developed purification method is wholly food–grade, because to the use of only water and ethanol, which are nontoxic solvents. The best condition to purify the compounds of interest were found by varying different variables, i.e. amount of water extracts or bergamot juice, pH value, volume of washing water, volume of eluting solvents and amount of resin employed were studied.

Macroporous polymer, used as the first resin in the purification process, is characterized by the presence of cove on internal surface of its constituent particles, which has allowed the selective absorption of the flavonoid glycosides. The washing step with water was necessary to remove other minor phenolic compounds, such as aminoacids, amines and sugar from the resin surface. The final elution with ethanol has allowed the desorption of flavonoid fraction. The resulting product was obtained with a purity degree ranged from 27 to 40% of HMG-flavonoids, and from 55 to 60% of the other flavonoids, such as neoeriocitrin, naringin and neohesperidin. Therefore, a product containing the whole flavonoid fraction also up to 90% was obtained. In the first step of procedure, it was important the optimization of amount of resin employed, amount of starting material (juice and water extracts), the volume of water for the washing and the volume of ethanol for the final elution. Ethanol removed from product solution could be used again as fresh solvent in a further purification. This is a fundamental aspect, for example, for an industrial procedure. Finally, the amount of the resulting extract depends on the amount and type of starting materials.

In the second step of procedure a polymeric resin was used , which has diverse chemical features than the macroporous resin. Also in this case, the process can be seen as a filtration through the material.

To optimize the purification through this resin, it was necessary also to study the pH value influence, as well as the above mentioned variables. In this case, a strong relationships between the separation efficiency of resin and the pH conditions was demonstrated. The product previously obtained and containing the total flavonoid fraction was re-dissolved in acid water, and the best absorption conditions were found using a pH value ranging from 2 to 3. Also the second resin adsorbs all flavonoid fraction, but the elution with different mixture of water/ethanol has allowed the fractionation of different flavonoid glycosides. In particular, simple flavonoid glycosides were desorbed with a mixture of water/ethanol or also with an appropriate volume of water; while the HMG-conjugates were desorbed using a basic ethanol (food grade). An enriched extract of simple flavonoid glycosides (neoeriocitrin, naringin, neohesperidin, etc) was obtained by first elution with water/ethanol or only water. Second elution has allowed to obtain an extract containing 3-hydroxy-3-methyl glutaryl flavanones with a purity ranging from 70 to 95%.

Bergamot fruit

In bergamot juice, the amount of 3-hydroxy-3-methyl glutaryl flavanones was found ranged from 0,05 to 0,3 %, in addition to the others flavonoid glycosides, other phenolic compounds, sugar etc. The figure 2 displays the UV chromatogram of the bergamot juice.

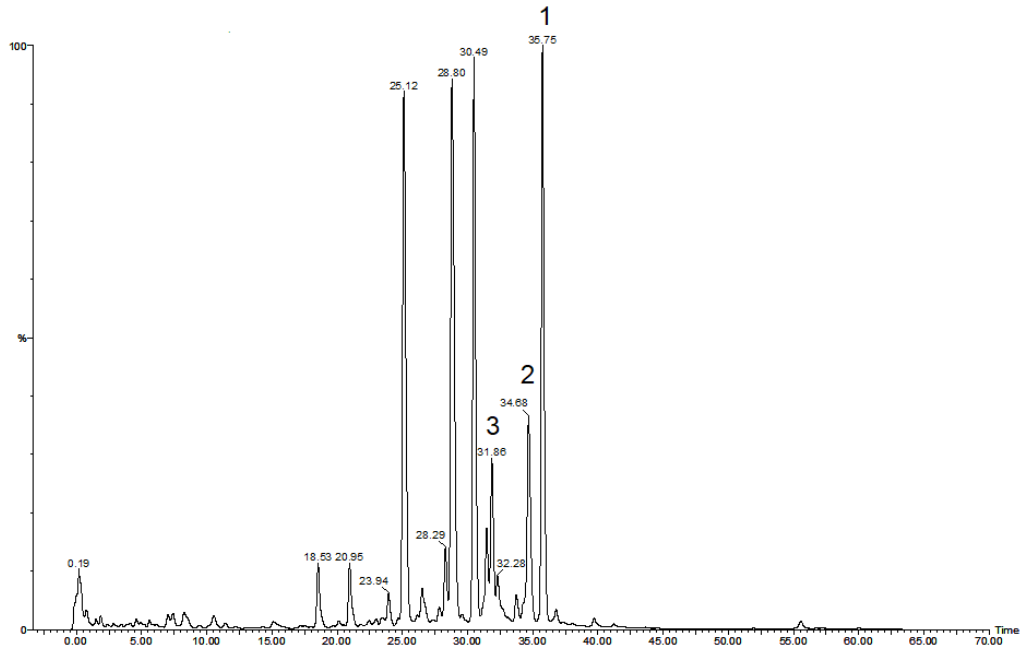

Figure 2 LC-UV chromatogram of flavonoid fraction in bergamot juice; 1- brutieridin, 2- melitidin, 3- peripolin

The purification process using the macroporous resin, allowed to obtain a first extract with a concentration of HMG-flavonoids ranged from 27 to 40%, with other flavonoids at 55-60% (Figure 3). From 400 ml of bergamot juice, 1g of dried extract was recovered.

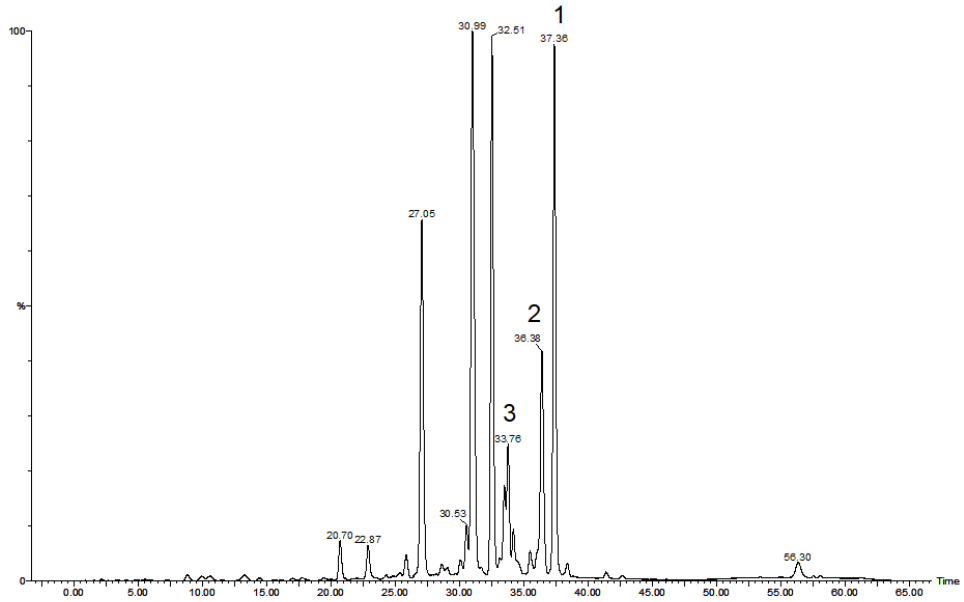

Figure 3 LC-UV chromatogram of the fraction obtained from macroporous resin process

The contact between the dissolved first extract and the second resin permitted to get an extract with a concentration of flavonoids HMG-conjugates ranging from 85-95%. The Figure 4 shows the UV chromatogram of the last extract, in which only the relative signals of the flavonoids HMG-conjugates are present.

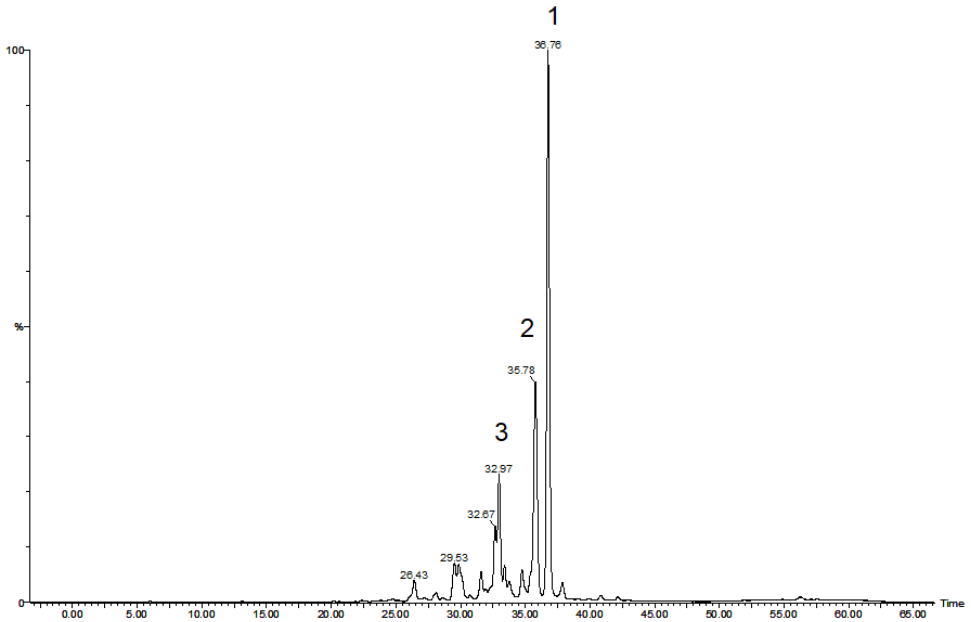

Figure 4 LC-UV chromatogram of HMG-flavonoids fraction obtained from second purification step

The same procedure was developed for the water extracts of pulp and squeezing residues, because also these parts of bergamot fruit are rich in flavonoids and flavonoid HMG-conjugates.
The extract obtained by first purification procedure contains 20-30% of HMG-flavonoids. This fraction was dissolved in acid water and subjected to the second purification step by polymeric material, to obtained a final dried extract with a concentration of HMG-flavonoids ranged from 60% to 75%.

Bergamot, sour orange and chinotto leaves

As already mentioned, crude extracts of citrus leaves were obtained by a simple and fast extraction process, using distilled or drinking water.
The purification procedure was the same for all type of citrus leaves. Crude extract, dissolved in water, was in contact with macroporous polymeric material for 1h, to allows the absorption of flavonoids fraction. After filtration and washing the resin with water, elution with food-grade ethanol has enabled to get an HMG-flavonoid extract with different purity degree, also containing the other flavonoid glycosides.
Crude extract of sour orange leaves contains an higher amount of flavonoids HMG-conjugates, ranging from 5% to 9%. The product obtained by the first purification step contains 35-40% of flavonoids HMG-conjugates, and 50-55% of other flavonoids. The final product obtained with the second purification process has a higher concentration of HMG-flavonoids, ranging from 85% to 95%.
Chinotto and bergamot leaves contain a less amount of these flavonoids than bitter orange leaves. In particular, 3-5% and 4-7% respectively.
For chinotto leaves, the first purification product was obtained at 20-25% of HMG-flavonoid and 60-75% of flavonoid glycosides. After second process, the purity of final product was at 65-70%.
Finally, the first extract of bergamot leaves was characterized by a purity degree in the range 15-20% of flavonoid HMG-conjugates, and 60-65% of the others. The second purification product was obtained at 60-64% of HMG-flavonoids.

Hypocholesterolaemic activity of 3-hydroxy-3-methyl glutaryl flavanones enriched extract form sour orange leaves

As already performed on bergamot enriched extracts (6), it was investigated the hypocholesterolaemic effects of 3-hydroxy-3-methylgutaryl flavanones enriched extract form sour orange leaves, obtained by the developed procedure. The study was conducted at the Department of Pharmacy of the University of Calabria.

Its activity was compared with one of the most used cholesterol lowering statins, i.e. simvastatin, in a rat model. Before the experiment, the animals received the hypercholesterolaemic diet for 3 weeks, and then were divided in three groups. For a time of 4 weeks, the group 1 was the untreated control, the group 2 was treated with simvastatin (60 mg/kg bw/day), and the group 3 with HMG-flavonoids (60 mg/kg bw/day). The results of the study have highlighted that the HMG-flavonoids extract reduced the total cholesterol (TC), triacylglycerols (TG) and low-density lipoproteins levels (LDL), while an increase of the high-density lipoproteins (HDL) content was observed exclusively in the rats treated with the HMG-flavonoid extract. The results of the experiment are shown in figure 5, 6, 7, 8.

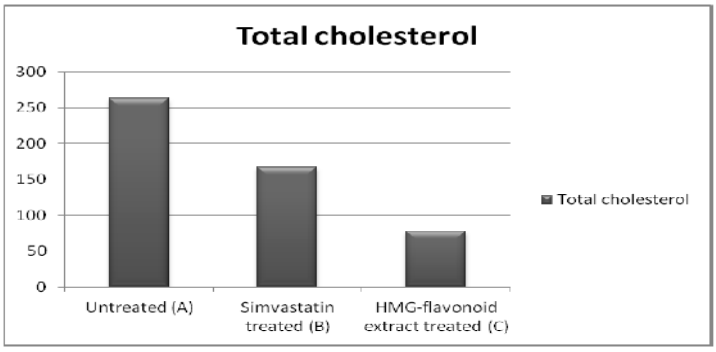

Figure 5 Effect of simvastatin and HMG-flavonoid extract on the Total Cholesterol values

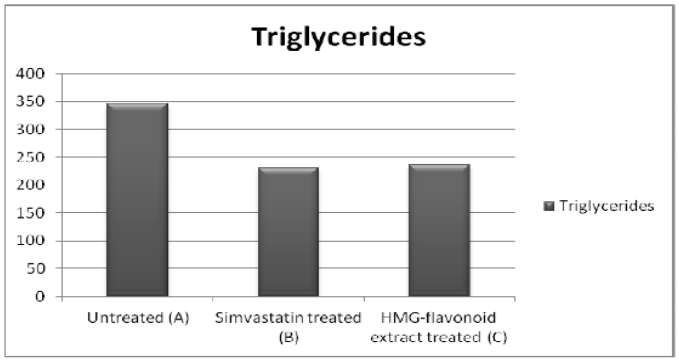

Figure 6 Effect of simvastatin and HMG-flavonoid extract on the Triglycerides values

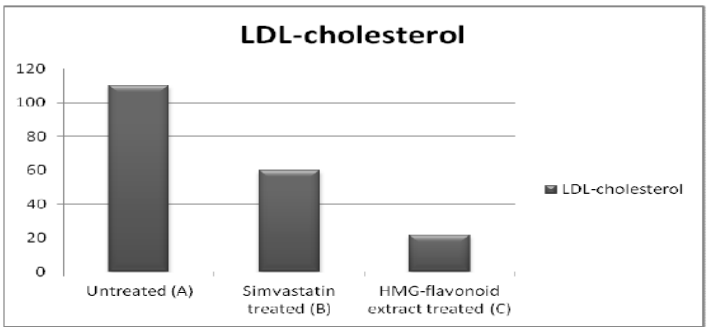

Figure 7 Effect of simvastatin and HMG-flavonoid extract on the LDL-cholesterol values

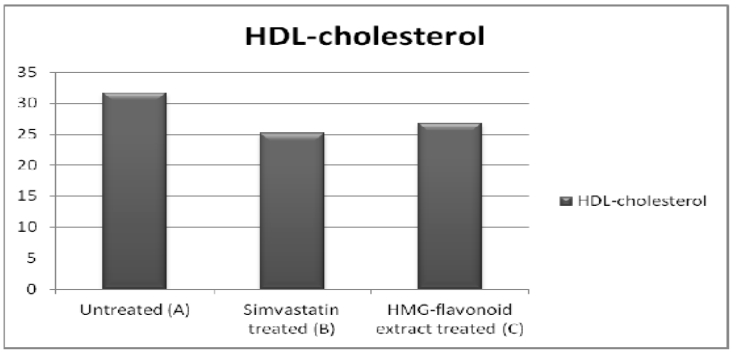

Figure 8 Effect of simvastatin and HMG-flavonoid extract on the HDL-cholesterol values

4. CONCLUSIONS

A new methodology to prepare enriched extracts in 3-hydroxy-3-methyl glutaryl flavanones was developed. For all starting natural matrices, the final enriched extract was obtained with a high purity degree. The use of food-grade adsorbent materials and non toxic solvents, as water and ethanol has allowed to get a safe and high quality extract, which can be used for clinical trials. Therefore, the methodology is a very simple “filtration”, which does not need of any particular equipment.

REFERENCES

1. Z. Liu (2008) Preparation of Botanical Samples for Biomedical Research. *Endocr Metab Immune Disord Drug Targets*; 8(2): 112–121.

2. Koehn FE, Carter GT. (2005) The evolving role of natural products in drug discovery. *Nat Rev Drug Discov;* 4(3):206–220.

3. F. Chemat, J. Strube (2015) Green extraction of natural products: theory and practice. *Green Process Synth* 4: 453–454

4. F. Chemat, M. A. Vian, G. Cravotto (2012). Green extraction of Natural products: concept and principles. *Int. J. Mol. Sci.* 13, 8615-8627

5. J. Li, A. Howard. (2010) Chase Development of adsorptive (non-ionic) macroporous resins and their uses in the purification of pharmacologically-active natural products from plant sources. *Nat Prod Rep* 27(10): 1493-510

6. Di Donna L., Iacopetta D., Cappello A.R., Gallucci G., Martello E., Fiorillo M., Dolce V., Sindona G. (2014). Hypocholesterolaemic activity of 3-hydroxy-3-methyl-glutaryl flavanones enriched fraction from bergamot fruit (Citrus bergamia): ‘‘In vivo’’ studies. *Journal of Functional Food*, 7(1), pp 558-568

III. FUNCTIONAL FOODS: NEW PROCEDURE FOR THE ENRICHEMENT OF FOODSTUFFS IN HYDROXYTYROSOL

1. INTRODUCTION

Over the past few decades, many non-nutrient compounds were identified in different food products. Olive oil for example, is considered a functional food of Mediterranean diet thanks to the presence of minor amounts of active principles, belonging to the nutraceuticals family, such as polyhydroxylated aromatic compounds. In particular, Hydroxytyrosol (3,4 dihydroxyphenilethanol - Htyr) is one of the most important phenolic compound of olive oil, which has a strong antioxidant effect. (1,2) Numerous studies have shown its protection activity against metabolic diseases (3) and digestive disorders (4), its anti-carcinogenic (5), anti-inflammatory (6) and antimicrobial activity (7). Furthermore, Hydroxytyrosol has no-genotoxic and no-mutagenic effects (8); this enhance its potential as nutraceuticals for functional foods. Recently, also the European Food Safety Authority (EFSA) recognized beneficial properties of olive oil phenolic compounds and in particular of Hydroxytyrosol, authorizing a health claim that may be used only for olive oil which contains at least 5 mg of hydroxytyrosol and its derivatives (e.g. oleuropein complex and tyrosol) per 20 g of olive oil (COMMISSION REGULATION (EU) No 432/2012). (9)

Several studies have shown that the concentration of simple phenols, such as hydroxytyrosol increase during the storage of olive oil because of the degradation of their derivatives. In particular, the degradation of oleuropein, its aglycone and oleacin causes a simultaneous increase of hydroxytyrosol. (10-13) However, it is fundamental to remember that during the storage, olive oil is subjected to the lipid oxidation process. This oxidation was recognized as the major problem affecting edible oils because it is the cause of important deteriorative changes in their chemical, sensory, and nutritional properties. Even if the olive oil is considered to be resistant to oxidative degradation due the presence of natural antioxidant such as phenolic compounds, this degradation is also in the case of olive oil, the most important cause of the loss of its nutritional properties. (14)

Therefore, an aged olive oil which has lost its sensory and nutritional features could be used as source of simple phenolic compounds, such as hydroxytyrosol.

According to EFSA health claim, the beneficial effects can be obtained with a daily intake of 20g of olive oil contains at least 5 mg of hydroxytyrosol and its derivatives. Hence,

another effective approach to increase the intake of hydroxytyrosol and its derivatives may be the enrichment of frequently consumed foods with the active principle from olive oil.

The goal of this work was to develop a new methodology to create enriched foods with hydroxytyrosol using aged olive oil as starting material.
The developed method was tested on foodstuffs usually consumed in daily diet, as flour, whole wheat flour and sugar. The methodology can be considered an innovative procedure to enrich foods, because it is not based on the addition of a standard or purified compound, but on the transfer of hydroxytyrosol from oil to food matrices with a simple contact. To remove the fat constituents of oil, the mixture was submitted to supercritical CO_2 fluid extraction, obtaining an enriched food indistinguishable from original food (non-enriched).
Finally, the antioxidant activity of the new food products was evaluated by DPPH test. The results highlighted that the enriched foods have a higher capability for scavenging the free radicals than the original matrices.

2. MATERIALS AND METHODS

2.1 Food Samples

Commercial food products: flour, whole wheat flour, sugar and olive oil were purchased from local market and stored at ambient temperature.

2.2 Chemicals

Analytical grade methanol, ethanol, formic acid and DMSO were supplied by VWR International (Radnor, Pennsylvania, USA). Ultrapure water was obtained from Milli-Q plus system (Millipore, Bedford, MA). Hydroxytyrosol was purchased from Extrasynthese (Genay Cedex, France), and d_2-hydroxytyrosol was obtained in our laboratory by literature method (15)

2.3 Enrichment procedure

24 g of each food sample were mixed with 6 g of olive oil using an agate mortar for 5 minutes to allow a homogeneous dispersion of oil in food matrix. The mixture was subjected to supercritical fluid extraction using carbon dioxide as solvent. The extraction

was carried out by a Spe–ed SFE 2 system (Applied Separation, Allentown, PA), which consisted of a CO_2 tank, a pump to pressurize the gas, an oven with two extractor vessels, a restrictor to maintain a high pressure in the extraction system, and a flow meter for collection of samples. The previously prepared mixture was placed in a 50 ml extractor vessel. Supercritical process was performed in combined mode, with 60 min in closed system at 40°C with a pressure of 100 bar, and 30 min in open system at 40°C and 300 bar. The supercritical CO_2 flow was set at 5 ml/min and the restrictor temperature at 120°C. Food products and olive oil obtained after the process were submitted to LC-MS/MS analysis to verify the hydroxytyrosol transfer from the oil to the selected foodstuffs.

2.4 LC- UV/MS analysis

Sample preparation 1 g of oil sample was extracted with 10 ml of MeOH. *n*-hexane was used to completely remove the lipid fraction from the solution . The methanolic extract was concentrated under vacuum, dissolved in 300 µl of extraction solvent and finally analyzed by HPLC-MS/UV.

For food matrices, 4 g of each sample were extracted with 20 ml of MeOH. After centrifugation, the methanolic extract was directly analyzed.

Instrumental analysis LC-ESI-MS/UV analysis was performed using a Waters FractionLynx system (Milford, MA) working in analytical mode, equipped with a Acquity QDa mass spectrometer and a 2489 UV/visible detector. The chromatographic separation was carried out using a C_{18} reversed-phase column, Luna (250 × 4.6 mm, 5 µm, Phenomenex), at a flow rate of 1 ml/min, injecting a volume of 20 µl. The run time was 70 min, and the gradient built using 0.1% HCOOH in H_2O (solvent A) and CH_3OH (solvent B) as mobile phases. The elution gradient was composed of the following step: isocratic elution 95% A for 7 min; linear gradient from 95% A to 60% A in 33 min, linear gradient from 60% A to 40% A in 5 min, linear gradient from 40% A to 10% A in 5 min; isocratic elution 10% A for 7 min; linear gradient from 10% A to 95% A in 5 min; equilibration of the column for 8 min.

2.5 Mass Spectrometry analysis

Sample preparation Twenty microlitres of a solution of labeled internal standard at 500 mg/L were mixed to 1 g of olive oil. The mixture was homogenized by vortex for three

minutes and then 100 mg were extracted with 900 µl of MeOH. After the extraction the supernatant was opportunely diluted with MeOH and injected into the instrument.

For each food samples, 1 g of sample was added with twenty microlitres of a solution of d_2 – Hydroxytyrosol at 50 mg/L, mixed by vortex for three minutes and finally extracted with 10 ml of MeOH. The extract solution was directly analyzed.

Instrumental analysis LC-MS/MS analysis was carried out using a system from Thermo Scientific composed by a UHPLC Accela pump coupled to a TSQ Quantum Vantage triple-stage quadrupole mass spectrometer (Thermo Fisher Scientific, San José, CA). The chromatographic analysis was performed with a C_{18} reversed-phase column, Hypersil (2.1 × 50mm, 3 µm particle size, Thermo Fisher Scientific). H_2O (A) and ACN (B) were used as solvent for chromatographic separation and the elution gradient was the following: at t = 0.0min, 100% A; at t = 1.0 min, 100% A; at t = 6.0 min, 10% A and 90% B; at t = 8.0 min, 10% A and 90% B; at t = 9.0 min, 100% A; at t = 12.0 min, 95% A and 5% B. The flow rate was set at 0.3 mL/min, and the sample injection volume was 10 µL. A further switching valve located on the mass spectrometer was used to divert the LC flow to waste for the initial 1 min as well as the final 4.70 min of each injection to allow the protection of the MS source from contamination. Mass spectrometry was performed acquiring spectral data on a triple-quadrupole mass analyzer equipped with a heated electrospray ionization (HESI II) source operating in negative ion mode with the following conditions: spray voltage, -3.5 kV; vaporizer and capillary temperatures, 280 and 270 °C, respectively; sheath and auxiliary gas at 40 and 46 arbitrary units (au), respectively. Quantitative analysis was performed by multiple reaction monitoring (MRM) scan mode following two transition; the first one for quantification, and second one for validation. In particular: m/z 153 → m/z 123 (assay, CE = 25 eV) and m/z 153 → m/z 122 (confirmation, CE = 17 eV). In analogy for d_2 – hydroxytyrosol m/z 155 → m/z 123 (CE = 25 eV) and m/z 155 → m/z 122 (CE = 17 eV). The collision induced argon pressure (CID) was set at 1.0 mTorr, and the mass resolution at the first (Q1) and third (Q3) quadrupoles was set at 0.7 Da at full width at half maximum (FWHM). The S-Lens values ranging from 50 – 60 eV, whilst CE values ranging from 17 to 25 eV. All valve positions and instrument parameters were controlled by Xcalibur software, version 2.0.0 (Thermo Fisher Scientific). The total LC-MS/MS method run time was 12 min.

2.6 Antioxidant capacity assays

Sample preparation 4 g of each food products were extracted with 20 ml of methanol. The resulting mixture was stirred by vortex for 5 min and then it was centrifuged at 6000 rpm for 5 min. The methanolic extract was filtered, concentrated using a rotary evaporator and dissolved in 1 ml of DMSO.

DPPH radical scavenging activity DPPH radical scavenging activity was determined spectrophotometrically at 517 nm measuring the DPPH concentration after the reaction with an antioxidant. (16) Briefly, 100 µl of extracted sample in DMSO were mixed with 800 µl ethanolic solution of DPPH radical (40 mg/L) into a cuvette. The DPPH absorbance was measured every 30 seconds for 30 minutes. Lower absorbance values of the reactive mixture indicate a higher free radical scavenging activity. The results of the DPPH experiments were expressed as percent of inhibition of DPPH solution, calculated as following: $I\% = [(A_{control} - A_{sample}) / A_{control}] *100$, where $A_{control}$ is the absorbance of 800 µl of DPPH solution with 100µl of DMSO and A_{sample} is the absorbance of DPPH in the presence of food samples.

Spectrophotometric analysis were carried out using a spectrophotometer Evolution 600 – Thermo (Thermo Fisher Scientific, San José, CA)

3. RESULTS AND DISCUSSION

In this section a novel method to produce new functional foods is presented. This methodology use the supercritical CO_2 fluid extraction to enrich foodstuffs generally consumed in daily diet with hydroxytyrosol, an important nutraceutical phenolic compound contained in olive oil. The Figure 1 shows the step of enrichment procedure.

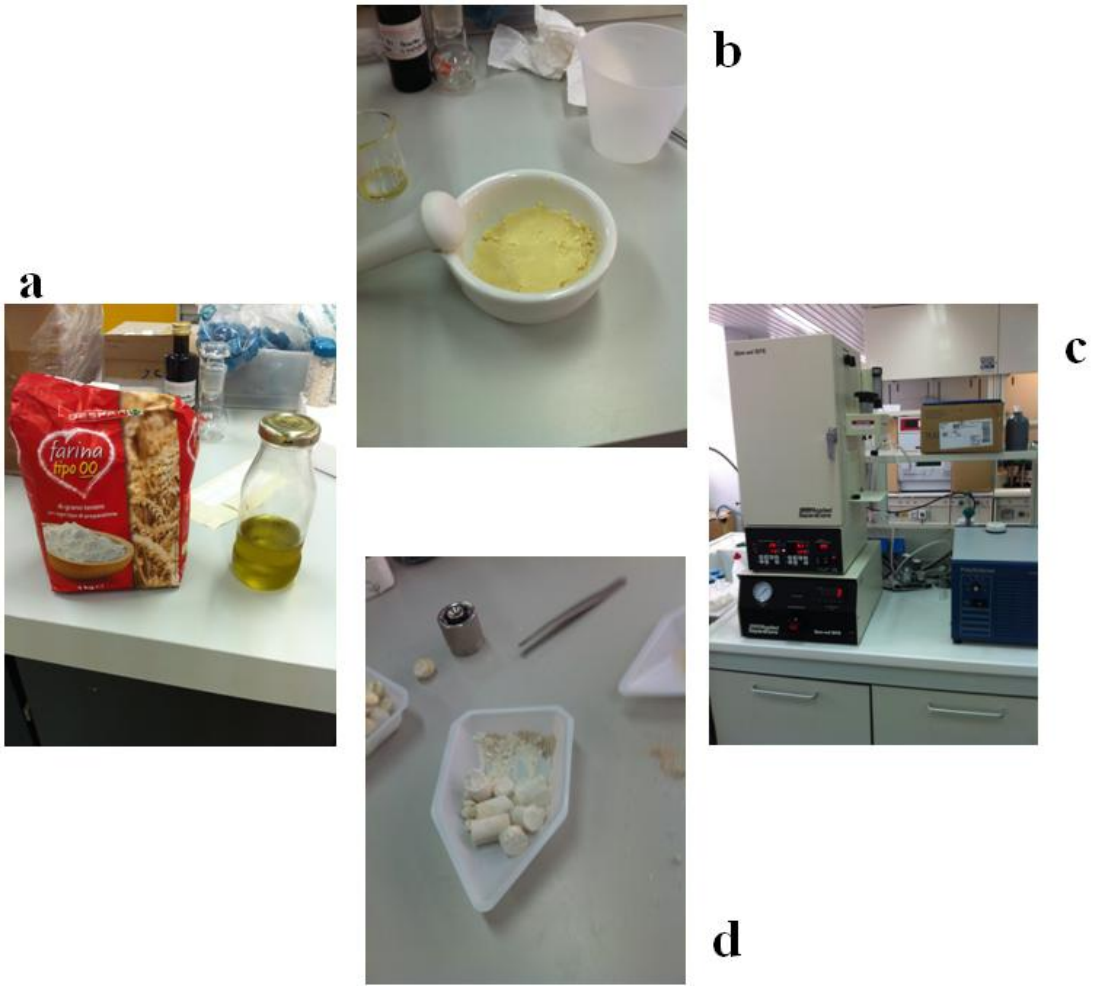

Figure 5 Workflow of enrichment process: a) starting materials b) mixture of starting materials c) supercritical CO_2 extractor d) enriched flour after process

The starting materials were mixed to allow the dispersion of the oil in the food matrices, and then submitted to the supercritical fluid process to obtain the final hydroxytyrosol enriched and fat free product.

Carbon dioxide becomes supercritical at temperature of 31.2 °C and pressure of 72.9 atm. In this state it is compressible such us a gas but possessing a density and a solvating power similar to a liquid; it has a low viscosity, an high diffusivity, and diffuses easily through solid materials providing faster extraction yields. Furthermore, supercritical CO_2 is a non-

toxic solvent. For all of these reasons today, supercritical fluid extraction is considered an important green technology which can be used in alternative to the traditional extraction methods. (17)

In this work, the process was not used in the traditional way, i.e. to extract apolar compounds, but to remove the fat constituents from mixture prepared by the olive oil and the selected foods. However, the use of supercritical CO_2 assists the selective absorption of hydroxytyrosol to food products.

The procedure was optimized to obtain a fast and quantitative transfer of hydroxytyrosol from oil to foodstuffs. Several experiments were performed on the flour matrix using an olive oil sample spiked with hydroxytyrosol standard at concentration of 100 mg/L. The experiments were carried out varying the supercritical process conditions, i.e. the temperature, pressure and the time of whole process. These tests were needed because, generally, the solubility of an analyte in a solvent is highly influenced by the density of the solvent; and the density of a fluid state is particularly sensitive to small changes in pressure and temperature (18,19).

The first experiments were performed at a pressure of 400 bar, and varying the temperature (from 40°C to 70°C) and the time (from 1 hour to 3 hours). It was observed that the temperature rise does not improve the transfer of hydroxytyrosol to the flour matrix. Therefore, the subsequent experiments were carried out at the minimum values of temperature and pressure: 40°C and 100 bar, varying the time from 1 hours to 3 hours. The results of these experiments have highlighted that the quantitative transfer of hydroxytyrosol is achieved after 3 hours. In order to decrease the time of process, other experiments in combined mode were performed. In particular, in the first step the system worked in static mode (closed system), at constant values of temperature and pressure (40°C, 100 bar) and subsequent in dynamic mode (open system) increasing the pressure up to 300 bar. The best results were obtained with the following conditions: static mode at 40°C and 100 bar for 1 hours and dynamic mode at 40°C and 300 bar for 30 minutes.

The Figure 2 shows the LC-UV chromatograms of flour extract and enriched flour extract obtained after the supercritical CO_2 process in the latest experimental conditions

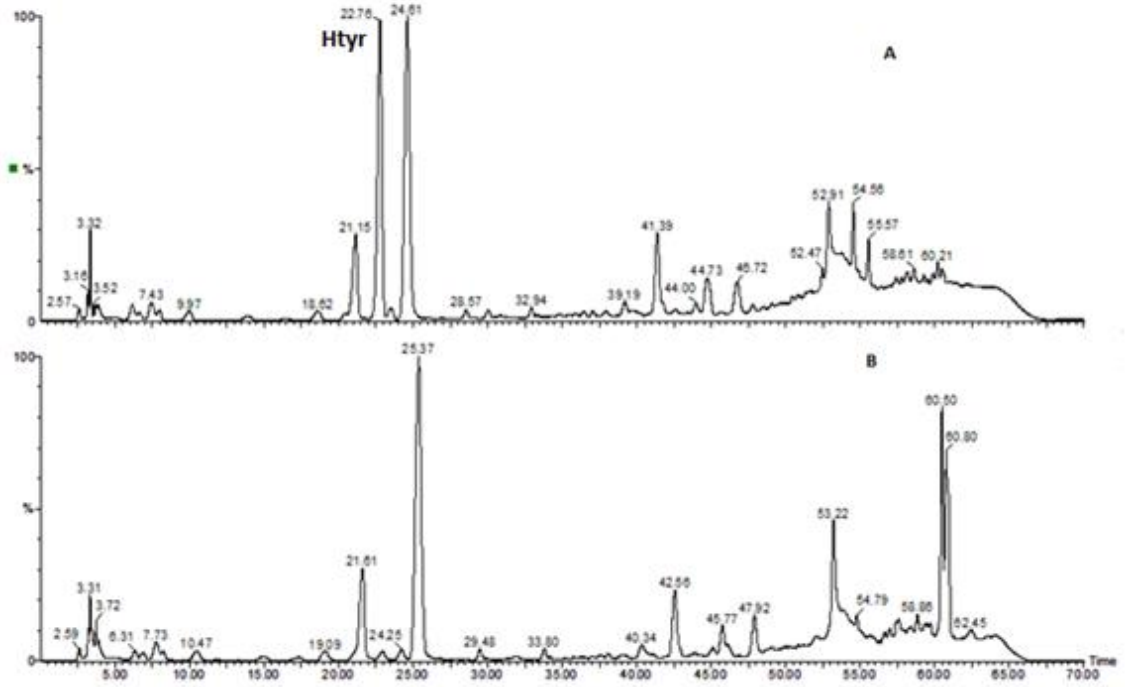

Figure 6 HPLC-UV chromatograms of flour after (A) and (B) before enrichment procedure

The chromatogram A shows clearly the presence of the hydroxytyrosol signal in the extracted flour. The quantitative assay performed by LC-UV analysis with external standard method have highlighted the quantitative transfer of hydroxytyrosol from the oil to the flour.

Probably, in the first 60 minutes of experiment, the closed system promotes the establishment of an equilibrium between the matrix and the supercritical fluid. This equilibrium improves the fat solubility in the supercritical CO_2 and the complete adsorption of hydroxytyrosol in the food matrices.

After the conditions optimization, the procedure was applied on the selected foods: flour, whole wheat flour and sugar, after homogenization with a commercial olive oil with a concentration of 14 mg/kg of hydroxytyrosol.

At the end of enriched process, each sample was extracted and analyzed by LC-MS/MS under MRM conditions following the optimized transition for hydroxytyrosol and d_2-hydroxytyrosol. (20) The Figure 2 shows a representative MRM chromatogram of an enriched sample revealing the signals of hydroxytyrosol and labeled internal standard transitions.

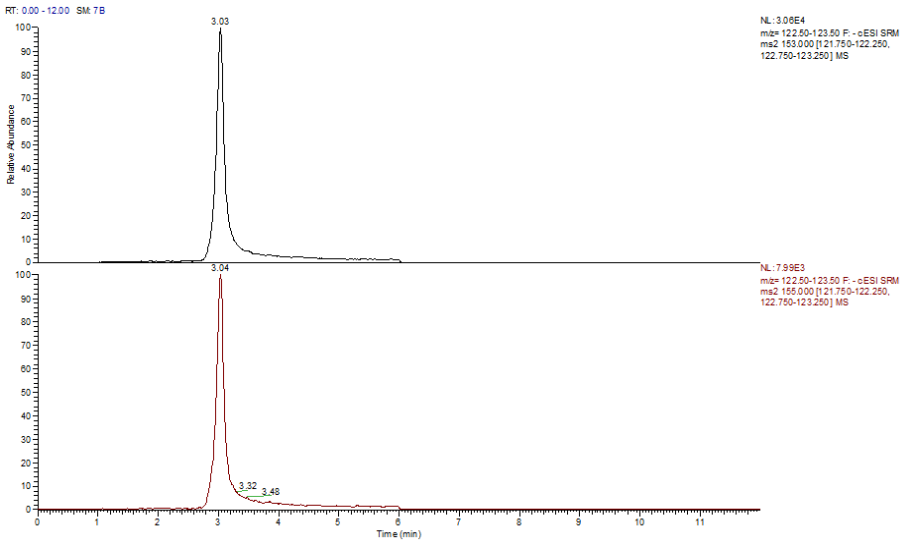

Figure 7 MRM chromatogram of followed transitions for hydroxytyrosol and d_2-hydroxytyrosol

The Table 1 discloses the amount of hydroxytyrosol found in enriched foods and the recovery values.

Table 1 Amount of hydroxytyrosol transfer to food samples and recovery values

Amount of Htyr per 6g of olive oil (µg)	**Enriched foods**	**Amount of Htyr per 24g of foods (µg)**	**Recovery %**
82.32	Flour	80.20	97.42
	Whole wheat flour	81.20	98.64
	Sugar	81.92	99.51

The recovery values are near 100%, this means a complete transfer of hydroxytyrosol from olive oil to food products.

To verify that the enriched food products can be really used in daily diet, it was simulated the preparation of a pizza/bread dough using the enriched flour. The dough was submitted to a simple procedure cooking at 180°C for 30 minutes.

At the end of cooking the outer and the inner parts of the "enriched bread" (Figure 4) were extracted and analyzed by HPLC-MS/MS, in order to verify that no degradation of hydroxytyrosol occurs.

Figure 8 Bread obtained from enriched flour

The table 2 shows the amount of hydroxytyrosol in "bread" obtained from enriched flour.

Table 2 Amount of hydroxytyrosol found in "enriched bread"

Amount of Htyr per g enriched four (µg)	Amount of Htyr per g of bread outside (µg)	Recovery %	Amount of Htyr per g of bread inside (µg)	Recovery %
13.72	12.95	94.38	13.23	96.43

Also in this case, the recovery values are near 100%, this highlights that no degradation of hydroxytyrosol occurs.

Finally, it was evaluate the ability of the enriched novel food for scavenging of free radicals by means the DPPH test.

There are several methods to evaluate the antioxidant activity of compounds, plant extracts and foods, such as FRAP (ferric reducing antioxidant power), ORAC (oxygen radical absorbance), CUPRAC (cupric reducing antioxidant capacity), but the most popular and employed method is the DPPH. (21-23)

In this work, the antioxidant capacity of enriched foods was determined by DPPH assay. This test involved the measurement of DPPH radical absorbance at 517 nm during the reaction with antioxidant compounds present in foods. DPPH radical is an organic nitrogen radical with a deep purple color, and when it is mixed with an antioxidant/reducing

compound its color changes from purple to yellow which indicates to the formation of hydrazine.

For each food sample two independent assays were performed; the first on original matrices and the second on enriched foods. Different conditions can be used for this assay, but in the experiments an excess of DPPH was used in order to exhaust the H-donating capacity of antioxidant compounds. The spectrophotomentric measurements were performed for 30 min until the reaction has reached the equilibrium. The kinetic curves were obtained plotting the DPPH radical absorbance against the time of experiment (Figure 4, 5, 6).

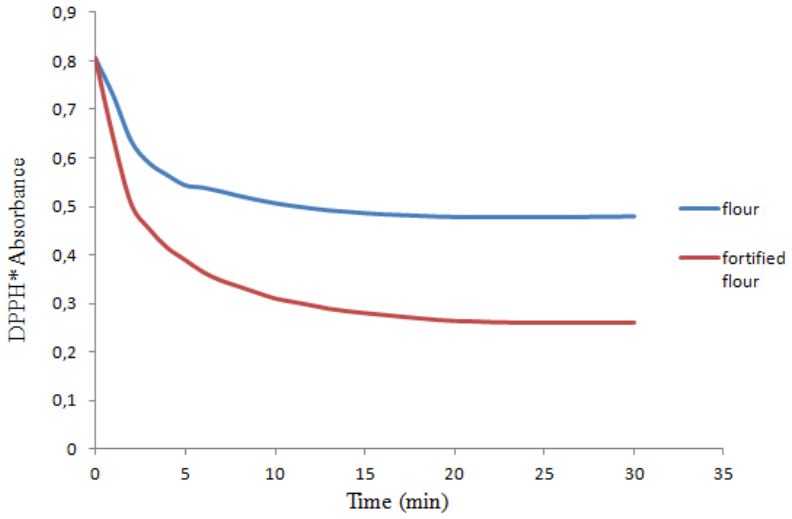

Figure 4 The kinetic curves of the scavenged DPPH by flour (blue) and enriched flour (red)

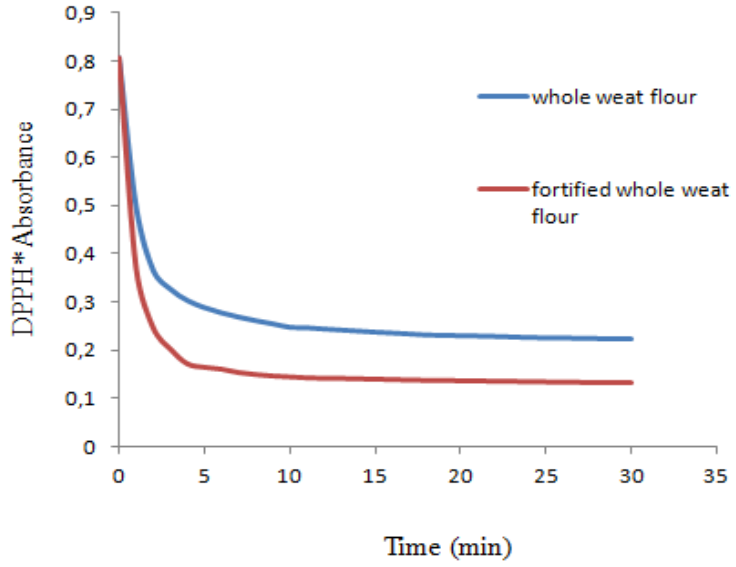

Figure 5 The kinetic curves of scavenged DPPH by whole wheat flour (blue) and enriched whole wheat flour (red)

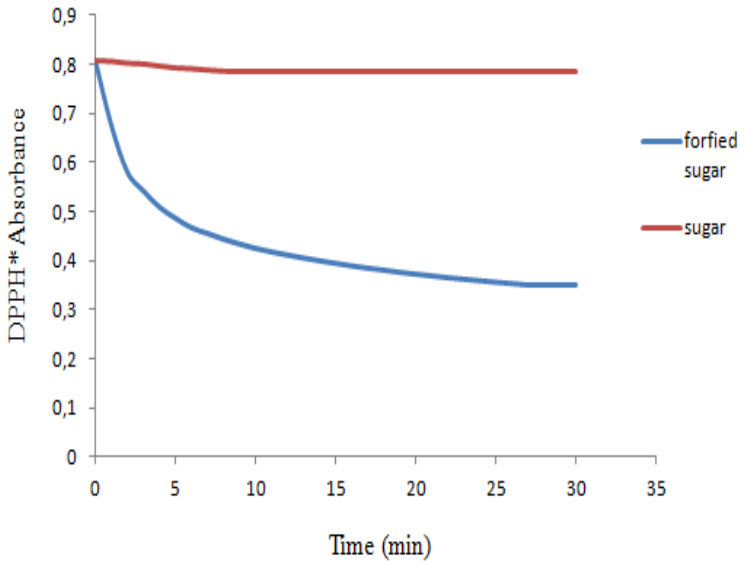

Figure 6 The kinetic curves of scavenged DPPH by sugar (blue) and enriched sugar (red)

The kinetic behaviour showed a lower DPPH absorbance value for fortified foods at the end of reaction compared to the original products. In particular, the kinetic curve of fortified flour shows that the disappearance of DPPH radical is faster than the original sample, and the same effect is observed for whole wheat flour sample. For sugar, the absorbance difference between the two samples is much higher, because the original sugar matrix doesn't show any radical scavenging activity (Figure 4). For all experiments, the reaction with DPPH was biphasic, with a fast decay in absorbance in the first few minutes and a slower step in which the equilibrium was reached, when the DPPH reagent was degraded. The results were expressed in terms of reduction percentage of DPPH solution or percent of inhibition, through the absorbance values at the beginning and after the time of 30 min (Table 3).

Table 3 percent of inhibition of foodstuffs

	% Inhibition
Flour	38.80
Enriched flour	**64.38**
Whole wheat flour	74.65
Enriched whole wheat flour	**86.11**
Sugar	2.55
Enriched sugar	**58.28**

These values display a higher radical scavenging activity for fortified foods.

4. CONCLUSIONS

The developed procedure based on the use of supercritical CO_2 fluid extraction, allows to create new functional foodstuffs enriched in hydroxytyrosol which may increase the daily intake of this nutraceutical compound. The results obtained have highlighted that the transfer of hydroxytyrosol from olive oil to food matrices is quantitative, and the new product can really used in diet because the hydroxytyrosol doesn't not suffer any degradation under cooking conditions.

Supercritical carbon dioxide is economic, non-toxic solvent with a high extraction efficiency. Therefore, the processes using the supercritical CO_2 fluid are considered the most important green technology in the industrial production.

The presented procedure can be used to enrich food products with other similar active principle.

REFERENCES

1. De Leonardis, A.; Aretini, A.; Alfano, G.; Macciola, V.; Ranalli, G. (2008). Isolation of a hydroxytyrosol-rich extract from olive leaves (Olea europaea L.) and evaluation of its antioxidant properties and bioactivity. *Eur Food Res Technol* 226(4), 653–659

2. Pérez-Bonilla, M.; Salido, S.; van Beek, T. A., Altarejos, J. (2013). Radical scavenging compounds from olive tree (Olea europaea L.) wood. *Journal of Agriculture and Food Chemistry* 62(1), 144–151

3. Bulotta, S.; Celano, M.; Lepore, S. M.; Montalcini, T,; Pujia, A.; Russo, D. (2014). Beneficial effects of the olive oil phenolic components oleuropein and hydroxytyrosol: focus on protection against cardiovascular and metabolic diseases. *Journal of Translational Medicine* 12(1):219

4. Sánchez-Fidalgo, S.; de Ibargüen, L. S.; Cárdeno, A.; de la Lastra, C. A. (2012). Influence of extra virgin olive oil diet enriched with hydroxytyrosol in a chronic DSS colitis model. *European Journal of Nutrition* 51(4):497–506

5. Burattini, S.; Salucci, S.; Baldassarri, V.; Accorsi, A.; Piatti, E.; Madrona, A.; Espartero, J. L.; Candiracci, M.; Zappia, G.; Falcieri, E.; (2013) Antiapoptotic activity of hydroxytyrosol and hydroxytyrosyl laurate. *Food Chemistry Toxicology* 55:248–256

6. Takeda, Y.; Bui, V. N.; Iwasaki, K.; Kobayashi, T.; Ogawa, H.; Imai, K.; (2014). Influence of olive-derived hydroxytyrosol on the toll like receptor 4-dependent inflammatory response of mouse peritoneal macrophages. *Biochemical and Biophysical Research Communications* 446(4):1225–1230

7. Bisignano, C.; Filocamo, A.; Ginestra, G.; Giofre, S. V.; Navarra, M.; Romeo, R.; Mandalari, G. (2014). 3, 4-DHPEA-EA from Olea Europaea L. is effective against

standard and clinical isolates of Staphylococcus sp. *Annals Clinical Microbioloby Antimicrobials* 13(1):24–28

8. Auñon-Calles, D.; Canut, L.; Visioli, F. (2013) Toxicological evaluation of pure hydroxytyrosol. *Food Chemical Toxicoly* 55:498–504

9. COMMISSION REGULATION (EU) No 432/2012

10. Baiano, A., Gambacorta, G., Terrcone, C., Previtali, M. A., Lamacchia, C., & La Notte, E. (2009). Changes in phenolic content and antioxidant activity of Italian extra-virgin olive oils during storage. *Journal of Food Science*, 74, 177–183.

11. Brenes, M., Garcia, A., Garcia, P., & Garrido, A. (2001). Acid hydrolysis of secoiridoids aglycons during storage of virgin olive oil. *Journal of Agricultural and Food Chemistry*, 49(11), 5609–5614.

12. Stefanoudaki, E., Williams, M., & Harwood, J. (2010). Changes in virgin olive oil characteristics during different storage conditions. *European Journal of Lipid Science and Technology*, 112, 906–914.

13. Morello, J. R. (2004). Changes in commercial virgin olive oil (cv Arbequina) during storage, with special emphasis on the phenolic fraction. *Food* Chemistry, 85, 357–364.

14. M.T. Morales, R. Przybylsky (2000) Handbook of Olive Oil 459-490

15. Kuwajima, H.; Takai, Y.; Takaishi, K.; Inoue, K. Synthesis of ^{13}C-labeled possible intermediates in the biosynthesis of phenylethanoid derivatives, cornoside and rengyosides. *Chem. Pharm. Bull.* **1998**, *46* (4), 581–586.

16. Pyrzynska K. and Pekal A. (2013). Applicant of free radical diphenylpicrylhydrazyl (DPPH) to estimate the antioxidant capacity of food samples. *Analytical Methods*, 5, 4288-4295

17. Anklam, E., Berg, H., Mathiasson, L., Sharman, M., & Ulberth, F. (1998). Supercritical fluid extraction (SFE) in food analysis: a review. *Food Additives and Contaminants*, 15, 729–750.

18. Del Valle, J. M., & Aguilera, J. M. (1999). Review: high pressure CO2 extraction. Fundamentals and applications in the food industry. *Food Science and Technology International*, 5, 1–24.

19. Raventòs, M., Duarte, S., & Alarcòn, R. (2002). Application and possibilities of supercritical CO2 extraction in food processing industry: an overview. *Food Science and Technology International*, 8, 269–284.

20. Mazzotti, F.; Benabdelkamel, H.; Di Donna, L.; Maiuolo, L.; Napoli, A.; Sindona, G. (2012) Assay of tyrosol and hydroxytyrosol in olive oil by tandem mass spectrometry and isotope dilution method. *Food Chem. 135* (3), 1006–1010.

21. Prior R. L.; Wu X. and Schaich K., J. (2005). Standardized Methods for the Determination of Antioxidant Capacity and Phenolics in Foods and Dietary Supplements, *Journal of Agriculture and Food Chemistry*, 53, 4290–4302

22. Moon J. K. and Shibamoto T. (2009), Antioxidant assays for plant and food components. *Journal of Agriculture and Food Chemistry*, 57, 1555–1666.

23. Kedare S. B. and Singh R. P. (2011). Genesis and development of DPPH method of antioxidant assay *Journal of Food Science and Technology*, 48, 412-422.

CHAPTER 3

Mass Spectrometric Advanced Approaches for Quality Assessment of Foods

I. Determination of Hydroxytyrosol and Tyrosol derivatives compounds in Extra Virgin olive oil by Microwave Hydrolysis and LC-MS/MS analysis

1. INTRODUCTION

Extra virgin olive oil is a fundamental ingredient of Mediterranean diet. It is considered a functional food for the presence of polyhydroxylated aromatic compounds, which may act as nutraceuticals. Its constant intake may provide potential health benefits to humans, lowering the incidence of cardiovascular and metabolic diseases. It was suggested that this effect is largely due to the antioxidant properties of the phenolic compounds present in the oil. (1-3)

Among those, hydroxytyrosol and tyrosol present in olive oils either in the free form or as conjugates play an important role in the prevention of certain diseases. (4-8)

Recently, the European Food Safety Authority approved a health claim on olive oil polyphenols (Commission Regulation (EU) 432/2012) which states that:

Olive oil polyphenols contribute to the protection of blood lipids from oxidative stress. The claim may be used only for olive oil, containing at least 5 mg of hydroxytyrosol and its derivatives (e.g. oleuropein complex and tyrosol) per 20 g of olive oil. In order to bear the claim information shall be given to the consumer that the beneficial effect is obtained with a daily intake of 20 g of olive oil. (9)

This may be an important tool for the oil makers, which intend to raise the economic value of their extra virgin olive oil if it contains these quality markers; in fact, it is possible to report this sentence directly on the label of the oil packaging: nevertheless, it is necessary to use an accurate and reliable analytical method to evaluate the exact amount of these compounds.

To date, there are not trustworthy methods to determine the absolute amount of "polyphenols" in olive oil. The International Olive Council (IOC) recommends the use of a classical procedure, which consists in a HPLC analysis, which uses the UV detection and tyrosol and syringic acid as internal standards. Unfortunately, the method is neither selective nor accurate, because the analysis relies on retention times and on the absorbance values recorded at 280 nm. (10)

The method developed in this section allows to determine the absolute amount of hydroxytyrosol and tyrosol derivatives, through a simple and fast microwave assisted acidic hydrolysis reaction. The instrumental analysis is based on the use of liquid chromatography combined with tandem mass spectrometry using isotope dilution method. Mass spectrometric analysis in MRM scan mode and labeled internal standards provide high specificity and accuracy to the method.

2. MATERIALS AND METHODS

2.1 Chemicals

Chemicals and reagents were commercially available (Sigma–Aldrich, St. Louis, MO). Hydroxytyrosol, tyrosol and oleuropein standards were purchased from Extrasynthese (Genay Cedex, France). Labelled standards, d_2-Hydroxytyrosol and d_2-Tyrosol were obtained by slightly modified literature methods. (11)

2.2 Synthesis and purification of d_2-Tyrosol standard

A stirred suspension of methyl 4-hydroxyphenilacetate (1g, 6 mmol) in D_2O (18 ml) was treated with $NaBD_4$ (1.88 g, 45.13 mmol) under stirring for 8 h at room temperature. 5 ml of a 2 N solution of HCl was added under ice-cooling for the decomposition of the excess reagent, and then the mixture was extracted with Et_2O. The organic layer was washed with brine and concentrated under vacuum. The purification of reaction residue was performed by semi-preparative chromatography, using a C18 reversed-phase column, Luna (250 × 10 mm, 5 μm particle size, Phenomenex), with an isocratic run using (A) ACN 7% and (B) H_2O (0.1% HCOOH) us solvents. The flow rate was fixed at 4.7 ml/min and the volume injected was of 1 ml.

2.3 Synthesis and purification of d_2-Hydroxytyrosol standard

0.66 g (15.84 mmol) of $NaBD_4$ were add in about 1 minute to 7 ml of ice labelled water (D_2O). A solution of 0.8 g (4.4 mmol) of methyl 3,4-hydroxyphenilacetate in 10.5 ml of D_2O was add to the mixture, and stirred was continued for 6.5 hours at room temperature. The reaction mixture was cooled to 0 °C and 21 ml of 2 N HCl were added drop by drop in 15 minutes. The mixture was extracted with 100 ml of ethyl acetate for six times. Each extract was washed with 50 ml of half saturated ammonium chloride solution, combined

and dried over sodium sulphate, and finally concentrated under vacuum. The purification of standard was performed by semi-preparative chromatography, using a C18 reversed-phase column, Luna (250 × 10 mm, 5 μm particle size, Phenomenex), with an isocratic run using (A) ACN 7% and (B) H_2O (0.1% HCOOH) as solvents. The flow rate was 4.7 ml/min and the volume injected was of 1 ml.

2.4 Extra virgin olive oil samples

Ten extra virgin oils were obtained from local oil producers and stored in amber glass bottles at 4°C until analysis.

2.5 Sample preparation

2.5.1 Determination of free Hydroxytyrosol and Tyrosol

Each olive oil sample was added to 50 μL of a solution of d_2-Hydroxytyrosol at 75 mg/L and 30 μL of a solution of d_2-Tyrosol at 250 mg/L up to a weight of 1.5 g. The mixture was stirred by ultra-turrax for three minutes to allow the homogeneous distribution of the standards; then 1 g was extracted using 1 ml of H_2O (0,1% HCOOH)/EtOH 3:7 v/v. The resulting mixture was centrifuged at 12000 rpm for three minutes, and the supernatant was diluted (1/10) with a solution of H_2O (0,1% HCOOH)/EtOH 3:7 v/v and analyzed by LC-MS/MS.

2.5.2 Determination of total Hydroxytyrosol and Tyrosol

Each olive oil sample was added to 50 μL of a solution of d_2-Hydroxytyrosol at 1000 mg/L and 40 μL of a solution of d_2-Tyrosol at 1000 mg/L up to a weight of 2 g. The mixture was homogenized vigorously by ultra-turrax for three minutes, and then 1 g was extracted using a solution 1 mL of H_2O (0,1% HCOOH)/EtOH 3:7 v/v. After the extraction 500 μL of supernatant were added to 500 μL of HCl 2M in a closed pyrex vessel, and submitted to acid hydrolysis for 4 minutes in a microwave Anton Paar Multiwave 3000 provided with a rotor 4×24 MC, operating at a temperature of 140 °C at the maximum power of 1400 W. The reaction mixture was then stirred to vortex for 1 minute, diluted (1/50) with H_2O (0,1% HCOOH)/EtOH 3:7 v/v and finally injected into the instrument.

2.6 Mass Spectrometry

LC-MS/MS analysis was performed using a LC/MSMS system from Thermo Scientific composed by a UHPLC Accela pump coupled to a TSQ Quantum Vantage triple-stage quadrupole mass spectrometer (Thermo Fisher Scientific, San José, CA). The HPLC separation was carried out using a C_{18} reversed-phase column, Hypersil (2.1 × 50mm, 3 μm particle size, Thermo Fisher Scientific), injecting 10 μL of sample solution. The flow rate was set at 0.25 mL/min using (A) H_2O and (B) ACN as elution solvents. The following gradient program was used: t = 0.0 min, 95% A and 5% B; t = 1.0 min, 95% A and 5% B; t = 6.0 min, 10% A and 90% B; t = 8.0 min, 10% A and 90% B; t = 9.0 min, 95% A and 5% B; equilibration time 3 min. A further switching valve located on the mass spectrometer was used to divert the LC flow to waste in the first minute and from 7 to 12 min to protect the ion source from contamination. Mass spectrometer was equipped with a heated electrospray ionization (HESI II) source operating in negative ion mode. The working conditions were: spray voltage, -3.5 kV; vaporizer and capillary temperatures, 280 and 270 °C, respectively; sheath and auxiliary gas at 40 and 46 arbitrary units (au), respectively. The collision gas pressure (Ar) in the collision cell (Q2) was set at 1.0 mTorr, and the mass resolution at the first (Q1) and third (Q3) quadrupole was set at 0.7 Da (FWHM). The S-lens rf amplitude and the collision energy (CE) were both optimized individually per compound.

For quantification purposes, MS/MS analysis was performed in multiple reaction monitoring (MRM) scan mode following two transitions per compound, the first one used for the quantitative analysis and the second used for confirmation. In particular, for Htyr *m/z* 153 → *m/z* 123 (assay, CE=17eV) and *m/z* 153 → *m/z* 122 (confirmation, CE=25eV), while for Tyr *m/z* 137 → *m/z* 106 (assay, CE=18eV) and *m/z* 139 → *m/z* 106 (confirmation, CE=18eV). (12)

Instrument control and data processing were carried out by means of Xcalibur software. The total LC-MS/MS method run time was 12 min.

2.7 LC-MS/UV analysis

LC-ESI-MS/UV analysis was performed using a Waters FractionLynx system (Milford, MA) working in analytical mode, equipped with a Acquity QDa mass spectrometer and a 2489 UV/visible detector. The chromatographic separation was carried out according to IOC methodology[3], using a C18 reversed-phase column, Luna (250 × 4.6 mm, 5 μm, Phenomenex), at a flow rate of 1 ml/min. The run time was 82 min and the injection volume 1 ml. The gradient was built using 0.1 % HCOOH (A), MeOH (B), ACN (C) as mobile phase, The elution gradient was composed of the following steps: at t = 0.0 min, 96% A, 2% B and 2% C; at t = 40 min, 50% A, 25% B and 25% C; at t = 45 min, 40% A, 30% B and 30% C; at t = 60 min, 0% A, 50% B and 50% C; at t = 70 min, 0% A, 50% B and 50% C; at t = 72 min, 96% A, 2% B and 2% C; at t = 82.0 min, 96% A, 2% B and 2% C.

3. RESULTS AND DISCUSSION

Hydroxytyrosol and Tyrosol are present in olive oil in part per million in their free form, The most abundant form are present as esters of elenolic acid at hundreds of part per million concentration (Figure 1). Oleuropein and ligstroside, the glycoside derivatives may be found at part per billion concentration.

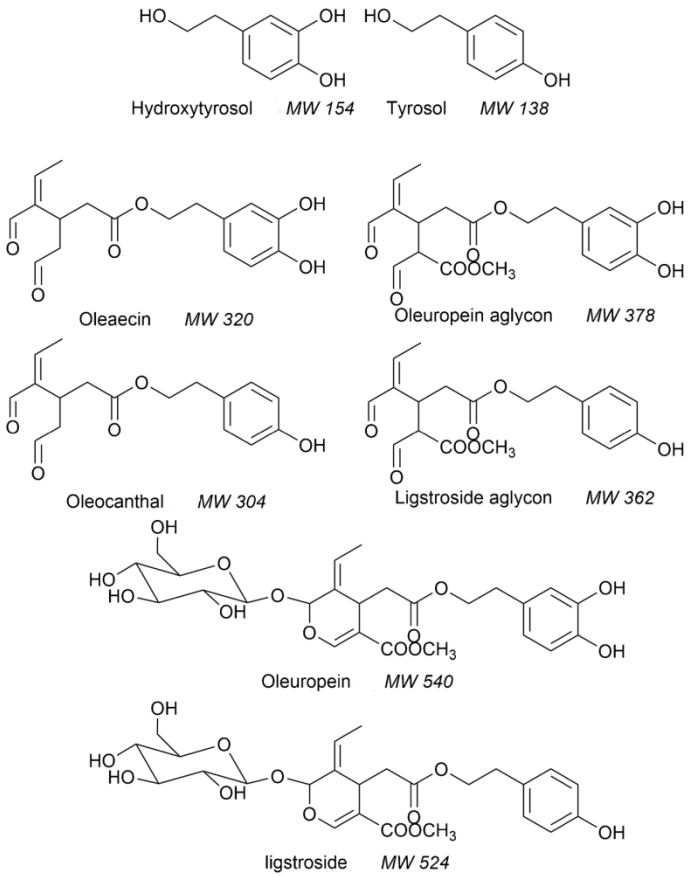

Figure 1 Chemical structure of tyrosol and hydroxytyrosol derivatives present in EVOO

The aim of the developed procedure is to determine the absolute content of hydroxytyrosol and tyrosol derivatives in extra virgin olive oil, according to the health claims of 432/2012 EU regulation. (9)

The method consists in a first assay of the free form of Htyr and Tyr, and in a second quantitative determination of their total amount, including their esterified forms that are the most abundant polyhydroxylated aromatic compounds present in extra virgin olive oil. For both analysis, the quantitative assay is carried out by LC-MS/MS and stable isotope dilution analysis, using d_2-Tyr and d_2-Htyr as deuterated internal standard, directly added to the samples. The analyzer was set in MRM mode following the optimized transition for

Tyr, Htyr, d_2-Tyr and d_2-Htyr, in order to obtain the best selectivity of analytes. (12) In particular, in the case of Htyr the monitored transition are: *m/z* 153 → *m/z* 123 for the hydrogenated compound and *m/z* 155 → *m/z* 123 for the deuterated standard; both reactions originate from the loss of formaldehyde from the deprotonated molecule $[M-H]^-$. The transition related to tyrosol are the following: *m/z* 137 → *m/z* 106 for the lightest analyte and *m/z* 139 → *m/z* 106 for the heaviest one, which arise from the loss of a methoxy radical from the negative pseudomolecular ion $[M-H]^-$.

The calibration curve for each analyte was obtained by injecting standard solutions at known concentration of the analyte and the internal standard.

For the free fraction, calibration curves were obtained as follows: the concentration of standard ranged from 0.125 to 0.750 mg/L for Hydroxytyrosol, with the internal standard at 0.250 mg/L; the concentration of standard Tyrosol ranged from 0.375 to 1 mg/L, with the concentration of the isotopomer internal standard fixed at 0.5 mg/L. The correlations obtained ($y = 0.9488x + 0.0556$; $R^2=0.9956$) for Tyr and ($y = 1.0295x + 0.0506$; $R^2=0.9991$) for Htyr, showed good linearity.

Similar solution were prepared for the analysis of the total fraction; in this case the concentration of Hydroxytyrosol standard solution ranged from 0.125 to 1.2 mg/L, while that of internal standard was fixed at 0.25 mg/Land the concentration of tyrosol standard solution ranged from 0.150 to 0.800 mg/L, while that of internal standard was fixed at 0.2 mg/L. Also in this case, the curves obtained ($y = 1.0671x + 0.2782$; $R^2=0.997$) for tyrosol and ($y = 1.1165x + 0.1667$; $R^2=0.997$) for hydroxytyrosol, showed good correlation.

To evaluate the amount of compounds in their free form, oil samples were submitted to the extraction of phenols with a mixture of ethanol and acid water and directly analyzed by LC-MS/MS, while the quantification of the total content of Htyr and Tyr was carried out through acidic hydrolysis.

Recently, some hydrolysis methods were developed to convert Tyr and Htyr derivatives in their simplest phenylethanol form. Mulinacci et al. proposed a hydrolysis reaction on the extracted phenolic fraction with H_2SO_4 for 2 hours at 80°C (13). In a more recent works, the acid hydrolysis was performed directly on the oil or on extracted solution of phenolic fraction using HCl. (14,15) These approaches present some disadvantage: for example, in the methodology proposed by Mulinacci et al., the sample preparation steps are laborious and the whole procedure (including instrumental analysis) takes a long time. While the

latter two mentioned methods are not based on mass spectrometry and internal standard calibration, causing loss in accuracy and selectivity.

In this study, a new and fast microwave assisted hydrolytic procedure was developed. The hydroalcoholic extract containing the phenolic fraction is diluted with hydrochloric acid 2M and submitted to hydrolysis reaction using a microwave oven in a closed vessel.

In order to optimize the hydrolysis reaction, several experiments were performed on a corn oil sample fortified with standard tyrosol, hydroxytyrosol and oleuropein at concentration of 100, 150 and 150 mg/kg, respectively, to simulate a high content phenols olive oil.

The tests were carried out varying the reaction conditions, i.e. time of reaction, watt power and temperature in the oven. After each hydrolysis reaction, the samples were opportunely diluted and analyzed by LC-MS/MS under MRM condition following the optimized transition for Tyr, Htyr, d_2-Tyr and d_2-Htyr.

It was demonstrated that the completeness of the reaction is obtained in 4 minutes with a temperature of 140°C and an oven power of 1400 W.

Figure 2 highlights the influences of the three variables on the reaction yield.

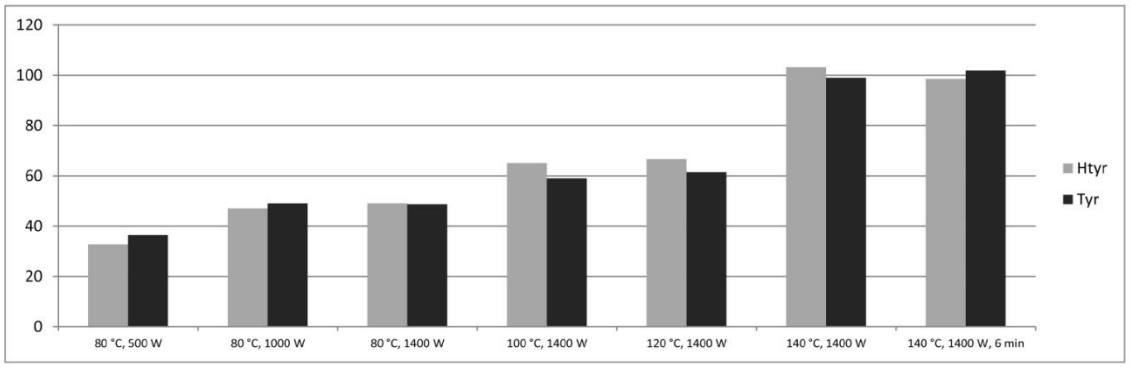

Figure 2 Variation of hydrolysis reaction accuracy depending on the different condition of temperature, power watt and time, employed to the microwave experiment.

The time of hydrolysis reaction was set at 4 minutes. In the first three experiments the temperature was fixed at 80°C as recommended by Mulinacci et al. method (13), and varying the watt power from 500W to 1400W. The amount of hydrolysis products increased from 500 W to 1000 W, remaining similar at 1400 W. For this reason, the next experiment was performed at the fixed value of power (1400W), increasing the temperature of microwave oven, from 80°C to 140°C. The best results indicated by the completeness of reaction, were obtained at a temperature of 140°C. Moreover, it was demonstrated that an increase in reaction time did not bring improvements.

Therefore, the best condition of hydrolysis reaction were the following: 140 °C, 140 Watt for 4 min.

After the optimization of hydrolysis procedure and before applying the method to real samples, some experiments were performed to calculate the accuracy of the methodology. Firstly, to verify that the acidic hydrolysis reaction did not affect the free form of Tyr and Htyr, the reaction was tested onto a standard mixture containing 20 mg/L of Tyr and 25 mg/L of Htyr. Internal standards (d_2-Tyr and d_2-Htyr) was added to the mixture, and the assay of analytes provides an accuracy of 104% and 100%, respectively after hydrolysis procedure (Table 1).

Table 3 Accuracy values performed on standard solution mixture

		Spiking concentration (mg/kg)	**Found concentration (mg/kg)**	**Accuracy (%)**	**RSD (%)**
Standard mixture	Tyr	20	20.89 ± 0.46	104	2.20
	Htyr	25	25.12 ± 0.61	100	2.43

Then, two corn oil fortified with Htyr, Tyr and Oleuropein, at two concentration levels were prepared. The first oil sample was prepared at 40 mg/kg Tyr, 30 mg/kg Htyr and 30 mg/kg oleuropein, to simulate a low content phenols olive oil, and the second sample at 100 mg/kg, 150 mg/kg and 150 mg/kg, representatives of a high content phenols olive oil. Table 2 shows the accuracy values obtained after hydrolysis procedure.

Table 2 Accuracy values performed on fortified soybean oils

Fortified sample		**Spiking concentration (mg/kg)**	**Found concentration (mg/kg)**	**Accuracy (%)**	**RSD (%)**
Corn oil (low content of phenols)	Tyr	40	40.73 ± 1.84	102	4.52
	Htyr	30	38.08 ± 0.77	99	2.02
	Oleuropein	30			
Corn oil (high content of phenols)	Tyr	100	99.02 ± 1.95	99	1.97
	Htyr	150	194.58 ± 2.25	103	1.16
	Oleuropein	150			

The accuracy values are near to 100%; this means that the hydrolysis procedure is complete and no collateral reactions occur. The RSD % values, calculated after three different preparation, show a good reproducibility.

In order to simulate the extra virgin olive oil matrix, the methodology was also tested onto a fortified pomace oil sample. Firstly, it was verified the absence of phenolic compounds in this type of oil by LC-MS/MS analysis, and then the sample was fortified with the following concentration of analytes: 100 mg/kg of Tyr, 150 mg/kg of Htyr and 150 mg/kg oleuropein. Table 3 shows the accuracy values obtained after hydrolysis reaction.

Table 3 Accuracy values performed on fortified pomace oils

Fortified sample		**Spiking concentration (mg/kg)**	**Found concentration (mg/kg)**	**Accuracy (%)**	**RSD (%)**
Fortified pomace oil	Tyr	100	102.76 ± 1.82	103	1.77
	Htyr	150	181.32 ± 3.65	96	2.01
	Oleuropein	150			

Also in this case, the accuracy values are near 100% and RSDs % highlight a good reproducibility.

LOQ and LOD values were calculated using the average signal given by the blank (pomace oil) sample plus its standard deviation multiplied by three times and ten times, respectively (Table 4).

Table 4 LOD and LOQ values

	LOD (mg/kg)	**LOQ (mg/kg)**
Tyr	0.041	0.043
Htyr	0.005	0.011

Limit of detection and quantification values highlight a good sensitivity of methods.

Finally, real EVOO samples were submitted to the developed methodology.

The figure 3 shows the LC-UV chromatograms of extracted phenols solution of an extra virgin olive oil sample before and after microwave assisted hydrolysis reaction.

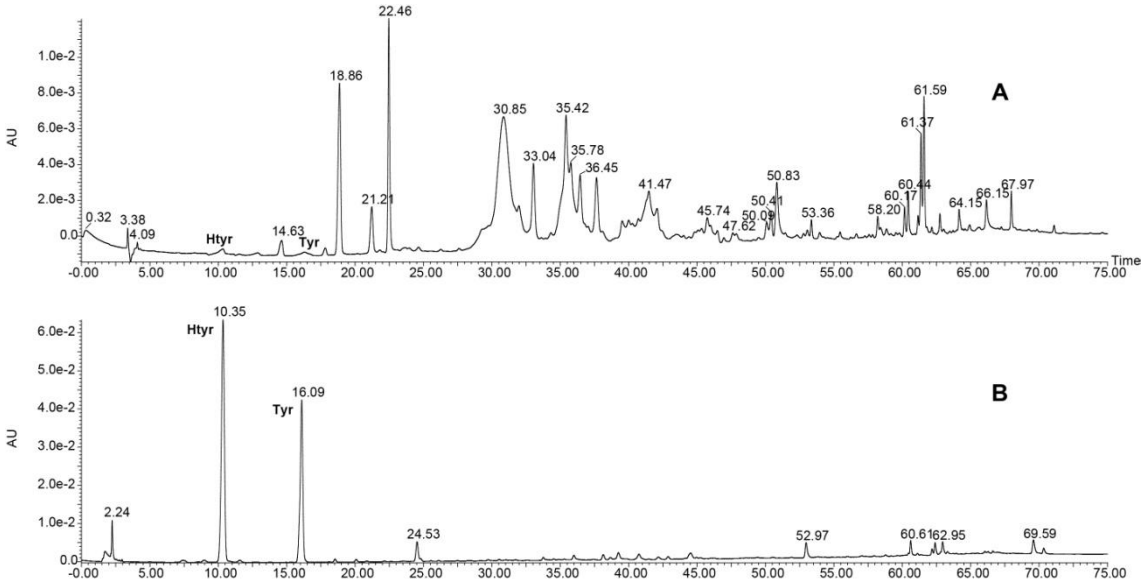

Figure 3 LC-UV chromatogram of a representative EVOO sample before and after hydrolysis procedure

The UV-chromatogram B shows, clearly, an increasing of the signals intensity relative to Htyr and Tyr and, at the same time, the complete disappearance of the other signals present in the UV-chromatogram, representative of their derivatives.

As indicated above, each EVOO sample was submitted to extraction procedure for the quantification of Htyr and Tyr in their free form.

Table 5 discloses the amount of Htyr and Tyr in their free form with RSD % values.

Table 5 Amount of free Htyr and Tyr in real samples

EVOO sample	Htyr (mg/Kg)	RSD (%)	Tyr (mg/Kg)	RSD (%)
O-1	2.96 ± 0.01	0.48	5.82 ± 0.15	2.66
O-2	Not detected	-	Not detected	-
O-3	7.11 ± 0.04	0.50	7.68 ± 0.06	0.82
O-4	21.19 ± 0.92	0.90	23.56 ± 0.21	0.90
O-5	0.98 ± 0.03	2.84	5.01 ± 0.14	2.84
O-6	6.48 ± 0.09	1.39	21.16 ± 0.16	0.76
O-7	1.97 ± 0.02	1.01	16.14 ± 0.23	1.43
O-8	10.71 ± 0.12	1.12	11.67 ±0.68	3.26
O-9	3.60 ± 0.04	1.11	4.07 ± 0.10	2.46
O-10	Not detected	-	10.52 ± 0.60	5.70

The amount of total Htyr and Tyr obtained after hydrolysis procedure are reported in Table 6.

Table 6 Amount of free Htyr and Tyr in real samples

EVOO sample	Total Htyr (mg/Kg)	RSD (%)	Total Tyr (mg/Kg)	RSD (%)
O-1	113.79 ± 4.17	3.67	86.15 ± 1.38	1.60
O-2	92.19 ± 5.35	5.80	83.63 ± 2.28	2.72
O-3	80.74 ± 1.36	1.69	55.10 ± 3.58	6.49
O-4	91.12 ± 3.82	4.19	83.24 ± 4.15	4.98
O-5	40.07 ± 1.22	3.05	78.30 ± 1.87	2.38
O-6	22.63 ± 0.64	2.84	41.61 ± 0.32	0.77
O-7	14.25 ± 0.13	0.94	61.97 ± 1.57	2.54
O-8	46.70 ± 0.34	0.72	55.49 ± 1.82	3.28
O-9	20.09 ± 0.29	1.42	23.85 ± 1.59	6.65
O-10	1.72 ± 0.06	3.67	76.15 ± 1.23	1.62

The figure 4 displays the MRM chromatogram relative to the transitions of the analytes and their labeled internal standards, in a EVOO sample after hydrolysis reaction.

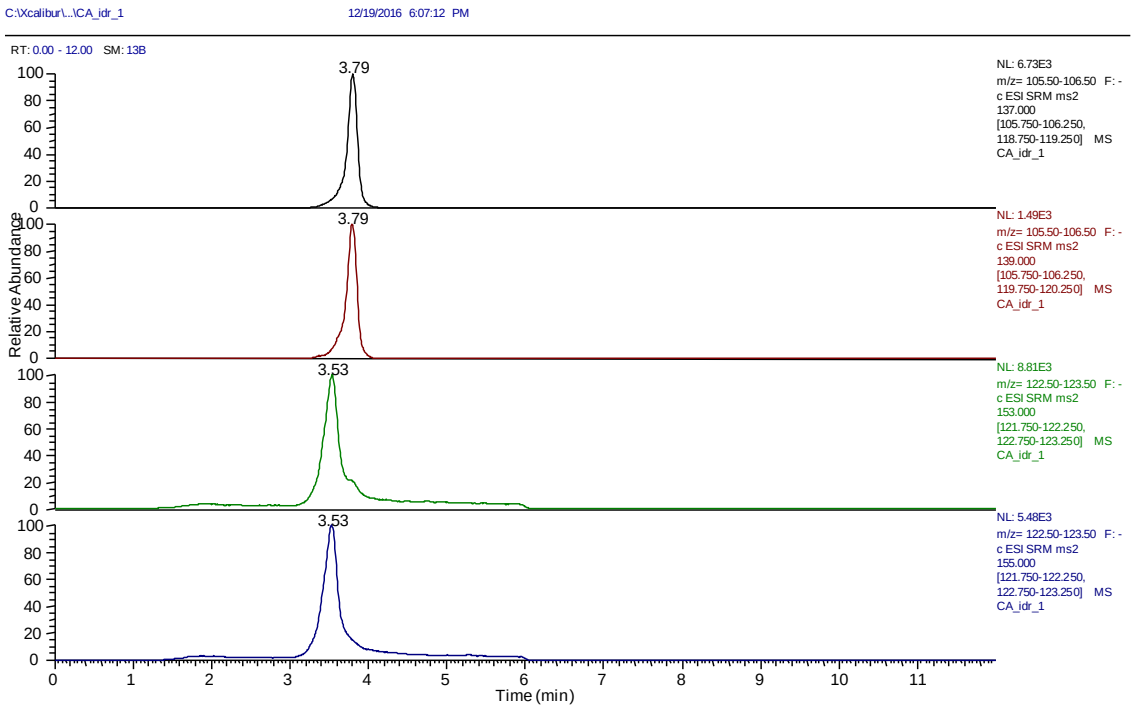

Figure 4 Representative MRM chromatogram of an EVOO sample revealing the signal of labeled and unlabeled standards after the hydrolysis reaction.

It is important to note that the total amount of Htyr and Tyr is the sum of their free form and their ester conjugates compounds. To evaluate the amount of phenylethanoid conjugates a correction on the molecular weight must be performed. First, the concentration of ester conjugates compounds are calculated subtracting the free form concentration from the total concentration (free and ester conjugates compounds) obtained from the two experiments described above. For Htyr derivatives, the result will be divided by the molecular weight of the hydroxytyrosol and multiplied by the average molecular weight of the Htyr ester aglycones, i.e. oleacin and oleuropein aglycone (see figure 1). While for the Tyrosol derivatives, the average molecular weight will be calculated using the molecular weight of oleocanthal and ligstroside aglycone. The secoridoides oleuropein and ligstroside were not considered in the calculation because of their trace concentrations in extra virgin olive oil. (18)

The value obtained above must be added to the amount of Htyr and Tyr in their free form, respectively in order to address the EU regulation.

The final results represent the amount of phenolic compounds present in EVOO, as required by EU directive 432/2012. (2) (table 6).

Table 6 Total amount of Htyr and Tyr per 20 g of oil

EVOO sample	Total Htyr derivatives (mg/kg)	Total Tyr derivatives (mg/kg)	Total amount Htyr and Tyr (free and derivatives) per 20 g of EVOO
O-1	254.13	199.66	9.07
O-2	208.92	201.80	8.21
O-3	173.97	122.11	5.92
O-4	179.67	167.57	6.94
O-5	89.56	181.86	5.43
O-6	42.97	70.35	2.27
O-7	29.72	126.39	3.12
O-8	92.03	117.09	4.18
O-9	40.86	51.65	1.85
O-10	3.89	168.41	3.45

4. CONCLUSION

A fast and reliable methodology to evaluate the amount of free and total hydroxytyrosol and tyrosol in extra virgin olive oil sample was developed. The main features of this method regard the rapidity of the whole experiment procedure, and the accuracy and sensitivity obtained thanks to the use of tandem mass spectrometry and isotope dilution analysis. The use of this methodology allows to assay the exact amount of nutraceutical compounds, providing added value to the oils that contain the amount requested by the EU directive 432/2012.

REFERENCES

1. Owen RW, Giacosa A, Hull WE, Haubner R, Wurtele G, Spiegelhalder B & Bartsch H (2000). Olive-oil consumption and health: the possible role of antioxidants. *Lancet Oncology* 1, 107–112.

2. Alarcon de la Lastra C, Barranco MD, Motilova V & Herrerias JM (2001) Mediterranean diet and health: biological importance of olive oil. *Current Pharmaceutical Design* 7, 933–950.

3. Bianco A & Uccella N (2000) Biophenolic components of olives. *Food Research International* 33, 475–485.

4. Victor R. Preedy, Ronald Ross Watson. (2010) Olives and Olive Oil in Health and Disease Prevention. *Technology & Engineering*

5. Bali EB, Ergin V, Rackova L, Bayraktar O, Kucukboyaci N, Karasu C (2014) Olive leaf extracts protect cardiomyocytes against 4-hydroxynonenal-induced toxicity in vitro: comparison with oleuropein, hydroxytyrosol, and quercetin. *Planta Med* 80(12):984–992

6. Bulotta S, CelanoM, Lepore SM, Montalcini T, Pujia A, Russo D (2014) Beneficial effects of the olive oil phenolic components oleuropein and hydroxytyrosol: focus on protection against cardiovascular and metabolic diseases. *J Transl Med* 12(1):219

7. Caruso, D., Berra, B., Giavarini, F., Cortesi, N., Fedeli, E., & Galli, G. (1999). Effect of virgin olive oil compounds on in vitro oxidation of human low density lipoproteins. *Nutrition, Metabolism and Cardiovascular Diseases*, 9, 102–107.

8. De la Puerta, R., Ruìz-Gutierrez, V., & Hoult, J. R. (1999). Inhibition of leukocyte 5-lipoxygenase by phenolics from virgin olive oil. *Biochemical Pharmacology*, 57, 445–449.

9. COMMISSION REGULATION (EU) No 432/2012: http://eur-lex.europa.eu/LexUriServ/LexUriServ.do?uri=OJ:L:2012:136:0001:0040:EN:PDF

10. http://www.internationaloliveoil.org/documents/viewfile/4141-met29eng

11. Kuwajima, H.; Takai, Y.; Takaishi, K.; Inoue, K. (1998). Synthesis of ^{13}C-labeled possible intermediates in the biosynthesis of phenylethanoid derivatives, cornoside and rengyosides. *Chem. Pharm. Bull. 46* (4), 581–586.

12. Mazzotti, F.; Benabdelkamel, H.; Di Donna, L.; Maiuolo, L.; Napoli, A.; Sindona, G. (2012) Assay of tyrosol and hydroxytyrosol in olive oil by tandem mass spectrometry and isotope dilution method. *Food Chem. 135* (3), 1006–1010.

13. Mulinacci, N.; Giaccherini, C.; Ieri, F.; Innocenti, M.; Romani, A.; Vincieri, F. (2006) F. *J. Sci. Food Agric. 86* (5), 757–764

14. Romero, C.; Brenes, M. (2012). Analysis of total content of Hydroxytyrosol and Tyrosol in olive oil. *J. Agric. Food Chem. 60* (36), 9017–9022.

15. Purcaro, G.; Codony, R.; Pizzale, L.; Mariani, C.; Conte, L. (2014) Evaluation of Total Hydroxytyrosol and Tyrosol in Extra Virgin Olive Oils. *Eur. J. Lipid Sci. Technol. 116*, 805–811.

APPLICATIONS OF PAPER SPRAY IONIZATION MASS SPECTROMETRY FOR RAPID QUALITY ASSESSMENT OF FOOD

The following analytical methodologies are based on the use of the paper spray mass spectrometry (PS-MS), developed by a paper spray source implemented *in house*.

PS-MS analyses were carried out using a triple-quadrupole mass spectrometer MS 320 from Varian (varian Inc., Palo Alto, Ca), originally equipped with an ESI source. The ESI source was removed and it was replaced by an *in house* built source consisting in a high voltage clip and a metallic stage for supporting (Figure 1a).

Whatman paper with a pore size of 11 µm was used to shape triangles, as solid support for sample manual spotting, with the following dimensions: 150 mm base, 250 mm height. The paper triangles were positioned in front of the mass spectrometer inlet similarly to the ESI source needle. The application of a high voltage and few microlitres of polar solvent such as methanol, allows the accumulation of charges at the apex of the paper triangle and the formation of a spray containing charged droplets. The latters, after solvent evaporation generate dry ions (Figure 1b).

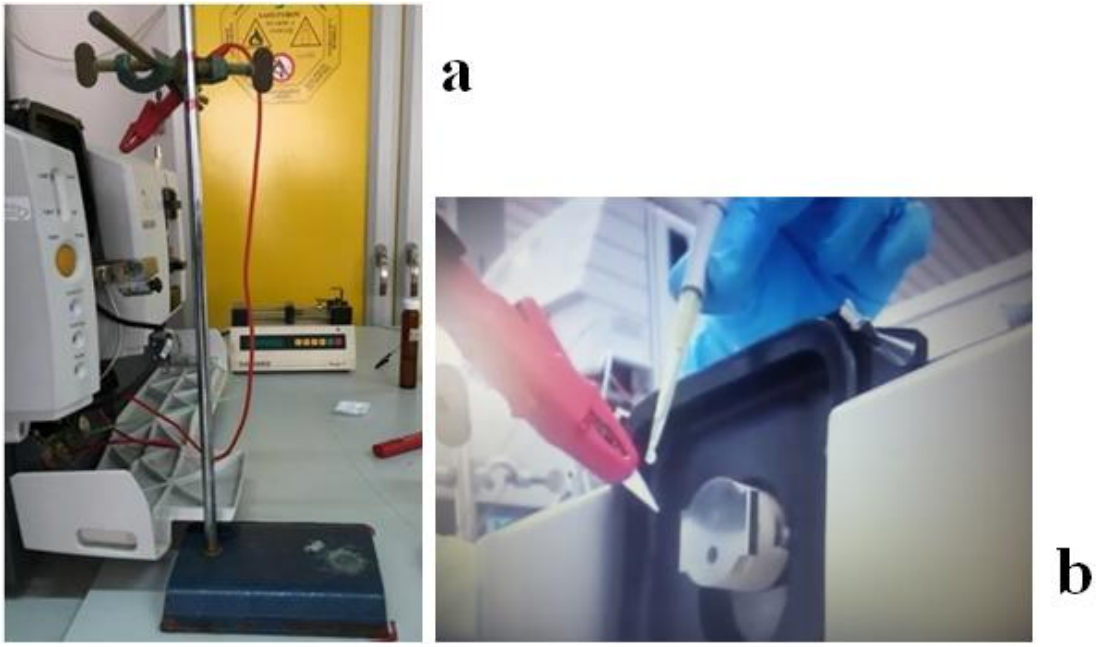

Figure 1 **a)** picture of *in house* implemented open source for PS-MS analysis, b) picture of manual spotting of solvent onto the paper triangle allowing the ionization of analytes

II. Absolute Evaluation of Hydroxytyrosol in Extra Virgin Olive Oil by Paper Spray Tandem Mass Spectrometry

1. INTRODUCTION

A novel approach for the evaluation of the absolute amount of Hydroxytyrosol in extra virgin olive oil has been set up. The method is based on the exploitation of paper spray ionization (PS) tandem mass spectrometry (MS/MS), which allows a fast assay of this active principle. (1-5) Also in this case, the total amount of Htyr has been evaluated summing the content of its free and esterified form.

The quantitative assay was based on the use of tandem mass spectrometry and isotope dilution method, and it was performed in multiple reaction monitoring (MRM) scan mode, following the transition m/z 153 → m/z 123 for hydroxytyrosol and m/z 155 → m/z 123 for labeled internal standard (d_2-hyroxytyrosol). (6)

Unlike the procedure described above, the determination of free form of Hydroxytyrosol was performed directly in matrix, without any extraction step, although, also in this case, to evaluate the total amount of Htyr the hydrolysis procedure was necessary.

The reliability and the accuracy of the proposed approach was evaluated testing the method onto a sample of seed oil spiked with a known amount of hydroxytyrosol and oleuropein. The accuracy values obtained ranged from 92% to 102%.

2. MATERIALS AND METHODS

2.1 Chemicals

Solvents and reagents were commercially available (Sigma-Aldrich, St. Louis, MO).

Labeled internal standard d_2-hydroxytyrosol was obtained by the same synthetic procedure described in the LC-MS/MS above described. (7)

2.2 Olive oil samples

Five extra virgin olive oil samples were purchased in a local market and stored in amber glass bottles at room temperature before the analysis.

2.3 Sample preparation

2.3.1 Determination of free Hydroxytyrosol

Extra virgin olive oil samples were added to 30 μL of a solution of d_2-Hydroxytyrosol at 350 mg/L up to a weight of 1g. The mixture was homogenized by ultra-turrax for three minutes, and directly spotted (15 μL) onto the paper triangle for PS-MS/MS analysis of the free fraction.

2.3.2 Determination of total Hydroxytyrosol

Each extra virgin olive oil sample was added to 30 μL of a solution of d_2-Hydroxytyrosol at 500 mg/L up to a weight of 2 g. The mixture was homogenized vigorously by ultra-turrax for three minutes, and then 1 g was extracted using a solution 1 mL of H_2O (0,1% HCOOH)/EtOH 3:7 v/v. After the extraction step, 500 μL of supernatant were added to 500 μL of HCl 2M in a closed pyrex vessel, and submitted to acid hydrolysis for 4 minutes in a microwave Anton Paar Multiwave 3000 provided with a rotor 4×24 MC, operating at a temperature of 140 °C at the maximum power of 1400 W, for 4 min. The reaction mixture was then stirred to vortex for 1 minute, diluted (1/1) with H_2O (0,1% HCOOH)/EtOH 3:7 v/v and finally spotted (15 μL) onto the paper triangle for PS-MS/MS analysis.

2.4 Paper spray mass spectrometry analysis

Mass spectrometry analyses were carried out in negative ionization mode using a LC 320 triple-stage quadrupole mass spectrometer (Varian Inc., Palo Alto, CA, USA), in-house implemented for PS-MS application (see above).

15 μL of each sample were spotted onto a paper triangle and left to dried for 1 min. The same volume of methanol was added to allow the spray desorption every 30 s for a total run time of 2 min.

The MS working conditions were optimized as following: needle voltage -4500 V; shield -400 V; capillary -90 V; housing temperature 35 °C, and the detector fixed at 1400 V. Collision gas was argon used at a pressure within the collision cell (Q2) of 2 mTorr, while the mass resolution at the first (Q1) and third (Q3) quadrupoles was set at 0.7 u at full width at half-maximum (FWHM). Scan time was set at 0.060 s. Collision energy (CE) was optimized and then set at 22 eV. MRM scan mode was used to quantify the analytes; in

particular, the transition m/z 153 → m/z 123 for hydroxytyrosol and m/z 155 → m/z 123 for the labeled internal standard were monitored. The ion current of each monitored transition, averaged over the total acquisition time, was used for the quantitative analysis.

2.5 LC-ESI-MS/UV analysis

LC-ESI-MS/UV analysis was performed using a Waters FractionLynx system (Milford, MA) working in analytical mode, equipped with a Acquity QDa mass spectrometer and a 2489 UV/visible detector. The chromatographic separation was carried out using a C18 reversed-phase column, Luna (250 × 4.6 mm, 5 μm, Phenomenex), with a flow rate of 1 ml/min. The run time was 50 min and the flow rate was fixed at 1 ml/min, injecting a volume of 1 ml. The eluents were 0.1 % HCOOH (A) and ACN (B). The following linear solvent gradient was applied: from 100% to 85% A in 5 min, to 70% A in 10 min and a plateau of 5 min, to 55% A in 7 min and a plateau of 5 min, to 100% B in 5 min and a final plateau of 3 min. (8)

3. RESULTS AND DISCUSSION

Paper spray is a simple and fast tecniques which allows a direct ionization of analytes with minimum sample treatment and at ambient conditions. Furthermore, the isotope dilution method combined with paper spray tandem mass spectrometry is a powerful tool for the quantification of analytes in complex natural matrices. The reliability of this method was highlighted for several food safety and quality applications. (9-11)

The use of stable isotopes as internal standards in MS assay represents an extremely accurate method for quantification, and the MS/MS experiment in MRM mode assure the greatest specificity.

The mass spectrometry experiment was performed in negative polarity mode according to previous studies on the ionization of this kind of molecules. (12) The transitions monitored were the following: *m/z* 153 → *m/z* 123 for d_0-hydroxytyrosol and *m/z* 155 → *m/z* 123 for d_2-hydroxytyrosol. These transitions were chosen basing on previous MS/MS experiments. (12) The hydroxytyrosol MS/MS spectrum, in negative ion mode, is characterized basically by a single diagnostic product ion at *m/z* 123, also present in the MS/MS spectrum of labeled internal standard d_2-hyroxytyrosol. This product ion results from the formal loss of a formaldehyde unit (Figure 2). (12)

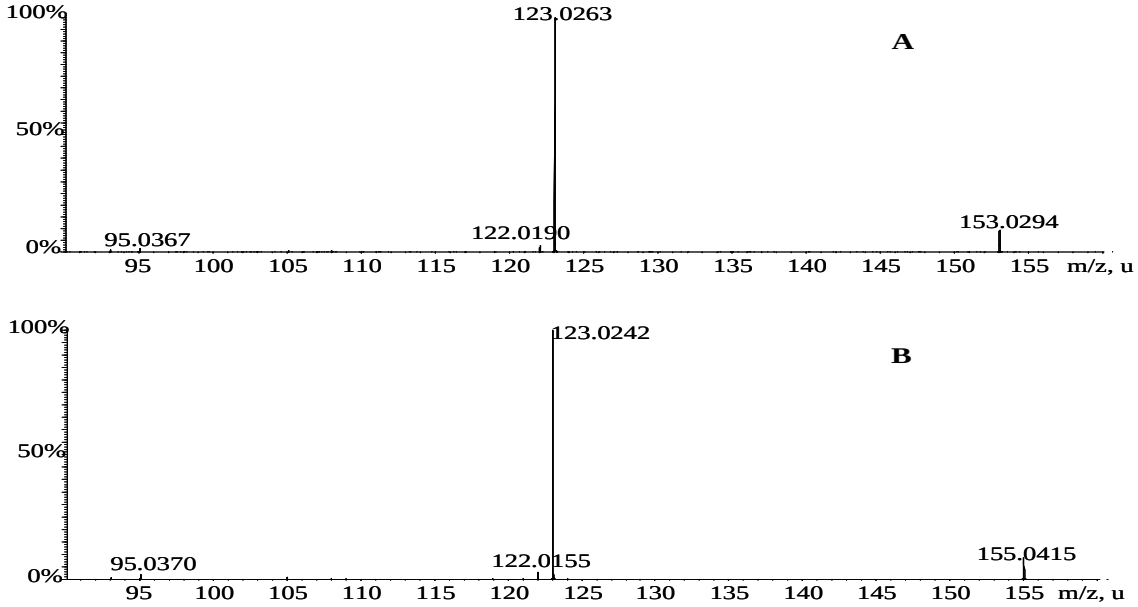

Figure 1 ESI (-) MSMS spectra of compound Htyr (A) and labelled Htyr (B).

The possible mechanism of the fragmentation is reported in Figure 2.

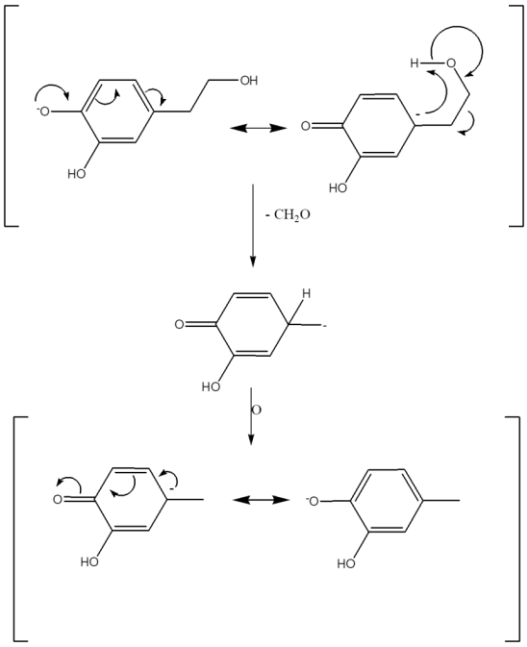

Figure 2 Fragmentation pattern of Hydroxytyrosol. (12)

In the PS-MS experiments, the center of the paper triangle was embedded with the sample solution or directly with few microlitres of sample; after the application of a high voltage, and few microlitres of methanol solvent, a sort of spray of charged droplets was generated

from the tip of the paper. The charged droplets after desolvation process generated dry ions, which were analyzed by mass spectrometer.

For the quantification of the free form of hydroxytyrosol, calibration curve was obtained by artificially adding to corn oil the analyte (Htyr) at concentration ranging between 2.5 and 15 mg/L and the internal standard (d_2-Htyr) at a fixed concentration of 7 mg/L (*in matrix* calibration curve). The equation obtained (y = 0.8047x + 0.1742 R^2=0.9951) by analyzing in triplicate each standard solution showed good linearity.

Figure 3 shows the ion current generated by the monitored gas-phase reactions from the standard solution of Htyr and labeled Htyr at the highest concentration (15 mg/L, Htyr and 7 mg/L, d_2-Htyr). The average ion currents over the total scan, were used for quantitative analyses.

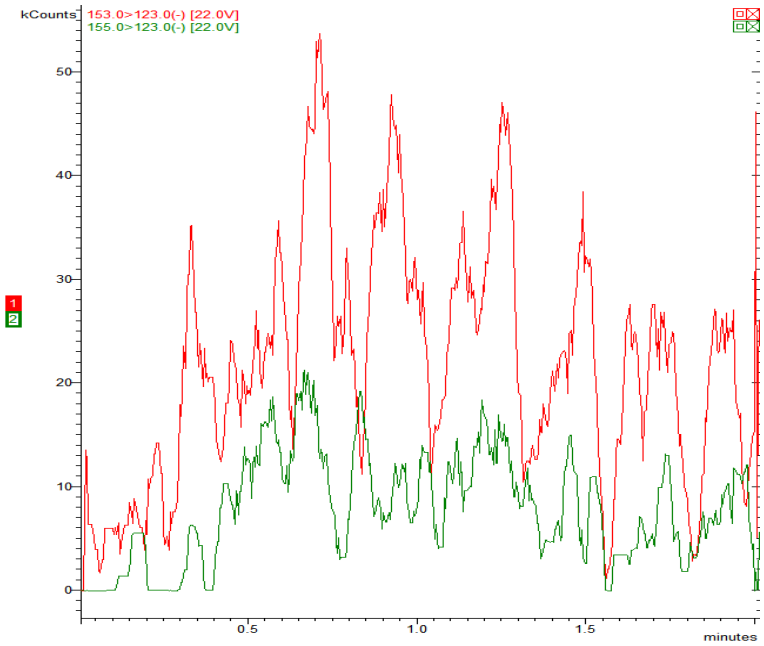

Figure 3 Ion current of MRM monitored transitions, respectively for Htyr (red) and d_2-Htyr (green) in the calibration curve sample at higher concentration

The accuracy values for the quantification of Htyr in its free form, was calculated preparing two fortified corn oil samples at two level of analyte concentration, 4 mg/kg and 16 mg/kg respectively, which represent the upper and the lower limits of the calibration curve. The accuracy values ranged from 93% to 103%, and the RSD values, lower than 7%, highlighted the precision of the methodology (Table 1).

Table 1 Accuracy values performed on spiked seed oils

Spiked samples (mg/kg)	Found concentration (mg/kg)	Accuracy (%)	RSD (%)
S1 4 mg/kg	3.72 ± 0.22	93.00	6.14
S2 16 mg/kg	16.42 ± 0.78	102.63	4.73

Hence, the developed method was applied to five real samples purchased from different local oil producers. After the addition of an opportune amount of labeled internal standard, the samples were directly submitted to PS-MS/MS analysis. The results are reported in Table 2.

Table 2 Amount of free Htyr in real samples

EVOO samples	Amount of free Htyr (mg/kg)	RSD (%)
Oil 1	2.81 ± 0.07	2.40
Oil 2	5.84 ± 0.13	2.20
Oil 3	6.35 ± 0.18	2.76
Oil 4	2.45 ± 0.11	4.50
Oil 5	Not detected	-

The limit of detection (LOD) and the limit of quantitation (LOQ) were calculated following the directives of IUPAC and the American Chemical Society's Committee on Environmental Analytical Chemistry, using the following equations:

$S_{LOD} = S_{RB} + 3\sigma_{RB}$

$S_{LOQ} = S_{RB} + 10\sigma_{RB}$

where S_{LOD} is the signal at the limit of detection, S_{LOQ} is the signal at the limit of quantitation, S_{RB} is the ratio of the signals given by the transitions of the analyte and of the internal standard from the blank sample (corn oil), and σ_{RB} is its standard deviation.

The concentrations were calculated by the standard curve (Table 3).

Table 4 Limit of detection and quantification values

	mg/kg
LOD	0.04
LOQ	0.81

Limit of quantification and limit of detection values demonstrate the sensitivity of the proposed method.

For the quantitative assay of total amount of hydroxytyrosol, oil samples were submitted to the same hydrolysis procedure described previously above. After the addition of the internal standards, 1g of each sample was extracted with 1 mL of acidic EtOH/H_2O; the final solution was diluted 1/1 with 2M hydrochloric acid for the microwave assisted hydrolysis reaction.

After the hydrolysis experiment, the solution obtained was directly spotted onto the paper triangle for PS-MS analysis, which was carried out at the same conditions used for the quantification of hydroxytyrosol in its free form.

Calibration curve was obtained by injecting standard solutions of analyte and internal standard. The concentration of the analyte in the standard solution ranged from 2.5 and 15 mg/L, while that of the internal standard (d_2-Htyr) was fixed at 5 mg/L. The equation obtained ($y = 1.4621x - 0.1591$ $R^2=0.9984$) by analyzing in triplicate each solution showed good linearity.

In order to verify the accuracy of the proposed method, a corn oil sample was fortified with Htyr and oleuropein. In particular, corn oil was prepared at 20 mg/kg of Htyr and 300 mg/kg of oleuropein. The sample was submitted to the hydrolysis reaction, opportunely diluted and directly analyzed by PS-MS. The accuracy value obtained is reported in Table 4.

Table 5 Accuracy values for hydrolysis procedure, preformed on fortified corn oil sample

		Spiking concentration (mg/Kg)	Accuracy (%)	RDS (%)
Fortified corn oil	Htyr	20	95.51	6.25
	Oleuropein	300		

The calculated values (Table 5) of LOQ and LOD, corresponding to 4.63 mg/kg and 3.51 mg/kg, also in this case show that the method for the quantification of total amount of Htyr in olive oil provides a good sensitivity.

Table 6 LOD and LOQ values for assay of total amount of Htyr

	mg/kg
LOD	3.51
LOQ	4.64

Total hydroxytyrosol amounts found in real samples are summarized in Table 6.
Each EVOO sample was analyzed in triplicate.

Table 7 Amount of total Htyr in real samples

EVOO samples	Amount of total Htyr (mg/kg)	RSD (%)
Oil 1	77.78 ± 1.95	2.50
Oil 2	28.55 ± 1.94	6.80
Oil 3	38.08 ± 0.88	2.33
Oil 4	19.26 ± 1.68	8.72
Oil 5	5.04 ± 0.64	12.70

For all the analyzed samples, and for both free and total Htyr, the RSD % values were lower than 13%, confirming the good repeatability of the developed approach.
The reproducibility of the measurements was evaluated by analyzing two samples in triplicate over a period of one week, ad also in this case the RSD % values were lower than 13%

Finally, to demonstrate the validity of the PS-MS/MS method, the real samples were also submitted to a classical HPLC-UV analysis. The results obtained were very similar to those obtained by PS-MS/MS analysis (Table 7).

Table 8 Amount of total Htyr obtained by PS-MS/MS and LC-UV analysis

EVOO samples	Amount of total Htyr (mg/kg) PS-MS/MS analysis	LC-UV analysis
Oil 1	77.78 ± 1.95	83.36
Oil 2	28.55 ± 1.94	26.74
Oil 3	38.08 ± 0.88	38.10
Oil 4	19.26 ± 1.68	21.52
Oil 5	5.04 ± 0.64	Not detected

4. CONCLUSION

In conclusion, a fast and reliable method for the quantification of free and total hydroxytyrosol in extra virgin olive oil was developed. The results obtained highlighted that the methodology may be a valid and more rapid alternative to the commonly used analytical method, such as HPLC-UV technique. The working time for each sample analysis, including sample preparation step, is shorter than 15 min, considering that the acquisition time for the MRM experiment is 2 min. The analytical parameters and the direct comparison with HPLC-UV analysis confirm the reliability and accuracy of the developed PS-MS/MS method.

REFERENCES

1. Bali EB, Ergin V, Rackova L, Bayraktar O, Kucukboyaci N, Karasu C (2014) Olive leaf extracts protect cardiomyocytes against 4-hydroxynonenal-induced toxicity in vitro: comparison with oleuropein, hydroxytyrosol, and quercetin. *Planta Med* 80(12):984–992

2. Bulotta S, CelanoM, Lepore SM, Montalcini T, Pujia A, Russo D (2014) Beneficial effects of the olive oil phenolic components oleuropein and hydroxytyrosol: focus on protection against cardiovascular and metabolic diseases. *J Transl Med* 12(1):219

3. Caruso, D., Berra, B., Giavarini, F., Cortesi, N., Fedeli, E., & Galli, G. (1999). Effect of virgin olive oil compounds on in vitro oxidation of human low density lipoproteins. *Nutrition, Metabolism and Cardiovascular Diseases*, 9, 102–107.

4. De la Puerta, R., Ruìz-Gutierrez, V., & Hoult, J. R. (1999). Inhibition of leukocyte 5-lipoxygenase by phenolics from virgin olive oil. *Biochemical Pharmacology*, 57, 445–449.

5. COMMISSION REGULATION (EU) No 432/2012: http://eur-lex.europa.eu/LexUriServ/LexUriServ.do?uri=OJ:L:2012:136:0001:0040:EN:PDF

6. Mazzotti, F.; Benabdelkamel, H.; Di Donna, L.; Maiuolo, L.; Napoli, A.; Sindona, G. (2012) Assay of tyrosol and hydroxytyrosol in olive oil by tandem mass spectrometry and isotope dilution method. *Food Chem. 135* (3), 1006–1010.

7. Kuwajima, H.; Takai, Y.; Takaishi, K.; Inoue, K. (1998). Synthesis of ^{13}C-labeled possible intermediates in the biosynthesis of phenylethanoid derivatives, cornoside and rengyosides. *Chem. Pharm. Bull. 46* (4), 581–586.

8. Mulinacci, N.; Giaccherini, C.; Ieri, F.; Innocenti, M.; Romani, A.; Vincieri, F. (2006) F. *J. Sci. Food Agric. 86* (5), 757–764

9. Di Donna, L.; Taverna, D.; Indelicato, S.; Napoli, A.; Sindona, G.; Mazzotti, F. (2017) Rapid assay of resveratrol in red wine by paper spray tandem mass spectrometry and isotope dilution. *Food Chem.* 229, 354-357

10. Taverna, D.; Di Donna, L.; Mazzotti, F.; Policicchio B.; Sindona, G.; (2013) High-throughput determination of Sudan Azo-dyes within powdered chili pepper by paper spray mass spectrometry. J. *Mass Spectrom.* 48, 544–547

11. Mazzotti, F.; Di Donna, L.; Taverna D.; Nardi M.; Aiello D.; Napoli, A.; Sindona, G. (2013). Evaluation of dialdehydic anti-inflammatory active principles inextra-virgin olive oil by reactive paper spray mass spectrometry. *International Journal of Mass Spectrometry* 352, 87– 91

12. Mazzotti, F.; Benabdelkamel, H.; Di Donna, L.; Maiuolo, L.; Napoli, A.; Sindona, G. (2012) Assay of tyrosol and hydroxytyrosol in olive oil by tandem mass spectrometry and isotope dilution method. *Food Chem. 135* (3), 1006–1010.

III. Discriminant Analysis of Vegetables Oils by Paper Spray Mass Spectrometry and Statistical Approach

1. INTRODUCTION

As already discussed, extra virgin olive oil is considered a functional food and a most popular ingredient of the Mediterranean diet; its success is due to its potential health benefits and its unique taste and flavour. (1,2)

The authenticity of olive oil is associated with genetic variety, geographical origin, and/or quality grade. (3) As regards of the latter aspect, various types of olive oils can be distinguished. The European Union Regulation defines several categories of virgin olive oil: extra virgin olive oil (EVOO), virgin olive oil (VOO), and lampante virgin olive oil (LVOO). Additionally, refined olive oil (ROO, refined VOO), and olive oil (OO, a mixture of ROO and VOO) are recognized. Olive pomace oils are classified as crude olive pomace oil (COPO, solvent-treated olive pomace), refined olive pomace oil (ROPO, refined COPO), and olive pomace oil (OPO, a mixture of ROPO and VOO). (4)

Extra virgin olive oil is much more expensive than other vegetable oils and, certainly, this is the cause of adulteration with lower grade seed, nut, pomace and refined oils.

Vegetable oils are a complex mixture containing a wide range of compounds, but principally, they are composed of triacylglycerols (TAGs) which represent the 95-98% of the whole oil composition and lower amount of diacylglycerols, free fatty acids (FAs), phospholipids and other minor component. TAGs consist of a glycerol molecule linked to three chain fatty acid residues. The variability of TAGs composition is due to the number and kind of free fatty acid combinations on the glycerol skeleton and the occurrence of positional isomers. TAGs profile can represent a fingerprinting of the vegetable oil, and the variation in TAGs composition after adulteration process can be used to evaluate the quality and the authenticity of the oil. (5,6)

Different analytical methods were developed for qualitative and quantitative determination of triacylglycerols in vegetable oils; classical spectroscopy methods such as Raman spectroscopy, nuclear magnetic resonance and infrared, liquid and gas chromatography techniques hyphenated with mass spectrometry. (7)

The latter, often require a laborious sample preparation step and a long time of analysis due to the complexity of TAGs composition. Today, there is continuing need for improved methods for assessing the adulteration in a fast and reliable way. Recently for example,

direct infusion MS methods using ESI and APCI sources with triple quadrupole (QqQ), quadrupole–time-of- flight (Q-TOF), or ion trap as mass analyzers have been developed. (7,8) In addition to the latter, also ambient mass spectrometry method using DART ionization was proposed. (9) Although the use of direct infusion methods allows eliminating the chromatographic separation step, the sample needs to be treated and purified before the analysis. Whereas, the ambient ionization source involves minimal or no sample preparation step.

In this study the ability of paper spray mass spectrometry to characterize the TAGs profile of different vegetables oil was investigated. Some encouraging data were obtained in combination with the chemometric analysis (Linear Discriminant Analysis – LDA and Soft Independent Modeling of Class Analogy – SIMCA) which have allowed to discriminate the extra virgin olive oil from the others vegetable oils commonly used as adulterants. Figure 1 shows the workflow of presented procedure: vegetables oils were submitted to PS-MS analysis, the TAGs profiles were used for chemometric analysis which has allowed the discrimination between the oils.

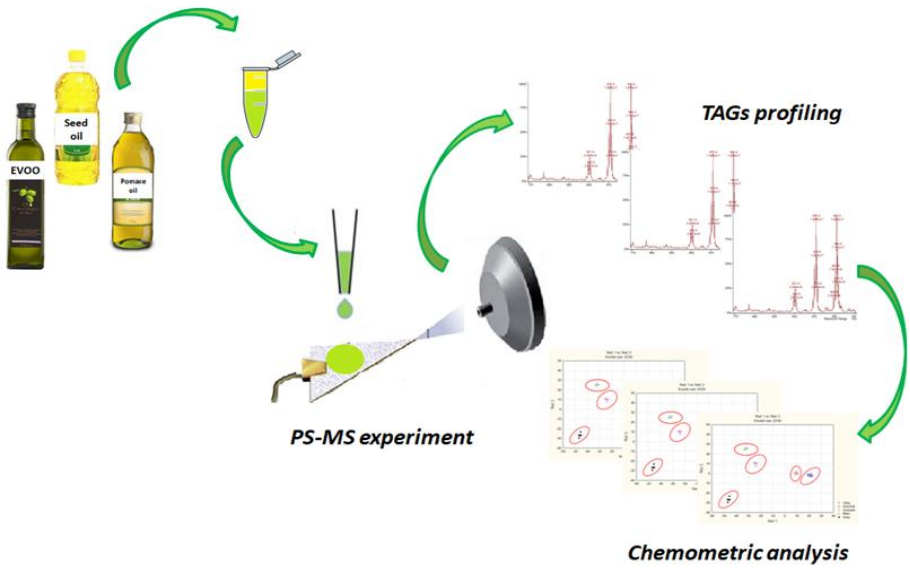

Figure 1 Workflow of developed methodology

2. MATERIALS AND METHODS

2.1 Chemicals

Reagents and solvents were commercially available (Sigma-Aldrich, St. Louis, MO).

2.2 Vegetable oil samples

The methodology was tested on N=10 samples of EVOO; N=10 samples of four different seed oils: corn, sunflower, peanut and soybean oils; N=10 samples of four cultivars from Puglia region (Southern of Italy): Peranzana, Coratina, Ogliarola, Cima di Mola. Seed oils sample were purchased in the local markets, while sample of extra virgin olive oil was obtained from the Research centre for Olive Growing and olive Oil Industry – CREA – Rende, Italy

2.3 Sample preparation

100 mg of each oil sample was treated with 200 mg of ammonium acetate, and then 500 µl of acetone was added to the mixture. The solution was stirred by vortex for 30 sec and 15 µL of the supernatant was directly deposited (manual spotting) onto the paper triangle, left to dry for 30 sec and analyzed by PS-MS.

2.4 Paper spray mass spectrometry analysis

Vegetable oils were analyzed using a triple quadrupole mass spectrometer MS 320 from Varian (Varian Inc., Palo Alto, Ca), equipped with a paper spray source developed *in house*.

15 µL of each sample were spotted onto a paper triangle and left to dry for 1 min. The same volume of methanol was added to allow the spray desorption every 15 s for a total acquisition time of 2 min.

The MS working conditions were the following: needle voltage 5000 V; shield 800 V; capillary 100 V; housing temperature 35 °C. Measurements were performed in full scan mode within 800 -1100 mass range, using positive polarity, with the detector fixed at 1400 V. For ESI (+) MS/MS investigations, collision energy was set at 25-35 eV, collision gas was argon used at a pressure within the collision cell (Q2) of 2 mTorr.

The mass resolution at the first (Q1) and third (Q3) quadrupoles was set at 0.7 u at full width at half-maximum (FWHM). Scan time was set at 0.1 sec.

2.5 Statistical analysis

Classification was performed by two multivariate chemometric techniques: linear discriminant analysis (LDA) and soft independent modeling of class analogy (SIMCA). LDA was carried out by Statistica 7.1 (StatSoft 2005 edition), and SIMCA was executed by V-Parvus 84 2004.

3. RESULTS AND DISCUSSION

Paper spray mass spectrometry was developed as a direct, fast and low-cost sampling and ionization method for the analysis of complex mixtures. This MS technique is now applied for the first time to the analysis of triacylglycerols profile for the identification and discrimination of vegetables oils.

Each oil sample was treated with ammonium acetate and then extracted with acetone. Ammonium acetate is a charge-transfer dopant, and its use is necessary because provides a significant improvement of TAGs signals compared to the intensity of the protonated molecules $[M+H]^+$ which are very low.

Several experiments were performed for the optimization of the weight ratio between oil and ammonium acetate to obtained a better ionization efficiency. The best result was obtained using a weight ratio of 1:2 preparing the sample as following: 50 mg of vegetable oils, 100 mg of ammonium acetate and 250 µl of acetone.

The sample preparation step is very simple and fast, considering that the homogenization and extraction time is 2 min, and there is no need for centrifugation.

The second part of the experiment was designed to optimize PS-MS experiment conditions. In particular, the voltage applied to the paper triangle, capillary voltage and scan time, which were set at 5000 V, 100 V and 0.1 s/scan, respectively.

PS-MS measurements were carried out in full scan mode, using positive polarity. 15 µl of acetone solution containing triacylglycerols fraction, were spotted onto the center of paper triangle, and after drying, 15 µl of methanol were spotted each 15 s for 2 min, to obtained

the desorption of ions. The total acquisition time was 2 min, and including the sample preparation, the whole experiment time is 5 min.

Ten samples of each different oils were analyzed by PS-MS: extra virgin olive oil, corn oil, soybean oil, sunflower oil, peanut oil.

The MS spectra were recorded in positive polarity within 800-1100 Da mass range showing the NH_4^+ adduct ions of TAGs. PS-MS profiling produces mass spectra highlighting similarity and differences among vegetables oils.

The Figure 2 shows the PS-MS mass spectrum of extra virgin olive oil. The full scan spectrum displays an almost unique molecular profile in the investigated mass range; the most intense TAGs ammonium adducts present are at m/z 850, m/z 876, m/z 902.

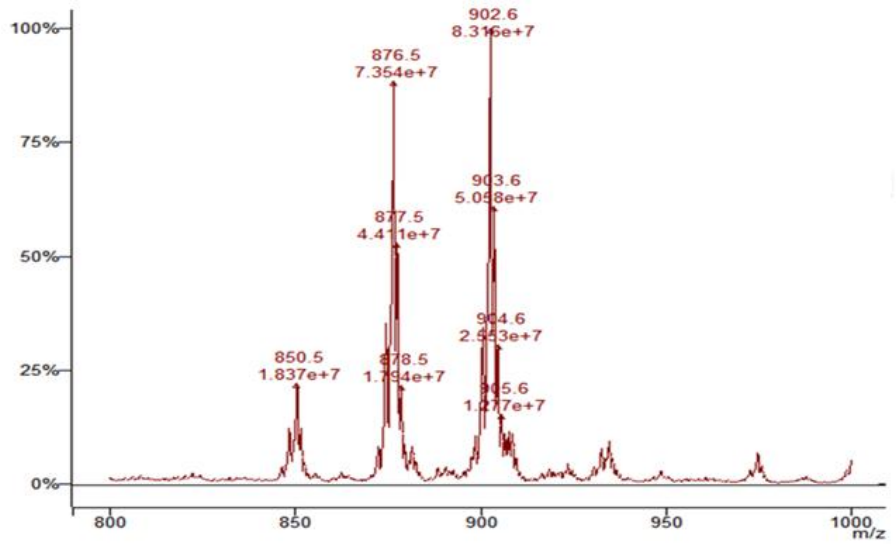

Figure 2 PS (+) -MS spectrum of TAGs profile in a representative EVOO sample

PS-MS TAGs fingerprinting of others vegetable oils, considered potential adulterants are shown in Figure 3.

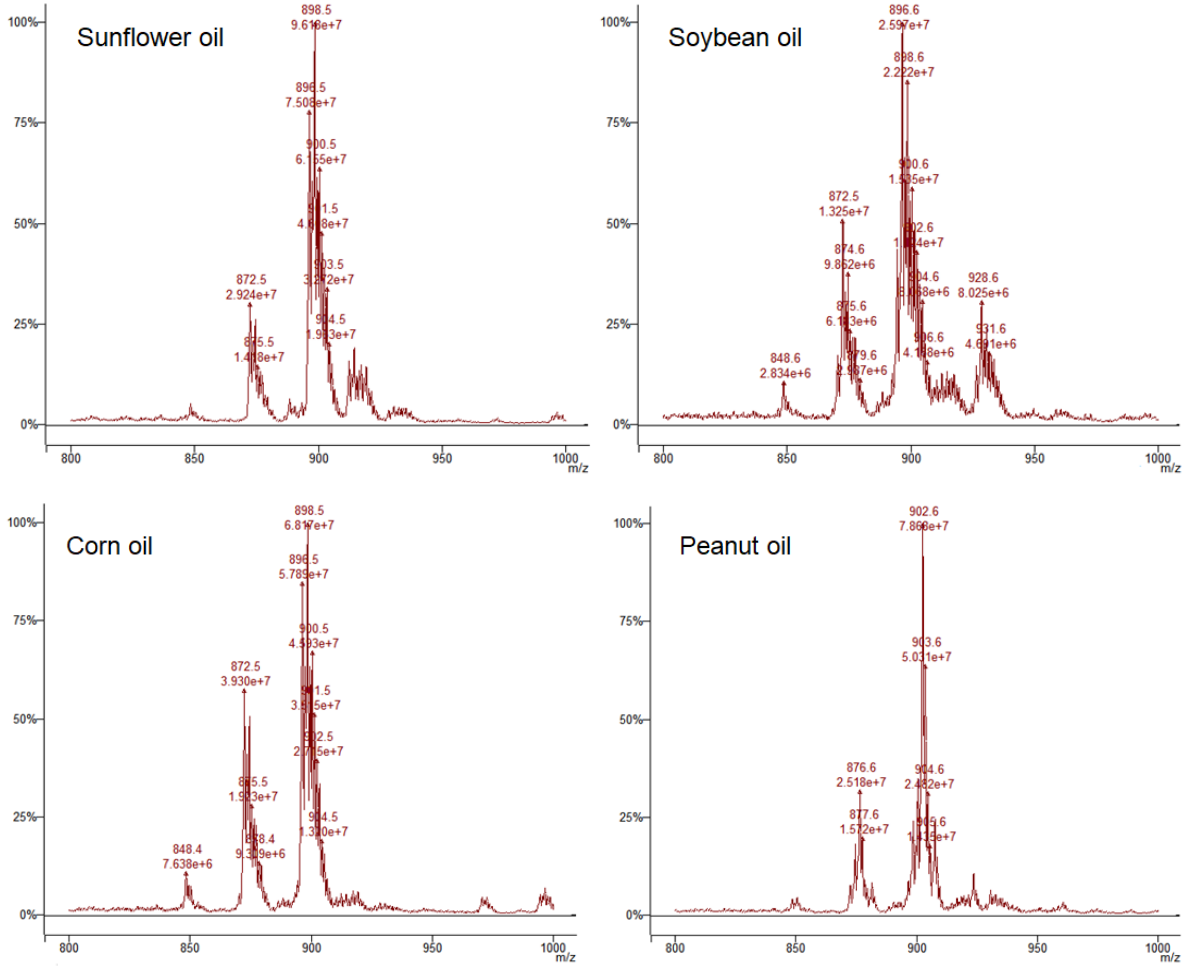

Figure 3 TAGs profile of different seed oils

The TAGs profile of vegetable oils which can be used as adulterants, such as sunflower, soybean and corn oil, show different most intense peaks respect to the olive oil. For example, the most intense TAGs ammonium adducts ions for soybean oil are at m/z 872, m/z 896 and m/z 898. Whereas, the TAGs mass spectrum of peanut oil highlights many similarity with the mass spectrum obtained from the olive oil; in fact the main representative ions are at m/z 876 and m/z 902.

Although not necessary for vegetable oils classification, PS (+) MS/MS experiments were performed to identify the diagnostic quasi molecular ions of each oil sample from their fragmentation pattern. MS/MS experiments were performed in a range of collision energy (from 25eV to 40eV) in order to obtained structural information.

Figure 4 displays the PS (+) MS/MS spectrum of the diagnostic ion at m/z 902 identified as triolein OOO, trioleoylglycerol. This ions is the most abundant in the MS spectrum of EVOO samples and peanut oil samples.

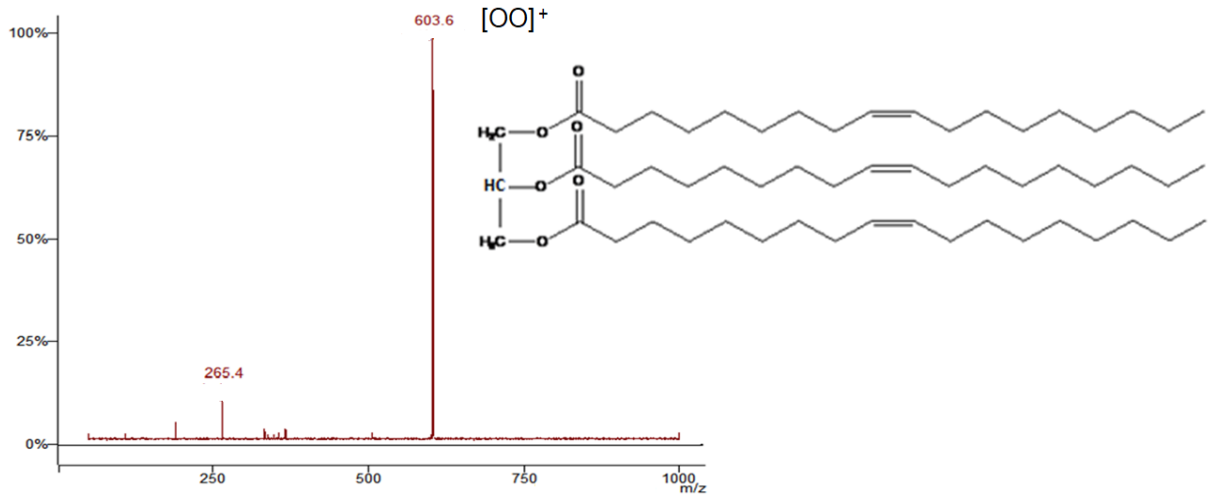

Figure 4 PS-MS/MS spectrum of triolein

As in the case of triolein, the MS/MS spectra of monoacid TAGs are relatively simple, because contain single diacylglycerol fragment ion and a single acylium ion. For the triolein in fact, the main ions present are that at m/z 603 that corresponds to the diacylglycerol ion $[OO]^+$, and the acylium ion at m/z 265, O^+.

The MS/MS of TAGs containing two different fatty acids, shows two diacylglycerol ions, as well as two acylium ion. While, the tandem mass spectrum of isobaric TAGs shows the presence of at least four diacylglycerol ions. For example, the ion at m/z 874 corresponds to two TAGs, OOPo and LOP (Figure 6).

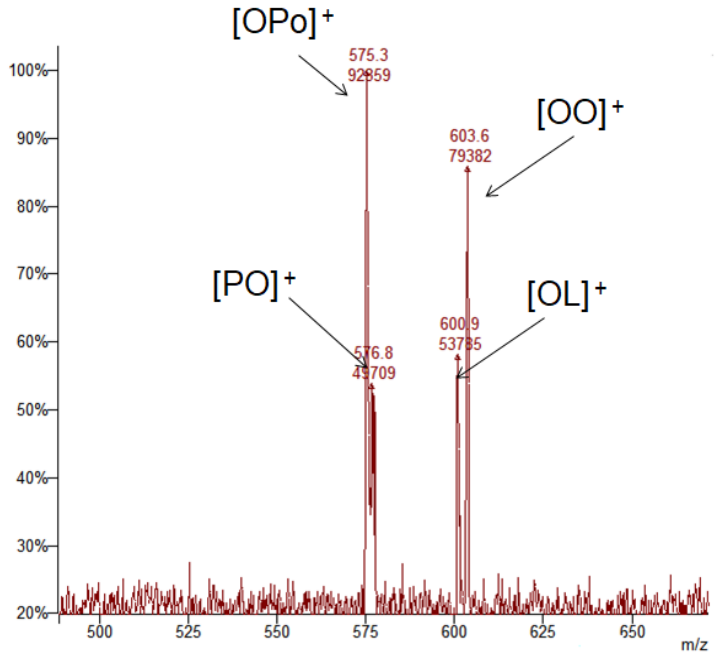

Figure 6 Diacylglycerol ions obtained by PS-MS/MS experiment of ion at m/z 874

Table 1 displays the most abundant triacylglycerols found in the vegetable oils, identified by paper spray tandem mass spectrometry experiments.

Table 1 Diagnostic $[M+NH_4]^+$ ions observed from the PS-MS/MS spectra

$[M+NH_4]^+$ m/z	**TAG**	**Vegetable oils**
850	POP	EVOO
872	LLP LnOP	corn oil sunflower oil soybean oil
874	LOP OOPo	EVOO
876	OOP	EVOO peanut oil
896	LLL	soybean oil
898	LLO OLnO	corn oil sunflower oil
900	OLO	corn oil sunflower oil soybean oil
902	OOO	EVOO peanut oil

P= Palmitic, Po= Palmitoleic, L= Linoleic, Ln= Linolenic, O= Oleic

These experiments confirm the ability of paper spray mass spectrometry technique not only to obtain fast molecular fingerprinting, but also for the molecular identification through tandem mass spectrometry experiments.

Statistical analysis

In order to differentiate the extra virgin olive oil from others vegetable oils considered potential adulterants, it is important to find a systematic, reproducible, and reliable method. This goal can be achieved by using multivariate statistical analysis.

In particular, in this work statistical analysis was carried out by two supervised chemometric tecniques: Linear Discriminant Analysis – LDA and Soft Independent Modeling of Class Analogy – SIMCA. The two approaches allowed to obtain classification rules to distinguish EVOO from other vegetable oils.

The two chemometric techniques were applied to the data matrix of the abundances of all ions acquired in the mass range m/z 800-1100. In particular, total ion current of each analysis was averaged over the total scan, and the absolute abundance of each ion was normalized to the sum of the abundances of all the ions in the range.

Linear discriminant analysis (LDA) is one of the most commonly used classification techniques. It defines a set of delimiters (depending on the number of considered categories) so that the multivariate space of the objects is divided in as many subspaces as the number of classes. Discriminant functions are obtained as a linear combination of descriptor that maximizes the ratio of variance between categories to variance within categories. In classification techniques such as LDA, even if the samples that will be predicted by LDA did not belong to any of the categories of the model, each object will be assigned anyway to one of them. Moreover, each object can fall into one and only one category because the multidimensional space is divided into many subspaces as classes.

LDA analysis were applied by considering all the ions in the acquired mass range (m/z 800-1100). Nevertheless, it means that several noise variables could be considered in the construction of the models. For this reason LDA class-modeling technique was again evaluated after a preliminary selection of relevant variables by means of stepwise linear discriminant analysis (S-LDA).

In this technique, the most significant variables involved in sample differentiation were selected using a Wilks' λ as a selection criterion. Accordingly, selection of the variables was performed by Stepwise LDA to discard redundant information and to select only those

variables that actually contributed to increase of classification ability. Again, the cross-validation procedure was performed in order to verify the goodness of the method in terms of prediction ability. (10-14)

Soft Independent Modeling of Class Analogy (SIMCA) is a class modeling technique in which an object can belong to one category, to more than one class simultaneously or to none of the categories. An important consequence of this feature is that SIMCA is able to detect the number of false positives/negatives for each class. Therefore, two parameters to validate the classification can be defined: sensitivity (SENS) and specificity (SPEC). SENS of a class is referred to the percentage of objects belonging to the class correctly accepted by the class model. SPEC of a class corresponds to the percentage of objects not belonging to the class correctly rejected by the class model. (15) In this work SIMCA analysis was performed using the variables selected by means of S-LDA.

The 2D – LDA plot calculated from PS-MS spectral data for different vegetables oils is shown in Figure 7.

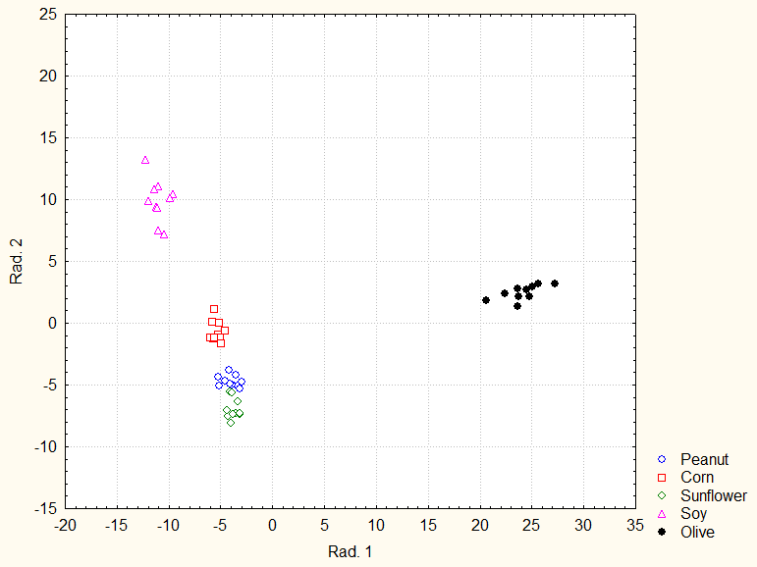

Figure 7 2D-LDA score plot of different vegetable oils

The Stepwise-LDA has retained 11 variables: the ion at m/z 850, 894, 873, 897, 886, 875, 899, 849, 881, 892, 907. Not all 11 variables were identified by tandem mass spectrometry but they can be ascribed to the vegetables oil molecular composition because these ions were not detected within the blank paper experiment, performed out using just solvent.

Again, the cross-validation procedure was performed in order to verify the goodness of the method in terms of prediction ability. The model has correctly predicted all samples for

each category and this suggests that the presented method may be a potential choice for discriminating EVOO from other vegetable oil as peanut oil, corn oil, soybean oil and sunflower oil. (Table 2).

Table 2 Number of correctly classified pure vegetable oil samples (prediction matrices) for Stepwise LDA

Stepwise LDA[a]

	Peanut	**Corn**	**Sunflower**	**Soy**	**Olive**
Peanut	10	0	0	0	0
Corn	0	10	0	0	0
Sunflower	0	0	10	0	0
Soy	0	0	0	10	0
Olive	0	0	0	0	10

[a] 11 variables retained after S-LDA (m/z 850, 894, 873, 897, 886, 875, 899, 849, 881, 892, 907 in decreasing order of discriminating capacity)

SIMCA analysis were based on 8 variables selected by means S-LDA, which in this case are the ions at m/z 850, 894, 897, 886, 875, 899, 849, in decreasing order of discriminating capacity. Validation of the model was carried out by a 5-fold cross-validation procedure. The SIMCA model has allowed the correct classification of all samples for each category and, moreover, has provided excellent sensitivity (100%) and specificity (100%) (Table 3).

Table 3 Number of correctly classified pure vegetable oil samples (prediction matrices) for SIMCA

SIMCA performed using the variables selected by means of S- LDA[b]

	Peanut	**Corn**	**Sunflower**	**Soy**	**Olive**	**SENS(%)**	**SPEC(%)**
Peanut	9	1	0	0	0	100	100
Corn	0	10	0	0	0	100	100
Sunflower	0	0	10	0	0	100	100
Soy	0	0	0	10	0	100	100
Olive	0	0	0	0	10	100	100

[b] 8 variables retained after S-LDA (m/z 850, 894, 873, 897, 886, 875, 899, 849 in decreasing order of discriminating capacity)

The next step was used to verify if the presented method can be applied for recognizing the adulteration of extra virgin olive oil. For this purpose, ten mixture samples of EVOO and different seed oils were prepared. In particular, PS-MS analysis were performed on N=10 samples consisting of olive oil 80% - peanut oil 20%, N=10 samples of olive oil 80% - soybean oil 20%, N=10 of olive oil 80% - corn oil 20%, and N=10 samples consisting of olive oil 80% - sunflower oil 20%.

2D-LDA plot obtained by PS-MS spectra of pure olive oil and mixture is shown in Figure 8. Also in this case the cluster corresponding to EVOO samples is well distinguished by other clusters.

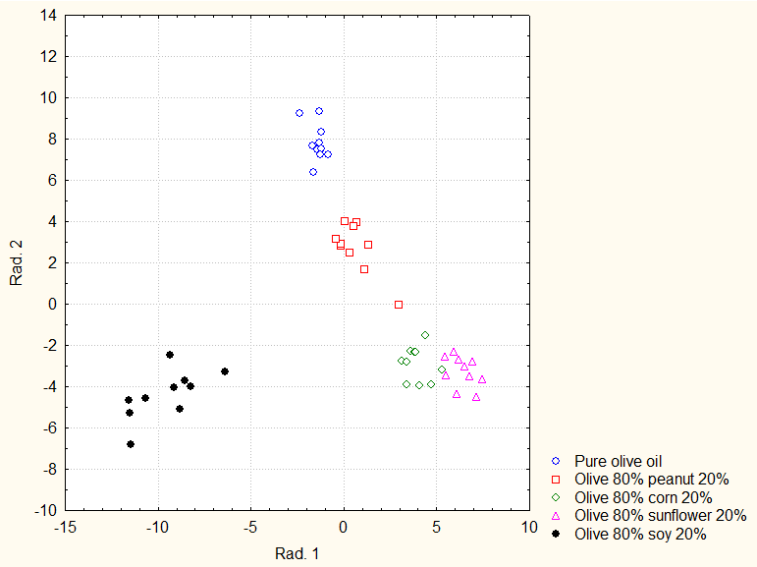

Figure 8 2D-LDA score plot pure olive oil and adulterated oil

In this experiment, the Stepwise-LDA has retained 10 variables: the ion at m/z 894, 896, 918, 872, 900, 847, 898, 922, 859, 925, in decreasing order of discriminating capacity.
With the cross-validation procedure, the model has classified correctly all the extra virgin olive oil, and almost of mixture oils, only two mixture of peanut oil samples were includes in the mixture of corn oil category (Table 4).

Table 4 Number of correctly classified pure vegetable oil samples (prediction matrices) for Stepwise LDA

Stepwise LDA[a]

	Olive 80% peanut 20%	**Olive 80% corn 20%**	**Olive 80% sunflower 20%**	**Olive 80% soy 20%**	**Pure olive oil**
Olive 80% peanut 20%	8	2	0	0	0
Olive 80% corn 20%	0	10	0	0	0
Olive 80% sunflower 20%	0	0	10	0	0
Olive 80% soy 20%	0	0	0	10	0
Pure olive Oil	0	0	0	0	10

[a] 10 variables retained after S-LDA (m/z 894, 896, 918, 872, 900, 847, 898, 922, 859, 925 in decreasing order of discriminating capacity)

SIMCA analysis has provided also in this case, excellent sensitivity and specificity. (Table 5)

Table 5 Number of correctly classified pure vegetable oil samples (prediction matrices) for SIMCA

SIMCA performed using the variables selected by means of S-LDA[b]

	Olive 80% peanut 20	**Olive 80% corn 20%**	**Olive 80% sunflower 20%**	**Olive 80% soybean 20%**	**Pure olive oil**	**SENS(%)**	**SPEC(%)**
Olive 80% peanut 20%	9	0	1	0	0	90	100
Olive 80% corn 20%	0	10	0	0	0	100	100
Olive 80% sunflower 20%	0	0	10	0	0	100	100
Olive 80% soybean 20%	0	0	0	10	0	100	100
Pure olive oil	0	0	0	0	10	100	100

[b] 8 variables retained after S-LDA (m/z 894, 896, 918, 872, 900, 847, 898, 922 in decreasing order of discriminating capacity)

Even in this case, the value of sensitivity and specificity are considered excellent. Almost the samples were classified correctly, only one sample of mixture olive oil 80% - peanut oil 20% was included in the soybean mixture category.

The same approach was tested to discriminate EVOO belonging to four Cultivar produced in Puglia region (Southern of Italy). Ten samples for each cultivar were analyzed: N=10 for Peranzana cultivar, N=10 for Ogliarola, N=10 for Cima di mola, and N=10 for Coratina. For this initial study, sample were taken from the north-western part of the region (Figure 9)

Figure 9 Maps of sample oils chosen; Peranzana (orange), Ogliarola (yellow),Cima di mola (green), Coratina (red)

Figure 10 displays the 2D-LDA plot for the EVOO from different cultivars.

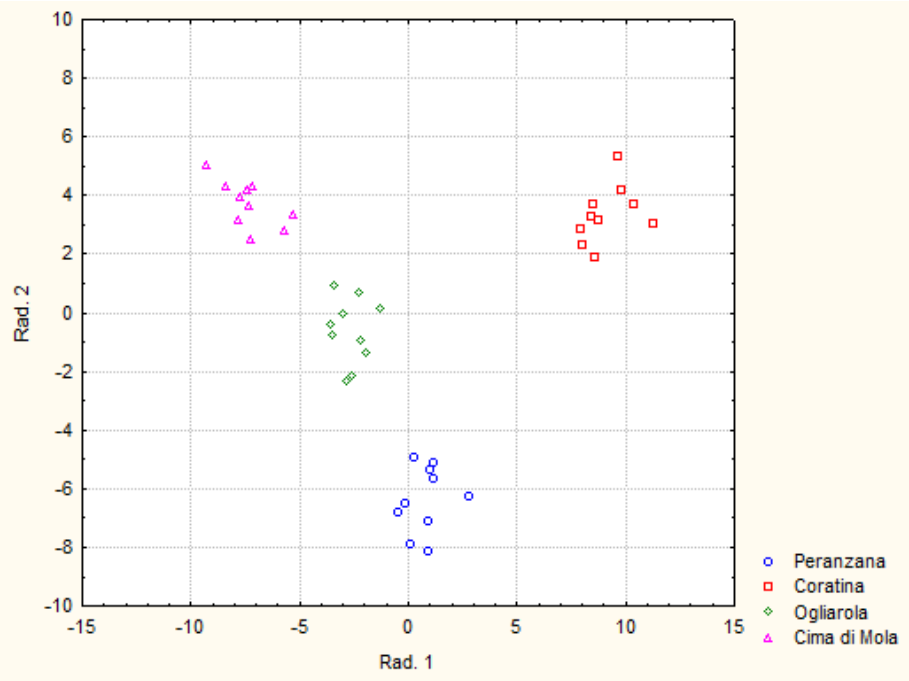

Figure 10 2D-LDA score plot EVOO samples from different cultivar

Stepwise-LDA has retained 18 variables and the model has classified correctly all samples of monovarietal oil; only one sample belonging to Ogliarola cultivar was classified as Cima di mola sample (Table 6).

Table 6 Number of correctly classified pure vegetable oil samples (prediction matrices) for Stepwise LDA

Stepwise LDA[a]

	Peranzana	**Coratina**	**Ogliarola**	**Cima di Mola**
Peranzana	10	0	0	0
Coratina	0	10	0	0
Ogliarola	0	0	9	1
Cima di Mola	0	0	0	10

[a] 18 variables retained after S-LDA (m/z 873, 879, 919, 893, 906, 912, 874, 905, 890, 903, 904, 880, 876, 884, 911, 883, 895, 907 in decreasing order of discriminating capacity)

The SIMCA analysis was performed using the 18 variables selected by S-LDA. The number of correctly classified sample were less than the S-LDA model, probably because in the case of monovarietal oils it is necessary to have a large number of samples to create a robust model. Table 7 shows the number of correctly classified sample and the values of specificity and sensitivity. The latter is less than 100%

Table 7 Number of correctly classified pure vegetable oil samples (prediction matrices) for SIMCA

SIMCA performed using the variables selected by means of S-LDA[b]

	Peranzana	Coratina	Ogliarola	Cima di Mola	SENS(%)	SPEC(%)
Peranzana	9	1	0	0	90	100
Coratina	0	10	0	0	80	100
Ogliarola	0	0	7	3	80	100
Cima di Mola	0	1	1	8	90	100

[b] 18 variables retained after S-LDA (m/z 873, 879, 919, 893, 906, 912, 874, 905, 890, 903, 904, 880, 876, 884, 911, 883, 895, 907 in decreasing order of discriminating capacity)

4. CONCLUSIONS

In conclusion, the presented method has highlighted that the combination of PS-MS measurements and chemometric approach can generate information to discriminate different vegetable oils.

Paper spray mass spectrometry approach offers several advantages: the rapidity of analysis, the minimum sample pre-treatment and the data processing easy and fast. For this reason, PS-MS is considered probably as one of the most rapid, economic and sensitive technique for quality control.

Multivariate statistical analysis has shown the capability of PS-MS TAGs profile to act as marker for the classification of vegetable oils. LDA and SIMCA has highlighted that olive oil can be clearly distinguished from other oils which are commonly used as adulterants, including soybean, corn, sunflower and peanut oil.

Furthermore, also the preliminary results obtained for classification of EVOO from different cultivars are encouraging and suggest that the developed approach can be used to investigate cultivars and regional origin.

REFERENCES

1. Alarcon de la Lastra C, Barranco MD, Motilova V & Herrerias JM (2001) Mediterranean diet and health: biological importance of olive oil. *Current Pharmaceutical Design* 7, 933–950.

2. Owen RW, Giacosa A, Hull WE, Haubner R, Wurtele G, Spiegelhalder B & Bartsch H (2000). Olive-oil consumption and health: the possible role of antioxidants. *Lancet Oncology* 1, 107–112.

3. G. Bianchi, Oils and Fats Authentication, CRC Press, Boca Raton, FL, 2002

4. European Union Commission Regulation EEC/1989/2003, Off. Journal of European Union, 2003, L295.

5. M.J. Lerma-García, R. Lusardi, E. Chiavaro, L. Cerretani, A. Bendini, G.Ramis-Ramos, E.F. Simó-Alfonso. (2011). Use of triacylglycerol profiles established by high performance liquid chromatography with ultraviolet-visible detection to predict the botanical origin of vegetable oils. *J. Chromatogr. A* 1218 7521–7527.

6. Y. Yang, M.D. Ferro, I. Cavaco, Y. Liang. (2013) Detection and identification of extravirgin olive oil adulteration by GC–MS combined with chemometrics. *J.Agric. Food Chem.* 61 3693–3702.

7. S. Indelicato, D. Bongiorno, R. Pitonzo, V. Di Stefano, V. Calabrese, S. Indelicato, G. Avellone. (2017). Triacylglycerols in edible oils: Determination, characterization, quantitation, chemometric approach and evaluation of adulterations. *J. Chromatogr. A* 1515, 1-167

8. R.R. Catharino, R. Haddad, L.G. Cabrini, I. B. S. Cunha, A.C. H. F. Sawaya, M.N. Eberlin. (2005) Characterization of Vegetable Oils by Electrospray Ionization Mass Spectrometry Fingerprinting: Classification, Quality, Adulteration, and Aging. *Anal. Chem.* 77, 7429-7433

9. L. Vaclavik, T. Cajka, V. Hrbek, J. Hajslova (2009). Ambient mass spectrometry employing direct analysis in real time (DART) ion source for olive oil quality and authenticity assessment. *Anal Chim Acta.*10;645(1-2):56-63

10. C. Benincasa, J. Lewis, E. Perri, G. Sindona, A. Tagarelli. Determination of trace element in Italian virgin olive oils and their characterization according to geographical origin by statistical analysis. (2007) *Anal. Chim. Acta.* 585, 366-370.

11. G. Lo Feudo, A. Naccarato, G. Sindona, A. Tagarelli. Investigating the origin of tomatoes and triple concentrated tomato pastes through multielement determination by inductively coupled plasma mass spectrometry and statistical analysis. (2010) *J. Agric. Food Chem.* 58, 3801-3807.

12. L. Di Donna, F. Mazzotti, A. Naccarato, R. Salerno, A. Tagarelli, D. Taverna, G. Sindona. Secondary metabolites of Olea europaea leaves as markers for the discrimination of cultivars and cultivation zones by multivariate analysis. (2010) *Food Chem.* 121, 492-496.

13. E. Furia, A. Naccarato, G. Sindona, G. Stabile, A. Tagarelli. Multielement Fingerprinting as a Tool in Origin Authentication of PGI Food Products: Tropea Red Onion. (2011) *J. Agric. Food Chem.* 59, 8450-8457.

14. G. Lo Feudo, B. Macchione, A. Naccarato, G. Sindona, A. Tagarelli. The volatile fraction profiling of fresh tomatoes and triple concentrate tomato pastes as parameter for the determination of geographical origin. (2011) *Food Res. Int.*44, 781-788.

15. M. Forina, C. Armanino, R. Leardi, G. Drava. A class-modelling technique based on potential functions. (1991) *J. Chemometrics.* 5, 435−453.

IV. Quantitative Evaluation of Caffeine in beverages and drugs by Paper spray tandem Mass Spectrometry

1. INTRODUCTION

Caffeine is an alkaloid found in plant species predominantly growing in the tropic or subtropic regions of the world. Plants use caffeine as a natural pesticide since it is toxic to insects. Caffeine is naturally found in more than 60 plants, including tea leaves, coffee beans, kola nuts. Most of them are used to flavor soft drinks such as colas and cacao pods, and to prepare chocolate products. (1) Caffeine is an ingredient of some energy drinks; it is often added in combination with synephrine in foods or food derivate usually used to induce weight loss or to increase sport performances. Moreover, some drugs and cosmetics contain caffeine. (2) Caffeine, like other natural compounds shows pharmacologic effects in humans, such as central nervous system stimulation, diuresis, and stimulation of cardiac muscle. This alkaloid is able to cause insomnia and increases blood pressure. (3-5)

Recently, the European Food Safety Authority (EFSA) recommended the daily dose of caffeine for an adult: for a safe intake, the suggested caffeine amount is 400 mg per day, corresponding to about four cups of coffee. Further, the maximum recommended dose for pregnant women is 200 mg. (6) Currently, several analytical methods for the quantification of caffeine within complex matrices are reported in literature, based on liquid and gas chromatography analysis, electrochemical analysis, and mass spectrometry. (7-11)

In this section, a simple and fast method based on the use of paper spray mass spectrometry to quantify caffeine in beverages and drugs is presented.

The quantitative assay was performed by isotope dilution method and tandem mass spectrometry in MRM mode, monitoring the following transitions: m/z 195 → m/z 138 for caffeine and m/z 198 → m/z 140 for the labeled internal standard. The reliability of the proposed method were calculated analyzing fortified samples, which have provided accuracy values near to 100%. LOQ and LOD value calculated suggest a good sensitivity of the method. Furthermore, the capability of PS-MS measurements was confirmed by classical HPLC-UV analysis performed on the real samples.

2. MATERIALS AND METHODS

2.1 Chemicals

Chemicals and reagents were commercially available (Sigma–Aldrich, St. Louis, MO).

2.2 Beverages and drugs samples

Beverages were purchased in a local market and drugs in a pharmacy.

2.3 Sample preparation

Beverages were centrifuged at 12000 rpm and for 3 min, and 30 μL of the internal standard solution at a concentration of 1000 mg/ L were added to 470 μL of each beverage sample. The solutions were homogenized by vortex for 30 sec, diluted 1/10 with water and directly spotted onto the paper triangle for PS-MS analysis.

Drugs were ground and extracted with 1 mL methanol. 60 μL of the internal standard solution at 100 mg/mL were added to 940 μL of extraction solution and mixed form 30 s by vortex.

The same samples were diluted and were submitted to HPLC-UV analysis.

2.4 Paper spray mass spectrometry analysis

Mass spectrometry analyses were performed in positive ionization mode with a MS 320 triple-stage quadrupole mass spectrometer (Varian Inc., Palo Alto, CA, USA), in-house implemented for PS-MS application.

15 μL of each sample were spotted onto a paper triangle and left to dried for 1 min. The same volume of methanol was added to allow the spray desorption every 30 s for a total run time of 2 min.

The MS working conditions were the following: needle voltage 5250 V; shield 800 V; capillary 60 V; housing temperature 35 °C, and the detector fixed at 1400 V. Collision gas was argon used at a pressure within the collision cell (Q2) of 2 mTorr, while the mass resolution at the first (Q1) and third (Q3) quadrupoles was set at 0.7 u at full width at half-maximum (FWHM). Scan time was set at 0.1 s. Collision energy (CE) was optimized and then set at 14 eV. MRM mode was used to quantify the analytes; in particular, the transition m/z 195 → m/z 138 for caffeine and m/z 198 → m/z 140 for the labeled internal

standard were monitored. The ion current of each monitored transition, averaged over the total acquisition time, was used for the quantitative analysis.

2.5 LC-UV analysis

LC analysis were carried out using an HPLC 1100 (Agilent Technologies, Waldbronn, Germany) equipped with a quaternary pump and a UV detector. Separation was achieved by using a reversed phase C18 column (Luna, Phenomenex, Torrance, CA, USA), using a flow rate of 1 mL/min and the detector set at 280 nm using a gradient water/methanol. (12)

3. RESULTS AND DISCASSION

Quantitative assay was performed using a combination of paper spray mass spectrometry and isotope dilution analysis; the isotopomer standard was caffeine-(trimethyl-$^{13}C_3$) (Figure 1).

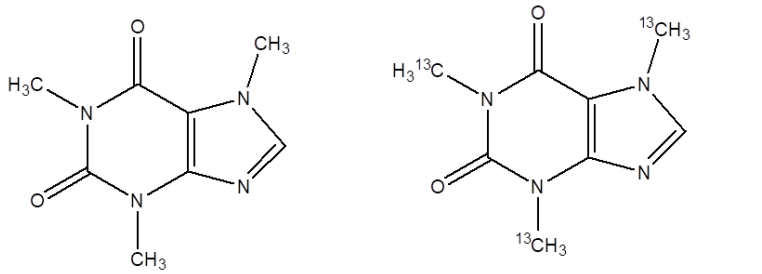

1. Caffeine
$C_8H_{10}N_4O_2$
MW 194

2. Caffeine-(trimethyl-$^{13}C_3$)
$C_5{}^{13}C_3H_{10}N_4O_2$
MW 197

Figure 1 Chemical structure of analyte (1) and labeled internal standard (2)

Tandem mass spectrometry experiments were carried out in positive ion mode monitoring the transition m/z 195 → m/z 138 for caffeine and m/z 198 → m/z 140 for the labeled internal standard. These transitions were chosen according to ESI (+) MS/MS experiments. The MS/MS spectrum of caffeine, in fact, is characterized by few diagnostic fragments; in particular, the ion at m/z 138, which represents the base peak of the spectrum. The same fragment, showing a m/z value increased of 2 Da was recorded in the MS/MS spectrum of the labeled standard, caffeine-(trimethyl-$^{13}C_3$); this ion probably is probably generated by the internal breakage of the six-membered ring of the molecule (Figure 2).

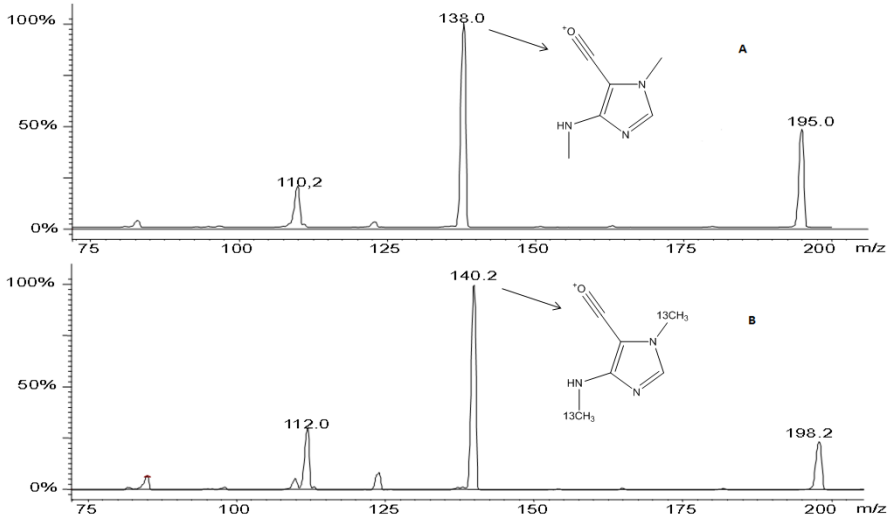

Figure 2 ESI-MS/MS spectra of caffeine (A) and caffeine-(trimethyl-$^{13}C_3$) (B)

For the PS-MS experiment, a high voltage was applied to the paper triangle embedded with 15 µL of sample and left drying; the same volume of methanol was spotted onto the paper every 30 sec, to allow the desorption of the ions. The acquisition time was 2 min.

The calibration curve was obtained by sampling five solutions of analyte at different concentrations, from 2 mg/L to 16 mg/L, mixed with the solution of labeled internal standard at ac concentration of 6 mg/L. Each solution was analyzed in triplicate. The equation obtained showed a good linearity (y = 0.8047x + 0.1742 R^2=0.9884). The ion currents averaged over the total acquisition time, were used for quantitative analyses (Figure 3). Each solution was analyzed in triplicate.

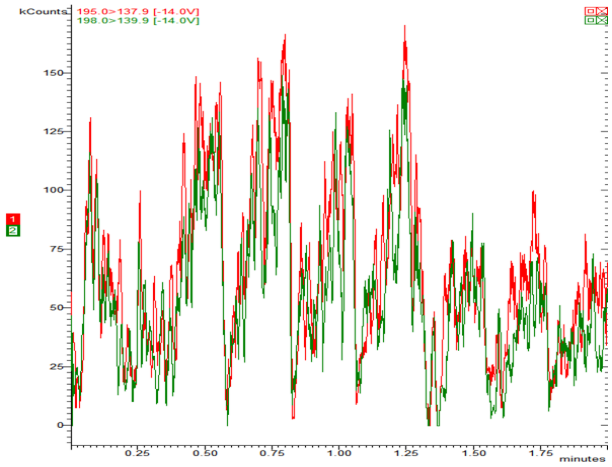

Figure 3 Ion current of MRM monitored transitions, respectively for Caffeine (red) and internal standard (green) in a calibration curve solution

The accuracy of the analytical method was determined by two spiked samples prepared by adding known amount of the caffeine to blank samples (soda drink). In particular the spiked samples were prepared at two different concentration of analyte, representing the limits of the calibration curve. In both cases the accuracy was near to 100 % (Table 1).

Table 1 Accuracy value calculated on fortified blank sample

Spiked samples (mg/L)	Found concentration (mg/L)	Accuracy (%)	RSD (%)
S1 5 mg/L	5.02 ± 0.69	100.40	13.70
S2 15 mg/L	14.60 ± 0.43	97.00	2.94

After evaluating the accuracy of the method, the real samples were submitted to the PS-MS/MS analysis. Table 2 shows the amount found in different matrixes.

Table 2 Amount of caffeine in real samples

Real samples	Amount of Caffeine (mg/L)	RSD (%)
Cola	115.90 ± 8.2	4.14
Coffee 1	6887.8 ± 203.9	3.38
Coffee 2	49.21 ± 154.1	3.13
Coffee 3	4074 ± 201.5	4.94
Coffee 4	7864 ± 305.6	3.9
Coffee 5	6742 ± 287.2	4.2
Tea	119.7 ± 15.3	12.7
Energy drink	381.5 ± 12.0	3.15
Drug 1	126.8 ± 8.9	7.03
Drug 2	164.3 ± 9.5	9.48

For all the analyzed samples, the RSD % values were lower than 13 %, confirming the good repeatability of the PS-MS/MS measurements.

The limit of detection (LOD) and the limit of quantification (LOQ) highlighted the sensitivity of the developed method (Table 3).

Table 3 Limit of detection and quantification values for both beverage and drugs

	mg/L for beverages	**mg/L for drugs**
LOD	1.2	1.2
LOQ	1.6	1.5

Also in this case, to prove the consistency of the PS-MS/MS measurements, the real samples were submitted to HPLC-UV analysis. Results were very similar that those obtained by PS-MRM measurements (Table 4)

Table 4 Amount of caffein obtained by PS-MS/MS and LC-UV analysis

Real samples	**Amount of Caffeine PS-MS/MS (mg/kg)**	**Amount of Caffeine LC-UV (mg/kg)**
Cola	115.90	123
Coffee 1	6887.8	6435
Coffee 2	49.21	4650
Coffee 3	4074	4190
Coffee 4	7864	8177
Coffee 5	6742	6600
Tea	119.7	378
Energy drink	381.5	121
Drug 1	126.8	122
Drug 2	164.3	165

4. CONCLUSION

A new analytical procedure for quantitative assay of caffeine in drinks and drugs has been developed. The method is based on PS-MS and isotope dilution method. The values of accuracy and LOQ and LOD show the reliability and the sensitivity of the procedure, and suggest a possible use of paper spray ionization technique for quantitative analysis in a rapid and convenient way.

REFERENCES

1. Ashihara H, Crozier A. Caffeine: a well known but little mentioned compound in plant science. (2001) *Trends Plant Sci.* 6:407–13.

2. James JE. In: Watson R, editor. Caffeine mental performance and mood. Cambridge: Woodhead Publishing Ltd. and CRC Press; 2003.

3. Buscemi S, Verga S, Batsis JA, Donatelli M, Tranchina MR, Belmonte S, et al.)2010) Acute effects of coffee on endothelial function in healthy subjects. *Eur J Clin Nutr*. 64:483–9.

4. Zhang Z, Hu G, Caballero B, Appel L. (2011) Habitual coffee consumption and risk of hypertension: a systematic review and meta-analysis of prospective observational studies. *Am J Clin Nutr*. 93: 1212–9.

5. James JE. (2004) Critical review of dietary caffeine and blood pressure: a relationship that should be taken more seriously. *Psychosom Med.* 66:63–71.

6. Scientific opinion on the safety of caffeine. EFSA J. 2015;13:4102.

7. Svorc L. (2013). Determination of Caffeine: A Comprehensive Review on Electrochemical Methods *Int J Electrochem Sci*. 8:5755–73

8. Horie H, Nesumi A, Ujihara T, Kohata K (2002). Rapid determination of caffeine in tea leaves. . *J Chromatogr A.* 942:271–3.

9. RostagnoMA, Manchon N, D'Arrigo M, Guillamon E, Villares A,Garcıa-Lafuente A, et al. Fast and simultaneous determination of phenolic compounds and caffeine in teas, mate, instant coffee, soft drink and energetic drink by high-performance liquid chromatography using a fused-core column. *Anal Chim Acta.* 2011;685:204–11.

10. Danhelova H, Hradecky J, Prinosilova S, Cajka T, Riddellova K, Vaclavik L, et al. Rapid analysis of caffeine in various coffee samples employing direct analysis in

real-time ionization-high-resolution mass spectrometry. *Anal Bioanal Chem.* 2012;403:2883–9.

11. Aranda M, Morlock G. New method for caffeine quantification by planar chromatography coupled with electropray ionization mass spectrometry using stable isotope dilution analysis. *Rapid Commun Mass Spectrom.* 2007;21:1297–303.

12. *Chena H, Dengb Y. Talanta. 2002;57:307–16*

GENERAL CONCLUSIONS

The strong relationship between the daily diet and human health, highlighted by many research studies, depends to the presence of several nutraceutical compounds in the foodstuffs. Current scientific knowledge supports that the active principles present in certain foods can modulate different body functions and prevent some diseases. In this field, it becomes fundamental the characterization of new potential active principles and the development of methodologies for their purification and enrichment.

In the first part of this thesis, two new flavanone glycosides 3-hydroxy-3-methylglutaril conjugates were identified from bergamot juice and structurally characterized. As the other HMG-flavonoids known (melitidin and brutieridin), these new molecules can be seen as statin-like compounds. For this reason, it was developed an innovative, fast and green methodology to obtain enriched extracts, containing the flavonoids HMG conjugates with a high purity degree (also up to 90 %), from different citrus fruits (bergamot, bergamot sour orange and chinotto leaves). The enriched extracts obtained through this methodology can be considered safe and highly quality. It was investigated the hypocholesterolaemic effect of HMG-flavonoids enriched extract respect to the activity of simvastatin, in a rat model. The study has provided excellent results on lowering total cholesterol level in blood, LDL and triglycerides level. The prospective for the future is to test the activity of the extracts through clinical trials.

New functional foods are obtained by the enrichment of frequently consumed foods with the hydroxytyrosol, an active principle of the olive oil. The methodology is an innovative procedure to enrich foodstuffs, because it is not based on the addition of a standard or purified compound, but on the transfer of hydroxytyrosol from oil to food matrices with a simple contact. The procedure is based on the use of supercritical CO_2 fluid extraction which allows the selective absorption of hydroxytyrosol on the food matrices. The antioxidant activity of new food products was evaluated by DPPH test. The results highlighted that the enriched foods have a higher capability for scavenging of free radicals than the original matrices.

Nutraceutical compounds are therefore considered quality markers of food, and the development of advanced analytical methodologies to quantify these marker compounds has became indispensable in this research field. The proper quantification of the

nutraceuticals can give an added value to the foods; hence, the use of advanced analytical techniques is necessary. In this field, mass spectrometry technique is one of the most important tools for its specificity and sensitivity features.

In this thesis, some innovative mass spectrometry-based approaches for the quantification and determination of target molecules were presented.

Novel, fast and reliable methodologies to evaluate the amount of polyhydroxylated aromatic compounds in extra virgin olive oil were developed. In particular, the first presented method was based on a fast microwave hydrolysis reaction followed by the LC-MRM analysis using labeled internal standard. The second approach has provided for the use of paper spray mass spectrometry technique. The results of the experiments have shown the accuracy of the procedures, and the analytical parameters have highlighted the sensitivity and reproducibility of the developed methods.

Also the analytical procedure for quantitative assay of caffeine in drinks and drugs was based on PS-MS and isotope dilution method. The values of accuracy and LOQ and LOD displayed the reliability and the sensitivity of the method.

The analytical methodologies developed by the exploitation of paper spray mass spectrometry suggest a possible use of this ionization technique for quantitative analysis in a rapid and convenient way.

Paper spray ionization technique was also used to discriminate different vegetable oils through the TAGs profile. The combination of PS-MS measurements and multivariate statistical analysis has shown the capability of PS-MS TAGs profile to act as marker for the classification of vegetable oils.

APPENDIX

Analytical and Bioanalytical Chemistry
https://doi.org/10.1007/s00216-018-0885-1

RESEARCH PAPER

A comprehensive evaluation of tyrosol and hydroxytyrosol derivatives in extra virgin olive oil by microwave-assisted hydrolysis and HPLC-MS/MS

Lucia Bartella[1] · Fabio Mazzotti[1] · Anna Napoli[1] · Giovanni Sindona[1] · Leonardo Di Donna[1]

Received: 10 November 2017 / Revised: 9 January 2018 / Accepted: 15 January 2018

Abstract
A rapid and reliable method to assay the total amount of tyrosol and hydroxytyrosol derivatives in extra virgin olive oil has been developed. The methodology intends to establish the nutritional quality of this edible oil addressing recent international health claim legislations (the European Commission Regulation No. 432/2012) and changing the classification of extra virgin olive oil to the status of nutraceutical. The method is based on the use of high-performance liquid chromatography coupled with tandem mass spectrometry and labeled internal standards preceded by a fast hydrolysis reaction step performed through the aid of microwaves under acid conditions. The overall process is particularly time saving, much shorter than any methodology previously reported. The developed approach represents a mix of rapidity and accuracy whose values have been found near 100% on different fortified vegetable oils, while the RSD% values, calculated from repeatability and reproducibility experiments, are in all cases under 7%.

Keywords Olive oil · Isotope dilution mass spectrometry · Microwave hydrolysis · 432/2012 EU regulation · Hydroxytyrosol · Phenolic compound

Introduction

The extra-virgin olive oil (EVOO) is believed to be one of the healthiest edible fat. The EVOO beneficial effects derive from its particular chemical composition which includes a high percent of triacylglycerols containing monounsaturated omega-9 fatty acids (above 70%), a good amount of triacylglycerols bearing omega-6 and -3 fatty acids, vitamin E, K and an appreciable presence of phenols. Each of these chemicals is known to exert different activities: for example, phenols are related to the protection and the improvement of the endothelium function [1], and may delay atherosclerosis [2]; triacylglycerols containing oleic acid moiety inhibit the formation of blood clots [3], and vitamin E may prevent the oxidation of cells-membrane lipids and plasma lipoproteins [4]. Phenols, in particular, possess antioxidant and anti-inflammatory activity [5, 6] as certified by the recent Regulation 432/2012 of the European Union [7]; the latter, with regard to olive oil, authorizes to report on the label of the food that "Olive oil polyphenols contribute to the protection of blood lipids from oxidative stress" and "that the beneficial effect is obtained with a daily intake of 20 g of olive oil...which contains at least 5 mg of hydroxytyrosol and its derivatives (e.g. oleuropein complex and tyrosol) per 20 g of olive oil" (Fig. 1).

It is essential, therefore, to use reliable analytical methods to determine the exact amount of the above mentioned compounds, in order to raise the value added of the extra virgin olive oil. To date, there is no official analytical method provided by the IOC (the International Olive Council) and approved by the EU legislation; a methodology commonly used to determine the "biophenols" in EVOO is based on HPLC coupled to UV detection together with tyrosol and syringic acid as internal standard. The method, however, lacks of selectivity because it relies on retention times and 280 nm UV absorbance [8]. Other methods, based essentially upon LC-MS/MS, have been developed to quantify the tyrosol (Tyr) and hydroxytyrosol (Htyr) derivatives. The latest one describes the assay of the dialdehydic form of Htyr and Tyr

✉ Leonardo Di Donna
l.didonna@unical.it

[1] Dipartimento di Chimica e Tecnologie Chimiche, Università della Calabria, via P. Bucci, cubo 12/D, 87030 Rende, CS, Italy

Published online: 26 January 2018

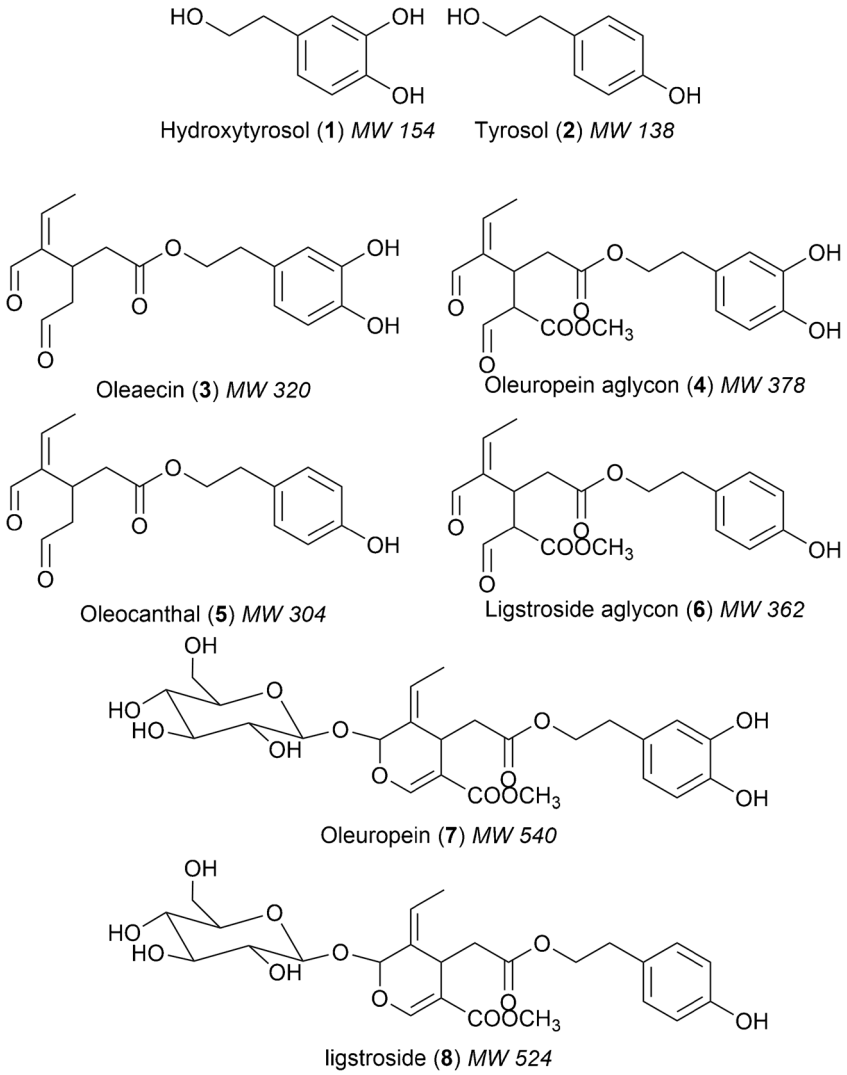

Fig. 1 Scheme of the tyrosol and hydroxytyrosol conjugates present in EVOO

(oleacein and oleocanthal, **3**,**4**) using purified standards [9]. Further procedures use the derivatization chemistry prior the mass spectrometric analysis [10–12], while recently, great attention was directed towards the use of hydrolysis reactions to convert all Tyr and Htyr derivatives (**3**–**8**) to the simplest form of the phenyl ethanoids (**1**,**2**) and their subsequent analysis. Mulinacci et al. [13] proposed a reaction with H_2SO_4 for 2 h at 80 °C performed on the extracted moiety of phenols, which was adopted by Mastralexi et al. [14] for the assay of the phenolic moiety, while a more recent approach is based on the use of HCl either directly on the oil [15] or onto the polar fraction [12]. The above described procedures have been shown to be reliable, however they involve a sample preparation step and instrumental analysis experiments that are often laborious and time consuming; on the other hand, when employing mass spectrometry, often the accuracy is not adequate unless a labeled internal standard is used [16, 17].

Here we present a fast and all-inclusive method to determine the amount of tyrosol and hydroxytyrosol derivatives, fulfilling the requirements of the legislation [7]; this novel method is based on microwave chemistry and isotope dilution mass spectrometry. The extracted molecules **3**–**8** (Fig. 1) are reduced to simple phenols by microwave digestion under acidic condition and then the total hydroxytyrosol and tyrosol amount were determined by LC-MS/MS using the selected reaction monitoring mode, in the presence of a deuterated internal standard.

Experimental

Chemicals

Chemicals and reagents were commercially available (Sigma–Aldrich, St. Louis, MO). Hydroxytyrosol, tyrosol and oleuropein standards were purchased from Extrasynthese (Genay Cedex, France). Labeled standards, d_2-Hydroxytyrosol and d_2-Tyrosol were obtained by slightly modified literature methods [18].

Synthesis of d_2-tyrosol

A stirred suspension of methyl 4-hydroxyphenylacetate (1 g, 6 mmol) in D_2O (18 mL) was treated with $NaBD_4$ (1.88 g, 45.13 mmol) under stirring for 8 h at room temperature. 5 mL of a 2 N solution of HCl was added under ice-cooling for the decomposition of the excess reagent, and then the mixture was extracted with Et_2O. The organic layer was washed with brine and concentrated under vacuum.

Synthesis of d_2-Hydroxytyrosol

0.66 g (15.84 mmol) of $NaBD_4$ were slowly added to 8 mL of D_2O cooled in an ice bath. A solution of methyl 3,4-dihydroxyphenylacetate (0.8 g, 4.4 mmol) in 10.5 mL of D_2O was added to the mixture, and the reaction mixture was stirred for 7 h at room temperature. The reaction mixture was cooled at 0 °C and HCl 2 N (21 mL) was added drop wise in 15 min. The residue was extracted with ethyl acetate (100 mL × 6). Each extract was washed with saturated ammonium chloride (50 mL), combined and dried using Na_2SO_4, and finally concentrated under vacuum.

Purification of standards

The final purification of d_2-tyrosol and d_2-hydroxytyrosol was performed by a Fractionlynx (Waters, Milford, MA) semi-preparative chromatography system, using a C_{18} reversed-phase column, Luna (250 × 10 mm, 5 μm particle size, Phenomenex, Torrance, CA), with an isocratic run using 0.1% HCOOH in water (93%) and CH_3CN (7%) as mobile phase. The flow rate was set at 4.7 mL/min and the volume injected was 1 mL. The collected fraction were evaporated under vacuum and then lyophilized. Deuterated standards were obtained at 99% purity.

Oil samples

Ten extra virgin olive oils were obtained from local oil-makers and stored in amber glass bottles at 4 °C until analysis.

Standard solution

Stock standard solutions of 2000 mg/L of hydroxytyrosol and tyrosol were prepared by dissolving the analytes in methanol. Stock solutions of d_2-hydroxytyrosol and d_2-tyrosol were prepared accordingly. The calibration curves were obtained using the following concentrations (mg/L) of analytes and internal standards: 0.125-0.250-0.500-0.750-1.200, hydroxytyrosol and 0.250 d_2-hydroxytyrosol; 0.200-0.400-0.600-0.800 tyrosol, 0.200 d_2-tyrosol.

Determination of free hydroxytyrosol and tyrosol

1.5 g of each extra virgin olive oil sample was mixed with 30 μL of a d_2-hydroxytyrosol solution at 125 mg/L and 30 μL from a d_2-tyrosol solution at 100 mg/L. The mixture was stirred by ultra-turrax for 3 min to allow the homogeneous distribution of the standards; then 1 g was extracted using 1 mL of H_2O (0.1% HCOOH)/EtOH 3:7 *v/v*. The resulting mixture was centrifuged at 13000 g for 3 min, and the supernatant was diluted (1/10) with a solution of H_2O (0.1% HCOOH)/EtOH 3:7 *v/v* and analyzed by LC-MS/MS.

Determination of total hydroxytyrosol and tyrosol

2 g of each extra virgin olive oil sample were mixed with 25 μL of a d_2-hydroxytyrosol solution at 2000 mg/L and 20 μL from a d_2-tyrosol solution at 2000 mg/L. The mixture was homogenized vigorously by ultra-turrax for 3 min, and then 1 g was extracted using a solution 1 mL of H_2O (0,1% HCOOH)/EtOH 3:7 *v/v*. After the extraction 500 μL of supernatant were added to 500 μL of HCl 2 M in a closed pyrex vessel, and submitted to acid hydrolysis for 4 min in a microwave Anton Paar Multiwave 3000 provided with a rotor 4 × 24 MC, operating at a temperature of 140 °C at the maximum power of 1400 W. The reaction mixture was then stirred to vortex for 1 min, diluted (1/50) with H_2O (0.1% HCOOH)/EtOH 3:7 *v/v* and finally injected into the instrument.

Mass spectrometry

LC-MS/MS analysis was performed using an instrument from Thermo Scientific composed by a UHPLC Accela pump coupled to a TSQ Quantum Vantage triple-stage quadrupole mass spectrometer (Thermo Fisher Scientific, San José, CA). The HPLC separation was carried out using a C_{18} reversed-phase column, Hypersil (2.1 × 50 mm, 3 μm particle size, Thermo Fisher Scientific), injecting 10 μL of sample solution. The flow rate was set at 0.3 mL/min using (A) H_2O and (B) ACN as elution solvents. The following gradient program was used: $t = 0.0$ min, 100% A; $t = 1.0$ min, 100% A; $t = 6.0$ min, 10% A; $t = 8.0$ min, 10% A; $t = 9.0$ min, 100% A; equilibration time 3 min. A further switching valve located on the mass spectrometer was used to divert the LC flow to waste in the first minute and from 7 to 12 min to protect the ion source from contamination. Mass spectrometer was equipped with a heated electrospray ionization (HESI II) source operating in negative ion mode. The working conditions were spray voltage, − 3.5 kV; vaporizer and capillary temperatures, 280 and 270 °C, respectively; sheath and auxiliary gas at 40 and 46 arbitrary units (au), respectively. The collision gas pressure (Ar) in the collision cell (Q2) was set at 1.0 mTorr, and the mass resolution at the first (Q1) and third (Q3) quadrupole was set at 0.7 Da (FWHM). The S-lens rf amplitude and the

collision energy (CE) were both optimized individually per compound (Table 1).

The multiple reaction monitoring (MRM) mode was used to quantify the analytes: the assay was performed following two transitions per compound, the first one for the quantitative analysis and the second for validation (Table 1). Instrument control and data processing were carried out by means of Xcalibur software. The total LC-MS/MS method run time was 12 min.

LC-ESI-MS/UV analysis was performed using the FractionLynx system from Waters (Milford, MA) working in analytical mode, equipped with a Acquity QDa mass spectrometer and a 2489 UV/visible detector. The chromatographic separation was carried out according to IOC methodology [8], using a C_{18} reversed-phase column, Luna (250 × 4.6 mm, 5 μm, Phenomenex), at a flow rate of 1 mL/min. The run time was 82 min and the flow rate was fixed at 1 mL/min, injecting a volume of 20 μl.

Results and discussion

The methodology here described aims at determining the content of Htyr and Tyr derivatives in the extra virgin olive oil, to address the claims described in the 432/2012 EU Regulation. The method consists of two steps: the first step concerns the assay of the free form of Htyr and Tyr naturally present in the EVOO, while the second step intends to determine the amount of the linked form of the phenylethanoids that are present for the most part as ester derivatives according to previous approaches [14].

Both analyses rely on the use of d_2-Tyr and d_2-Htyr isotopic standard diluted directly in the extra virgin olive oil; the homogenization step of the internal standards in the oil is crucial in order to obtain their best distribution in the matrix. Whereas the analysis of the free phenols may be performed by directly analyzing the solution of the olive oil extracted with a mixture of ethanol and acid water, the second determination is achieved by a hydrolysis step of the bound forms. We developed a fast hydrolysis reaction using a microwave oven in a closed vessel: in particular, the phenol solution, previously extracted from the standard enriched olive oil, is diluted with 2 M hydrochloric acid. The acid hydrolysis has been optimized by following the reaction on a spiked corn oil sample.

The corn oil, naturally missing of any phenols has been fortified with standard tyrosol, hydroxytyrosol and oleuropein at concentration of 100, 150 and 150 mg/kg, respectively, simulating a high content phenols olive oil: the trial experiments were performed varying the time of reaction, the power and the temperature parameters of the oven. At the end of the reaction, the samples were suitably diluted and analyzed by LC-MRM following the optimized transition for Tyr, Htyr, d_2-Tyr and d_2-Htyr (Table 1) [16]. Figure 2 shows how the three variables influence the reaction. In particular, the completeness of the reaction was accomplished at 1400 W, 140 °C and 4 min in the oven.

Figure 3 emphasizes the difference of the extracted phenols solution of an EVOO sample before and after the hydrolysis reaction analyzed by HPLC-UV using the gradient of the IOC method (see methods). In particular, Fig. 3B shows the complete disappearance of the Tyr and Htyr ester signals, and the increase of the free from peaks.

For both free and total Tyr and Htyr analysis the determination is based on the use of electrospray triple quadrupole mass spectrometry coupled to an HPLC; the analyzer is set in MRM mode in order to obtain the best selectivity for the analytes (Table 1).

The selected gas-phase transitions are those leading to the loss of methoxy radical (*m/z* 106) and formaldehyde (*m/z* 123) from the negative pseudomolecular ions $[M\text{-}H]^-$ of Tyr and Htyr, respectively [16]. In the case of d_2 standards the neutral mass lost is increased by 2 Da. Those transitions, which are the most abundant in term of signal, have used for the assay. Furthermore, Table 1 describes other gas phase reactions, used to validate the analysis; these are due to the loss of a formal molecule of water from the molecular ion of tyrosol and to the loss of a methoxy radical from the $[M\text{-}H]^-$ ion of hydroxytyrosol.

Table 2 discloses the values of accuracy of two fortified corn oils, representatives of a low and a high content phenols olive oil, after the microwave hydrolysis under the final reaction conditions. As shown, the accuracies are near 100%. These indicates that (i) the hydrolysis does not affect the free form of Tyr and Htyr, (ii) the hydrolysis of the ester is complete, and (iii) no side reaction takes place on the mixture of

Table 1 Optimized transition, collision energy and S-lens values for the analysis of Tyr and Htyr

Analyte	Transition (quantitative)	Transition (confirmative)	Collision energy (eV)		S-lens (V)
			quan	conf	
Tyr	*m/z* 137 → *m/z* 106	*m/z* 137 → *m/z* 119	18	20	50
Htyr	*m/z* 153 → *m/z* 123	*m/z* 153 → *m/z* 122	17	25	60
d_2-Tyr	*m/z* 139 → *m/z* 106	*m/z* 139 → *m/z* 120	18	20	50
d_2-Htyr	*m/z* 155 → *m/z* 123	*m/z* 155 → *m/z* 122	17	25	60

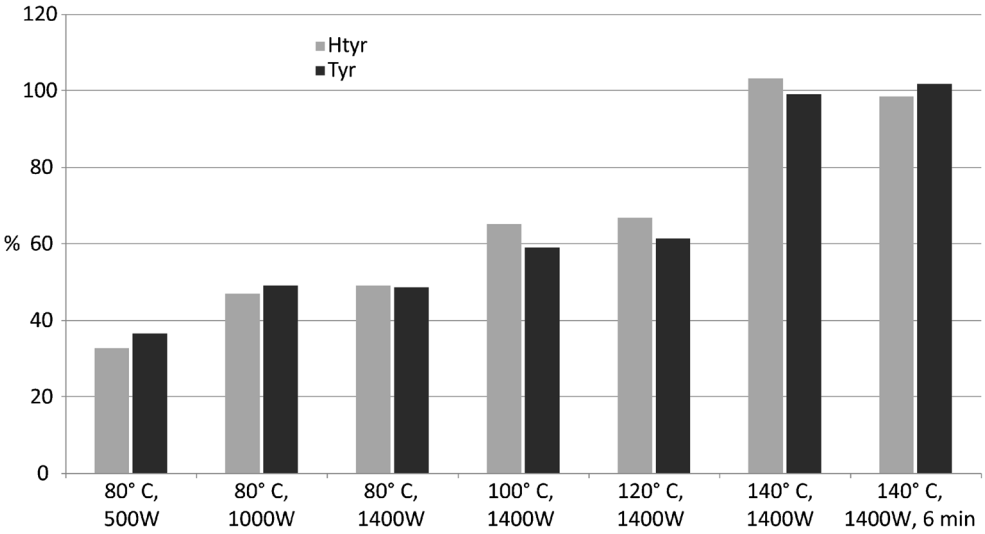

Fig. 2 Variation of accuracy depending on the different conditions employed to the microwave hydrolysis experiment. The reaction time was 4 min except where expressly stated. The experiments were performed on a fortified corn oil containing Tyr, Htyr, and Oleuropein at 100, 150, and 150 mg/kg, respectively

standards. Table 1 includes also the reproducibility results after three different preparations.

The reaction was tested also onto a standard mixture of Tyr, Htyr, d_2-Tyr and d_2-Htyr to ensure that the concentration of the four compounds remained unchanged after the reaction. In particular, the assay of an acidic solution at 20 ppm of Tyr and 25 ppm of Htyr after the microwave hydrolysis provided an accuracy of 104% and 100% respectively (Table 2). We tested the method also on a sample of fortified pomace olive oil in order to simulate at most the extra virgin olive oil matrix. Firstly we examined the presence of compound **1**–**8** in the pomace oil by submitting the polar extract to hydrolysis. These allowed us to calculate the LOQ and the LOD that, in principle, may be influenced by the reaction (Table 2). Ascertained the absence of phenols in the pomace oil (Fig. 4), the sample has been fortified with Tyr, Htyr and Oleuropein at concentration of 100, 150 and 150 mg/kg, respectively.

After hydrolysis and LC-MS/MS analysis we obtained a value of 102.76 and 185.06 mg/kg for Tyr and Htyr giving an accuracy of 103 and 96%, respectively. The results are summarized in Table 2.

At the end, we proceeded with the analysis of ten extra virgin olive oils collected from local oil-makers (Fig. 5).

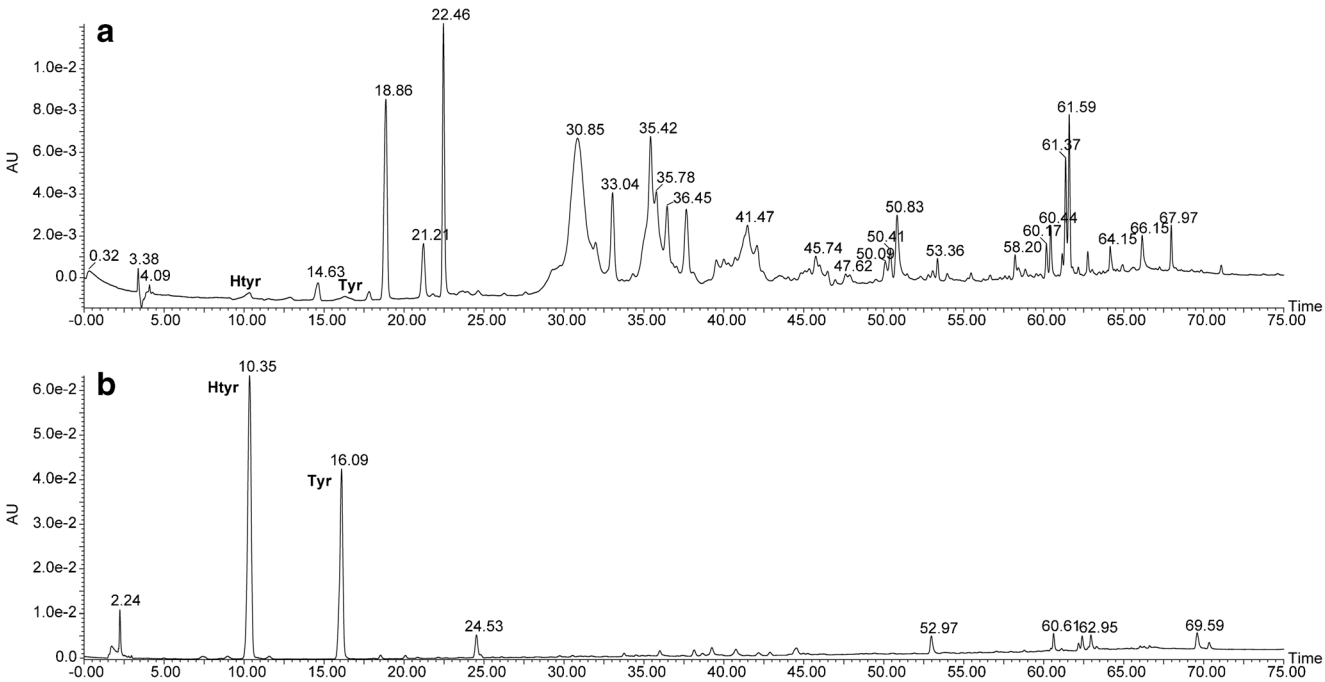

Fig. 3 Representative HPLC-UV chromatogram describing the signal of the olive oil phenols before (**A**) and after (**B**) the 4 min microwave hydrolysis reaction (sample DD)

Table 2 Accuracy values performed on fortified corn and pomace oils and standard solution mixture

Fortified sample		Spiking concentration (mg/kg)	Found concentration (mg/kg)	Mean accuracy (%)	RSD[a] (%)
Low phenols content corn oil	Tyr	40	40.73 ± 1.84	102	4.52
	Htyr	30	38.08 ± 0.77[c]	99	2.02
	Oleuropein	30	–		
High phenols content corn oil	Tyr	100	99.02 ± 1.95	99	1.97
	Htyr	150	194.58 ± 2.25[c]	103	1.16
	Oleuropein	150	–		
Standard mixture	Tyr	20	20.89 ± 0.46	104	2.20
	Htyr	25	25.12 ± 0.61	100	2.43
Fortified pomace oil	Tyr	100	102.76 ± 1.82	103	1.77
	Htyr	150	185.06 ± 3.65[c]	96	1.97
	Oleuropein	150			
		LOD (mg/kg)[b]		LOQ (mg/kg)[b]	
Fortified pomace oil	Tyr	0.041		0.043	
	Htyr	0.005		0.011	

[a] The reproducibility of the measurements were performed by analyzing each sample three times every 7 days

[b] LOD and LOQ values were calculated using the average signal given by the blank sample plus its standard deviation multiplied by three times and ten times, respectively

[c] The concentration of Htyr found in the oleuropein fortified samples is the sum of the contribution of free Htyr and linked Htyr

The results are described in Table 3, which also contains data on the reproducibility of the experiments over a period of 3 weeks. It is worth to note that the data reported in Table 3 refers only to the free and the total content of Tyr and Htyr,

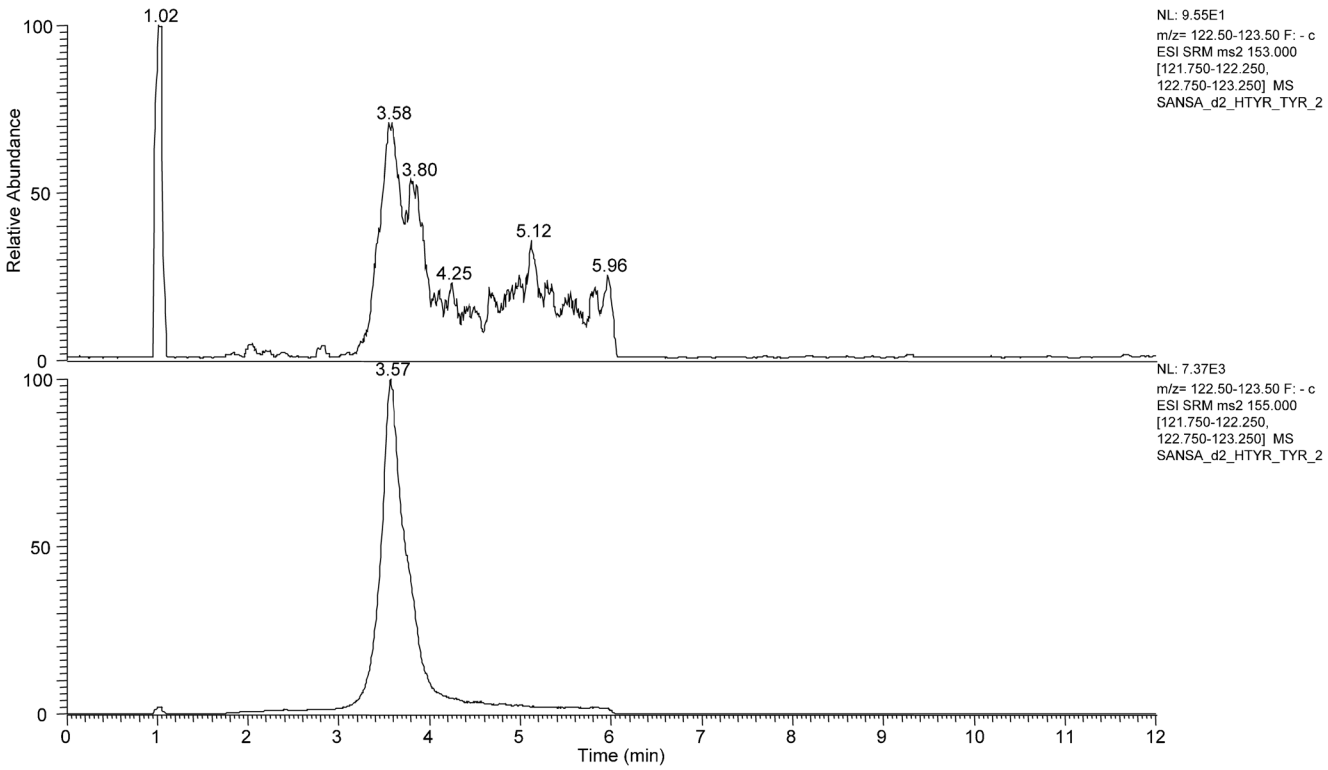

Fig. 4 SRM chromatograms relative to the hydroxytyrosol transitions of the pomace olive oil after hydrolysis. The signals were used to calculate LOD and LOQ

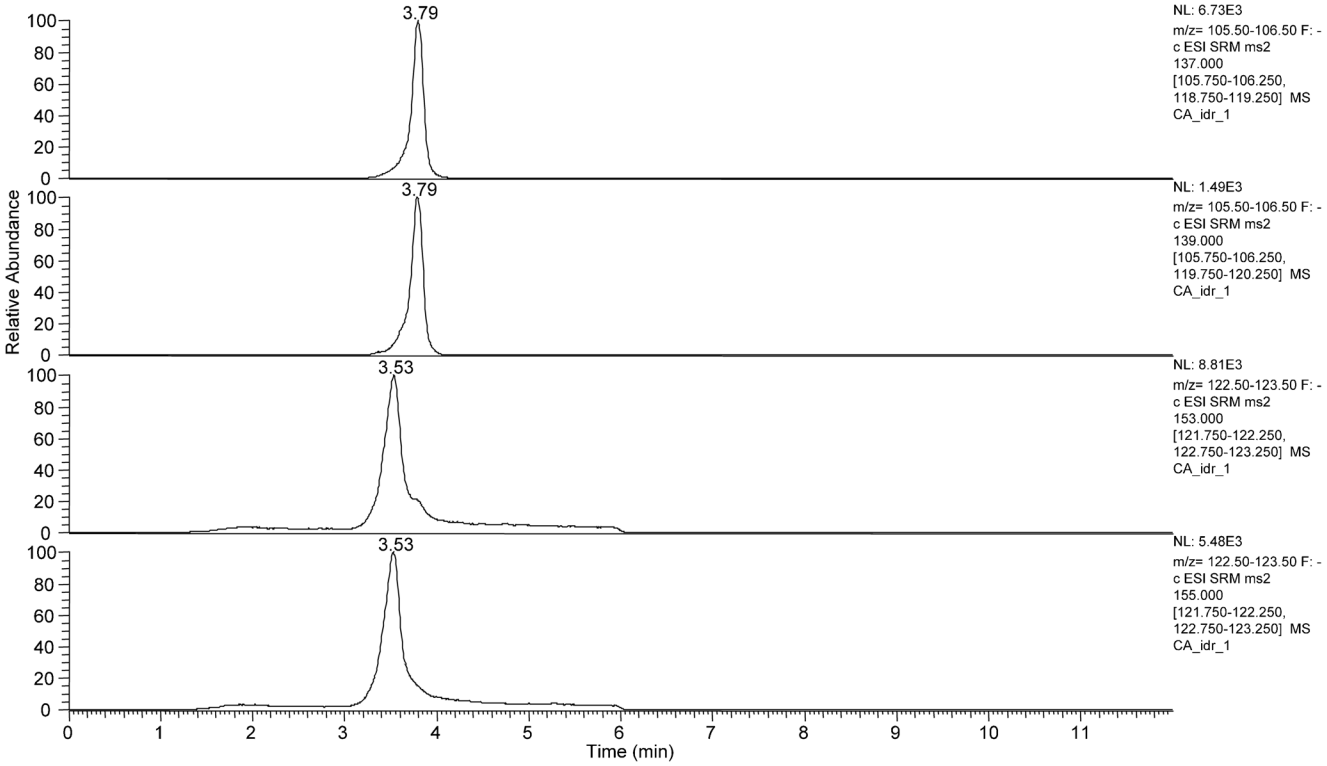

Fig. 5 Representative MRM chromatogram of the CA extra virgin olive oil sample revealing the signal of labeled and unlabeled standards after the hydrolysis reaction

keeping in mind that the total content is the sum of the free and the ester conjugate form of each compound. Hence, to evaluate the amount of the phenylethanoid conjugates (**3**–**8**) a correction on the molecular weight must be performed [14]. For example, the concentration of the Htyr released from the conjugated compounds after the hydrolysis reaction will be given by the total Htyr concentration minus the free Htyr concentration found in the two experiments above described. This result should be divided by the MW of the hydroxytyrosol and multiplied by the weighted average MW of the Htyr esters. The latter may be calculated as the average molecular weight of oleacein (**3**) and oleuropein aglycone (**4**), since the oleuropein (**7**) is present at trace amount in EVOO [19]. The number obtained is then added to the concentration of the free Htyr moiety. The final result should represent the concentration of the Htyr compounds in the EVOO as requested by the EU Regulation [7]. Similar calculation should be done for the Tyr derivatives. The EU Regulation conditions will be addressed by the sum of the two concentration obtained. Table 4 summarizes these values.

Table 3 Amount of free and total tyrosol and hydroxytyrosol in selected extra virgin olive oils

EVOO sample	Free Htyr (mg/kg)	Free Tyr (mg/kg)	Total Htyr (mg/kg)	RSD[a] (%)	Total Tyr (mg/kg)	RSD[a] (%)
DD	2.96 ± 0.15	5.82 ± 0.21	113.79 ± 4.17	3.66	86.15 ± 1.38	1.60
BR	Not detected	Not detected	92.19 ± 5.35	5.80	83.63 ± 2.28	2.72
PI	7.11 ± 0.38	7.68 ± 0.26	80.74 ± 1.36	1.68	55.10 ± 3.58	6.49
OL	21.19 ± 0.92	23.56 ± 1.02	91.12 ± 3.82	4.19	83.24 ± 4.15	4.98
CA	0.98 ± 0.03	5.01 ± 0.14	40.07 ± 1.22	3.04	78.30 ± 1.87	2.39
LA	6.48 ± 0.09	21.16 ± 0.16	22.63 ± 0.64	2.83	41.61 ± 0.32	0.77
OC	1.97 ± 0.02	16.14 ± 0.23	14.25 ± 0.13	0.91	61.97 ± 1.57	2.53
LU	10.71 ± 0.12	11.67 ± 0.68	46.70 ± 0.34	0.73	55.49 ± 1.82	3.28
RU	3.60 ± 0.04	4.07 ± 0.10	20.09 ± 0.29	1.39	23.85 ± 1.59	6.67
BE	Not detected	11.67 ± 0.68	1.72 ± 0.06	3.49	76.15 ± 1.23	1.61

[a] The reproducibility of the measurements was obtained by repeating the experiment for each sample three times (seven for sample CA) every seven days

Table 4 Total amount of tyrosol and hydroxytyrosol derivatives found in extra virgin olive oils

EVOO sample	Total Htyr derivatives[a] (mg/kg)	Total Tyr derivatives[a] (mg/kg)	Total amount of phenyl ethanoids per 20 g of EVOO[b]
DD	254.13	199.66	9.08
BR	208.92	201.80	8.21
PI	173.97	122.11	5.92
OL	179.67	167.57	6.94
CA	89.56	181.86	5.43
LA	43.08	70.51	2.27
OC	29.80	126.73	3.13
LU	92.27	117.41	4.19
RU	40.97	51.80	1.85
BE	3.90	167.26	3.42

[a] The total concentration of each analyte X is calculated using the formula $(X_t\text{-}X_f) \times c_f + X_f$, where X_t is the total concentration of the species, X_f is the free concentration of the species and c_f is the ratio between the average molecular weight of the ester conjugate (**3**,**4** and **5**,**6**) and the molecular weight of X

[b] Total amount of species reported as indicated by the EU directive 432/2012, i.e., sum of total amount of Htyr and Tyr derivatives expressed as mg per 20 g (EU regulation, 2012)

The calculation above performed are necessary because of the generic sentence reported in the official directive. Folkloristic definition of the active molecules aside [7], the document raises the problem on how to irrefutably determine the amount of both hydroxytyrosol and tyrosol and their conjugated, considering that this information can be reported on the label of the food; we strongly recommend to modify the claim reporting not the minimum concentration in mg/kg of the whole family of Htyr and Tyr compounds, but at least the minimum molar concentration, or in alternative the minimum amount per g, expressed as Tyr and Htyr concentration equivalent as suggested previously [15].

Conclusions

In conclusion a fast and reliable method to determine the amount of free and total tyrosol and hydroxytyrosol has been developed. The procedure meets the requirement of a recent EU Regulation on health claim which gives the opportunity to transform the extra virgin olive oil into a nutraceutical. Besides, the working time of the analysis (from the sample preparation to the analysis time) is limited to less than 30 min, much shorter than any previous methodology reported in the literature. The reliability of the method is assured by the use of LC-MS/MS and labeled internal standards, while the rapidity of the experiments is provided by the fast hydrolysis performed with the aid of the microwave chemistry. The developed methodology represents an unprecedented mix of rapidity and accuracy.

Acknowledgments The study has financial support from University of Calabria (Ex60%/2015).

Compliance with ethical standards

Conflict of interest The authors declare that they have no conflict of interest.

References

1. Visioli F, Caruso D, Grande S, Bosisio R, Villa M, Galli G, et al. Virgin olive oil study (VOLOS): vasoprotective potential of extra virgin olive oil in mildly dyslipidemic patients. Eur J Nutr. 2005;44:121–7.
2. Perez-Jimenez F, Alvarez de Cienfuegos G, Badimon L, Barja G, Battino M, Blanco A, et al. International conference on the healthy effect of virgin olive oil. Eur J Clin Investig. 2005;35:421–4.
3. Sánchez-Taínta A, Estruch R, Bulló M, Corella D, Gómez-Gracia E, Fiol M, et al. Adherence to a Mediterranean-type diet and reduced prevalence of clustered cardiovascular risk factors in a cohort of 3,204 high-risk patients. Eur J Cardiovasc Prev Rehabil. 2008;15:589–93.
4. Fitó M, Guxens M, Corella D, Sáez G, Estruch R, de la Torre R, et al. Effect of a traditional Mediterranean diet on lipoprotein oxidation: a randomized controlled trial. Arch Intern Med. 2007;167:1195–203.
5. EFSA Panel on Dietetic Products Nutrition and Allergies (NDA). Scientific opinion on the substantiation of health claims related to polyphenols in olive and protection of LDL particles from oxidative damage (ID 1333, 1638, 1639, 1696, 2865), maintenance of normal blood HDL-cholesterol concentrations (ID 1639), maintenance of normal blood pressure (ID 3781), "anti-inflammatory properties" (ID 1882), "contributes to the upper respiratory tract health" (ID 3468), "can help to maintain a normal function of gastrointestinal tract" (3779), and "contributes to body defences against external agents" (ID 3467) pursuant to Article 13(1) of Regulation (EC) No 1924/2006. EFSA J. 2011;9:2033. https://www.efsa.europa.eu/it/efsajournal/pub/2033. Accessed 09 Nov 2017.
6. Fitó M, Cladellas M, de la Torre R, Martí J, Alcántara M, Pujadas-Bastardes M, et al. Antioxidant effect of virgin olive oil in patients with stable coronary heart disease: a randomized, crossover, controlled, clinical trial. Atherosclerosis. 2005;181:149–58.

7. Commission of the European Communities. Commission Regulation No 432/2012 of 16 May 2012 establishing a list of permitted health claims made on foods, other than those referring to the reduction of disease risk and to children's development and health, Official Journal of the European Union. 2012. http://eur-lex.europa.eu/LexUriServ/LexUriServ.do?uri=OJ:L:2012:136:0001:0040:en:PDF. Accessed 09 Nov 2017.
8. IOC, International Olive Council. Determination of biophenols in olive oils by HPLC. 2009. http://www.internationaloliveoil.org/documents/viewfile/4141-met29eng. Accessed 09 Nov 2017.
9. Sánchez de Medina V, Mihod H, Mellioue E, Magiatise P, Priego-Capote F, de Castro L. Quantitative method for determination of oleocanthal and oleacein in virgin olive oils by liquid chromatography–tandem mass spectrometry. Talanta. 2017;162:24–31.
10. Di Donna L, Benabdelkamel H, Mazzotti F, Napoli A, Nardi M, Sindona G. High-throughput assay of oleopentanedialdheydes in extra virgin olive oil by the UHPLC-ESI-MS/MS and isotope dilution methods. Anal Chem. 2011;83:1990–5.
11. Mazzotti F, Di Donna L, Taverna D, Nardi M, Aiello D, Napoli A, et al. Evaluation of dialdehydic anti-inflammatory active principles in extra-virgin olive oil by reactive paper spray mass spectrometry. Int J Mass Spectrom. 2013;352:87–91.
12. Purcaro G, Codony R, Pizzale L, Mariani C, Conte L. Evaluation of total hydroxytyrosol and tyrosol in extra virgin olive oils. Eur J Lipid Sci Technol. 2014;116:805–11.
13. Mulinacci N, Giaccherini C, Ieri F, Innocenti M, Romani A, Vincieri FF. Evaluation of lignans and free and linked hydroxytyrosol and tyrosol in extra virgin olive oil after hydrolysis processes. J Sci Food Agric. 2006;86:757–64.
14. Mastralexi A, Nenadis N, Tsimidou MZ. Addressing analytical requirements to support health claims on "olive oil polyphenols" (EC Regulation 432/2012). J Agric Food Chem. 2014;62:2459–61.
15. Romero C, Brenes M. Analysis of total contents of hydroxytyrosol and tyrosol in olive oils. J Agric Food Chem. 2012;60:9017–22.
16. Mazzotti F, Benabdelkamel H, Di Donna L, Maiuolo L, Napoli A, Sindona G. Assay of tyrosol and hydroxytyrosol in olive oil by tandem mass spectrometry and isotope dilution method. Food Chem. 2012;135:1006–10.
17. Di Donna L, Mazzotti F, Benabdelkamel H, Gabriele B, Plastina P, Sindona G. Effect of H/D isotopomerization in the assay of resveratrol by tandem mass spectrometry and isotope dilution method. Anal Chem. 2009;81:8603–9.
18. Kuwajima H, Takai Y, Takaishi K, Inoue K. Synthesis of 13C-labeled possible intermediates in the biosynthesis of phenylethanoid derivatives, cornoside and rengyosides. Chem Phatm Bull. 1998;46:581–6.
19. De Nino A, Di Donna L, Mazzotti F, Muzzalupo E, Perri E, Sindona G, et al. Absolute method for the assay of oleuropein in olive oils by atmospheric pressure chemical ionization tandem mass spectrometry. Anal Chem. 2005;77:5961–4.

RSC Advances

PAPER

Cite this: *RSC Adv.*, 2017, **7**, 55264

Mass spectrometry and potentiometry studies of Al(III)–naringin complexes†

L. Bartella, E. Furia* and L. Di Donna

Received 9th November 2017
Accepted 30th November 2017

DOI: 10.1039/c7ra12281k

rsc.li/rsc-advances

Here we have studied the complexation of naringin with Al(III) under physiological conditions (*i.e.*, at 37 °C and in 0.16 mol L^{-1} NaCl). Solubility and protonation constants of the ligand were first determined in order to evaluate the competition of naringin for the Al(III) and H^+ ions. Speciation analysis made by potentiometric titrations and supported by UV data shows that a complexation occurs at a 1 : 1 ligand-to-Al(III) stoichiometric ratio. Notably, these data combined with mass spectrometry results indicate that the complexation site is located on the β-hydroxy ketone moiety.

Introduction

Several biological effects, including radical scavenging and metal chelation, are ascribed to polyphenolic compounds. Numerous epidemiological studies have shown a correlation between high dietary intakes of phenolics and reduced risk of cardiovascular disease and cancer.[1–5] Flavonoids, which contain a large group of polyphenolic phytochemicals with great therapeutic properties, have received much attention in the treatment of some diseases such as cancer, viral infection and inflammation. Most of their pharmacological activities are associated with enzymatic inhibition, anticancer and antioxidant activity and interference with reactions such as the formations of free radicals.[6–9] Flavonoids are naturally present in vegetables, fruits, and beverages such as tea and wine. *In vitro*, flavonoids inhibit the oxidation of low-density lipoprotein and reduce thrombotic tendency, but their effects on atherosclerotic complications in human beings are unknown. Naringin (4′,5,7-trihydroxy flavanone, HL, Scheme 1) is the major flavonoid in grapefruit; due to its metal chelating, antiulcer, antioxidant, superoxide scavenging and anti-inflammatory properties, this compound has attracted scientific interest.[10–13]

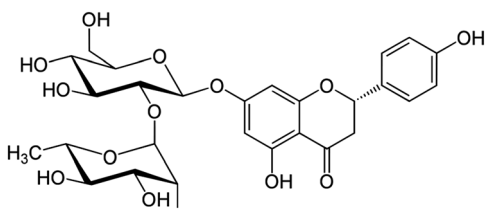

Scheme 1 Chemical structure of naringin.

In our continuous investigation on the complexation behaviour of biological ligands towards some bioavailable metal cations,[14–19] the purpose of this work was to study the sequestering ability of naringin with respect to aluminium cation under physiological conditions (*i.e.*, 37 °C and in 0.16 mol L^{-1} NaCl). Solubility as well as acidic constant of naringin were determined under the same experimental conditions, too. Although the interaction of this compound with water is important because of its antioxidative activity in biological media involves water as the natural solvent, most of the studies reported in literature refers to measurements carried out in mixed solvents due to its low solubility in water.[20–22]

The reason for choosing the aluminium cation is mainly due to the fact that human exposure to aluminium does not serve any essential function in human biochemistry. The aluminium cation can enter the brain where it persists for a long time causing neurotoxicity.[23] Some of the aluminium toxicity can be reduced by chelation, for this reason it was interesting to explore the sequestering ability of a natural product such as naringin to coordinate the Al(III) ion.

Experimental

Materials

The hydrochloric acid and the sodium chloride stock solutions, and the sodium hydroxide titrant solutions were prepared and standardized as described in a previous work.[24] Aluminium(III) chloride stock solution was prepared and standardized as previously reported.[18] Naringin (Sigma-Aldrich, ≥95%), used without further purification, was kept in a desiccator over silica gel. All solutions were prepared with bidistilled water.

Department of Chemistry and Chemical Technologies, University of Calabria, Via P. Bucci, Cubo 12/D, 87036, Arcavacata di Rende, CS, Italy. E-mail: emilia.furia@unical.it

† Electronic supplementary information (ESI) available: Fig. S1 relative to the further tandem mass spectrometry experiment performed on the isolated species at *m*/*z* 1185. Fig. S2 relative to the MS/MS spectrum of the other stable species at *m*/*z* 621. See DOI: 10.1039/c7ra12281k

Apparatus and experimental procedure

The potentiometric apparatus and Ag/AgCl electrodes were prepared as defined in a previous work.[14] The glass electrodes, manufactured by Metrohm, acquired a constant potential within 10 min, after the addition of the reagents, that remained unchanged within ±0.1 mV for several hours. The titrations were carried out with the same tool described in a previous work.[15] To avoid the carbonate interference a slow stream of nitrogen gas was passed through three bottles (a–c) containing: (a) 1 mol L^{-1} NaOH, (b) 1 mol L^{-1} H_2SO_4 and (c) 0.16 mol L^{-1} NaCl, and then into the test solutions, stirred during titrations, through the gas inlet tube. During the EMF measurements, the cell assembly was placed in a thermostat kept at (37.0 ± 0.1) °C.

The HPLC/UV analysis for the solubility measurements were performed by using a Fractionlynx HPLC system (Milford, MA) working in analytical mode equipped with a 2489 UV/Visible detector.[25] 20 μL of naringin saturated solutions were injected into a C18 reverse phase Luna column 4.6 × 250 mm from Phenomenex (Torrance, CA). The run time was 25 min, and the elution gradient comprises the following step (mobile phase: solvent A: 0.1% HCOOH/H_2O, solvent: B CH_3OH): isocratic elution 80% A for 2 min; linear gradient from 80% A to 40% A in 10 min, isocratic elution 40% A for 2 min, linear gradient from 40% A to 20% A in 3 min; isocratic elution 20% A for 2 min; linear gradient from 20% A to 80% A in 3 min; equilibration of the column: 3 min. The area of the signal recorded at 280 nm wavelength, was matched to a calibration curve built analysing five standard solutions whose concentration ranged from 37.5 to 300 mg L^{-1} in order to calculate the unknown concentration.

Information about the structure of complexes was gathered by recording the ESI MS and MS/MS spectra.[26] These were acquired by direct infusion of the solution (*i.e.*, naringin–aluminium complex at 60 mg kg^{-1} concentration) into a Thermo Scientific TSQ Quantum Vantage triple-stage quadrupole mass spectrometer (Thermo Fisher Scientific, San José, CA). The mass spectrometer was equipped with a heated electrospray ionization (HESI II) source operating in positive ion mode. The experimental conditions were the following: spray voltage, 3.5 kV; vaporizer and capillary temperatures, 280 and 270 °C, respectively; sheath and auxiliary gas: 40 and 46 arbitrary units (au), respectively. The collision gas pressure (Ar) in the collision cell (Q2) was set at 1.0 mTorr, and the mass resolution at the first (Q1) and third (Q3) quadrupole was set at 0.7 Da (FWHM). The S-lens rf amplitude and the collision energy (CE) were 110 V and 50 eV, respectively.

Results and discussion

The complex formation equilibria between Al(III) and naringin were studied by measuring with a glass electrode the competition of the ligand for the aluminium(III) and H^+ ions, using bidistilled water as solvent at 37.0 °C and in 0.16 mol L^{-1} NaCl. The present study has provided, at first, the determination of the solubility and of the acidic constant of ligand under the selected experimental conditions. To evaluate the influence of ionic strength and ionic media on the solubility of naringin, values at 37 °C were determined in pure water, in 1.0 and 3.0 mol L^{-1} NaCl and in 0.5, 1.0 and 3.0 mol L^{-1} $NaClO_4$, also. This knowledge is necessary when modelling the dependence of equilibrium constants on the ionic strength.

Solubility measurements

Solubility studies allow the determination of activity coefficients for nonelectrolyte solutes in aqueous solutions containing a large excess of salts, whose knowledge is necessary when modelling the dependence of equilibrium constants on ionic strength. It is well known from literature that the low solubilities in water of some solutes can be modified by the presence of cosolutes, such as inert salts, or by increasing the temperature.[27–30] Two different phenomena related to solubility changes caused by the presence of cosolutes can be observed: salting-in and salting-out effects.[31] Saturated naringin solutions were prepared as already described in a previous work.[32] Briefly, solid was wrapped up in a highly retentive filter paper (Whatman 42) bag and then was kept in a glass cylinder containing pure water as well as sodium chloride aqueous solution at pre-established ionic strength values (*i.e.*, 0.16 mol L^{-1}), under continuous stirring with a magnetic bar. The cylinders were then placed in a thermostatic water bath at (37.0 ± 0.1) °C, and the naringin concentrations were monitored over time, until it reached a constant value, which usually occurred in about (7 to 10) days. Finally, the solubility values were obtained by analysing naringin saturated solutions by HPLC/UV. Results obtained at the different ionic strengths and media are reported in Table 1.

As can be seen in Table 1, the solubility of naringin in $NaClO_4$ is higher than those in NaCl. In particular, naringin exhibits a salting out effect in NaCl medium, being the solubility in water higher than those in sodium chloride. On the contrary, a salting in effect is observed when the inert salt is $NaClO_4$, the solubility increasing with the ionic strength. It was not possible to compare our results with literature data, whose are referred to measurements performed in non-aqueous solvent.[21,22]

Potentiometric and mass spectrometric measurements

The metal (C_M) and ligand (C_L) concentrations were ranged from 0.5 × 10^{-3} to 1.5 × 10^{-3} mol L^{-1}. The upper limit was imposed by the low solubility of ligand under our experimental

Table 1 Solubility at 37.0 °C of naringin in water and in aqueous solutions of NaCl and $NaClO_4$ at different ionic strength. The uncertainties represent standard deviation

I, mol L^{-1}	$S \times 10^3$, mol L^{-1}
Pure water	1.015 ± 0.002
0.16 NaCl	0.999 ± 0.004
1.0 NaCl	0.932 ± 0.004
3.0 NaCl	0.775 ± 0.003
0.50 $NaClO_4$	1.539 ± 0.003
1.0 $NaClO_4$	1.769 ± 0.003
3.0 $NaClO_4$	2.333 ± 0.008

conditions. The ligand-to-metal ratio was varied between 1 and 3. The hydrogen ion concentration was ranged from 3.15×10^{-3} mol L^{-1} (pH 2.5) to incipient precipitation of basic salts which takes place in the range $[H^+] = 0.32–0.032 \times 10^{-3}$ mol L^{-1} (pH 3.5–4.5) depending on the specific ligand-to-metal ratio. The general equilibrium can be written as follows:

$$pAl^{3+} + rHL \rightleftarrows Al_pH_{-q}(HL)_r^{(3p-q)} + qH^+, \beta_{pqr} \quad (1)$$

which takes into account the possible formation of simple ($q = r$), mixed ($q \neq r$), mononuclear ($p = 1$) and polynuclear ($p > 1$) species. The most probable p, q and r values and the corresponding constants β_{pqr} were obtained by a least squares fitting of the potentiometric data.[33] In the numerical treatments, the acidic constant of naringin (equilibrium 2), determined by potentiometric measurements under the same experimental conditions (*i.e.*, 37.0 °C and in 0.16 mol L^{-1} NaCl) in the absence of metal ion, was maintained invariant:

$$HL \rightleftarrows L^- + H^+, \log K_a = -8.18 \pm 0.03 \quad (2)$$

the uncertainty on this constant represents 3σ. The reproducibility and reversibility of the latter equilibrium were verified by performing titrations in acidic and in alkaline directions. No attempts were made to evaluate the second acidic constant due to the ligand oxidation reaction which occurs at a pH value greater than 8.5. Like many other cations, Al^{3+} can be hydrolysed to form solutions of mononuclear as well as polynuclear hydroxide complexes which can be stable indefinitely. The species $Al(OH)^{2+}$ and $Al(OH)_2^+$ were considered the predominant hydrolysis products under our experimental conditions.[34] The relative equilibrium constants were taken from literature[18] and were unchanged during the numerical evaluation, whose details are reported below (Table 2). Experimental data comprised 4 titrations with 78 data points.

The complexes of Al(III) with naringin were characterized by the (1,−1,1) and (1,−3,1) stoichiometries. No other species, introduced to improve the fit, was retained. In order to visualize our results, the refined equilibrium constants were used to represent the distribution of Al^{3+} in the different species (Fig. 1). All proposed species reached concentration levels no lower than 25% with respect to the total metal amounts. Consequently, meaningful concentrations were obtained for each species, allowing a correct definition of the respective equilibrium constants. In the whole pH range investigated the predominant species is the complex with stoichiometry (1,−1,1), while the species with (1,−3,1) stoichiometry reaches significant percentages at a less acidic pH range (from 4.0 to 4.5). As can be seen the species generated by the metal hydrolysis reach concentration levels no higher than 10% confirming that the sequestering ability of naringin towards Al(III) is competitive with water.

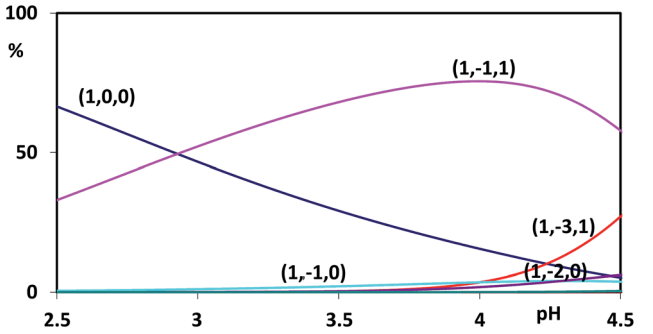

Fig. 1 Distribution diagram of aluminium cation in the presence of naringin ($C_M = 0.5 \times 10^{-3}$ mol L^{-1} and $C_L = 1.5 \times 10^{-3}$ mol L^{-1}).

To gain additional insight on the complexes formation, we have compared the UV-vis spectra of the free and bound ligand (Fig. 2). The naringin absorption spectrum displayed three bands (*i.e.*, 330, 282 and 225 nm); with an increase on metal cation concentration the absorption maxima were red shifted (385 and 307 nm) indicating that the complexation occurs. The bathochromic shift in the absorption spectra confirms that deprotonation takes place at the hydroxyl group which gives red shifted absorption and maxima.

Mass spectrometric methodologies provide a rapid and sensitive tool for the identification and characterization of the species in terms of structure and stoichiometry.[35,36] Therefore, the equilibrium behaviour and the speciation models were verified by analysing a naringin–aluminium solution, at pH 3.5 and in a stoichiometric ratio 1 : 1, with mass spectrometry in aqueous medium. The mass spectrum of the ions generated in source by ESI shows different species (Fig. 3). In particular, the molecular ions at m/z 1185 and m/z 623 correspond, respectively, to the aluminium complex bound to two and one molecules of deprotonated naringin. The further tandem mass spectrometry experiment performed on the isolated species at m/z 1185 shows a clear fragmentation pattern (Fig. S1†): the ion

Table 2 Survey of the log $\beta_{pqr} \pm (3\sigma)$, according to the general equilibrium 1, for aluminium(III)–naringin complexes obtained by numerical procedure

(p,q,r)	log $\beta_{pqr} \pm 3\sigma$
(1,−1,1)	1.01 ± 0.09
(1,−3,1)	−8.2 ± 0.2
σ	0.30
χ^2	4.28
U	3.14

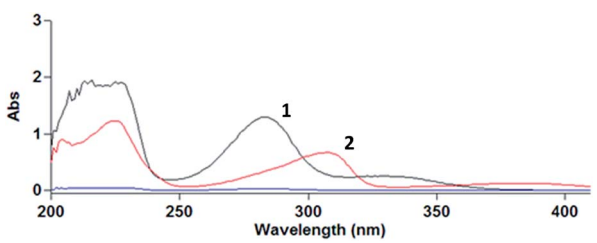

Fig. 2 UV-vis spectra of the free ligand 0.1×10^{-3} mol L^{-1} (line 1) and of the complexes formed between naringin and Al(III) 0.1×10^{-3} mol L^{-1} (line 2).

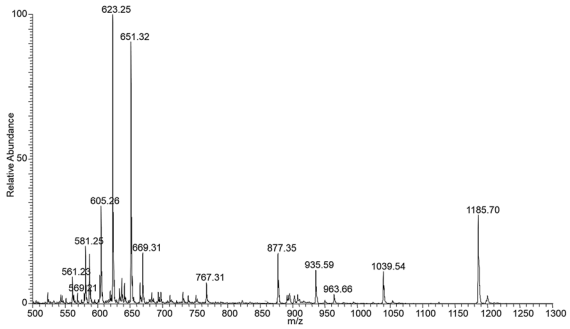

Fig. 3 ESI (+) MS spectrum of stable ion of the naringin–aluminium solution.

at *m*/*z* 1039 corresponds to the formal loss of one rhamnose unit from a naringin moiety, which subsequently fragment at the aglycon site generating the species at *m*/*z* 877 (loss of glucose unit).

Other diagnostic ions are those at *m*/*z* 731 and *m*/*z* 569, which are related to the loss of the rhamnose and glucose moieties from the second naringin molecule. The latter ion, present also as minor signal in the spectrum of stable ions (Fig. 3) and which contains two molecules of the aglycon naringenin linked to Al, indicates that the complexation site is on the aglycon moiety. By performing a MS/MS experiment on this ion (Fig. 4), it is possible to observe a particular fragmentation that leads to the formation of two complementary ions at *m*/*z* 463 and *m*/*z* 406 (Scheme 2), which suggests that the complexation site is located on the β-hydroxy ketone moiety. The MS/MS spectrum of the other stable species at *m*/*z* 621, which correspond to the complex (1,−1,1) shows significant fragment species at *m*/*z* 605 $[M - L]^+$, due to the loss of a formal unit of water, and *m*/*z* 459, which is generated by the subsequent loss of the rhamnose unit (Fig. S2†).

By combining results from potentiometric and MS measurements we can assume that, according to the stoichiometric coefficients (1,−1,1) and (1,−3,1), the structure of these species is AlL^{2+} and $Al(OH)_2L$, respectively, the other coordination sites of aluminium being occupied by water molecules.

No comparison with the literature data was possible. The only evaluation concerns the interactions between naringin and other metal ions.[37–39] In particular, as concern iron(III) ions, the formation of a single species of 1 : 1 stoichiometric ratio is studied from a kinetic point of view. Therefore, only a qualitative comparison between this data and our results is possible. The iron(III)–naringin complex contains a stable six-membered ring, according to the structure proposed for the aluminium–naringin complexes (Scheme 2).

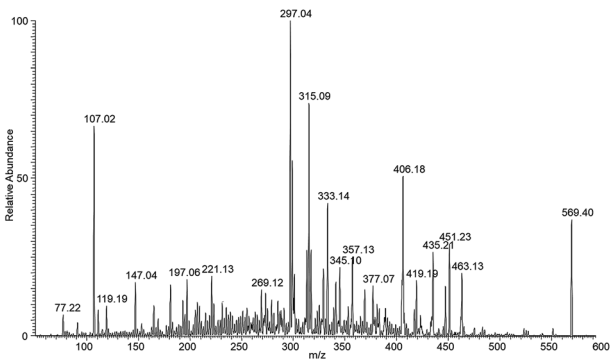

Fig. 4 ESI (+) Tandem mass spectrum on the isolated species at *m*/*z* 569.

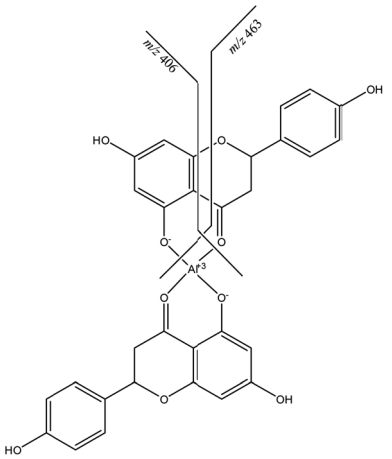

Scheme 2 Fragmentation of the ion at *m*/*z* 569.

Conclusions

In this study, the first under physiological conditions, the complexation of naringin with the Al(III) ion is reported. The speciation models and the formation constants proposed on the basis of potentiometric results were in agreement with Al(III)–naringin system MS data. The latter provided information regarding the structure of the complexes. From our results the following conclusions can be drawn:

– an accurate speciation study of this system by potentiometric measurements allowed us to clearly identify the stoichiometry of the complexes. This was the starting point necessary for understanding the relative structures;

– in the pH range investigated complexes with 1 : 1 stoichiometric ratio between aluminium and naringin, *i.e.*, AlL^{2+} and $Al(OH)_2L$, are possible;

– in agreement with previous data[6] the complex formation induces a bathochromic shift of the UV-vis absorption bands;

– as confirmed by mass spectrometry results the complexation site is located on the β-hydroxy ketone moiety.

Conflicts of interest

There are no conflicts to declare.

Acknowledgements

This research was supported by University of Calabria.

Notes and references

1 M. G. L. Hertog, E. J. M. Feskens, P. C. H. Hollman, M. B. Katan and D. Kromhout, *Lancet*, 1993, **342**, 1007–1011.
2 C. S. Yang and Z.-Y. Wang, *J. Natl. Cancer Inst.*, 1993, **85**, 1038–1049.
3 M. R. Sowers, S. Crawford, D. S. McConnell, J. F. Randolph, E. B. Gold, M. K. Wilkin and B. Lasley, *J. Nutr.*, 2006, **136**, 1588–1595.
4 G. J. Soleas, L. Grass, P. D. Josephy, D. M. Goldberg and E. P. Diamandis, *Clin. Biochem.*, 2006, **39**, 492–497.
5 G. Mantovani, A. Maccio, C. Madeddu, G. Gramignano, M. R. Lusso, R. Serpe, E. Massa, G. Astara and L. Deiana, *Cancer Epidemiol., Biomarkers Prev.*, 2006, **15**, 1030–1034.
6 R. M. S. Pereira, N. E. D. Andrades, N. Paulino, A. C. H. F. Sawaya, M. N. Eberlin and M. C. Marcucci, *Molecules*, 2007, **12**, 1352–1366.
7 F. Billes, I. Mohammed-Ziegler, H. Mikosch and E. Tyihák, *Spectrochim. Acta, Part A*, 2007, **68**, 669–679.
8 M. M. Kasprzak, A. Erxleben and J. Ochocki, *RSC Adv.*, 2015, **5**, 45853–45877.
9 X. Deng, Z. Wang, J. Liu, S. Xiong, R. Xiong, X. Cao, Y. Chen, X. Zhenga and G. Tang, *RSC Adv.*, 2017, **7**, 38171–38178.
10 A. Garg, S. Garg, L. J. D. Zaneveld and A. K. Singla, *Phytother. Res.*, 2001, **15**, 655–669.
11 D. Susanti, H. M. Sirat, F. Ahmad, R. M. Ali, N. Aimi and M. Kitajima, *Food Chem.*, 2007, **103**, 710–716.
12 S. Kanno, A. Tomizawa, T. Ohtake, K. Koiwai, M. Ujibe and M. Ishikawa, *Toxicol. Lett.*, 2006, **166**, 131–139.
13 H. Ccedilelik, M. Kosar and E. Arinc, *Toxicology*, 2013, **308**, 34–40.
14 E. Furia and R. Porto, *J. Chem. Eng. Data*, 2008, **53**, 2739–2745.
15 E. Furia, A. Napoli, A. Tagarelli and G. Sindona, *J. Chem. Eng. Data*, 2013, **58**, 1349–1353.
16 E. Furia, D. Aiello, L. Di Donna, F. Mazzotti, A. Tagarelli, H. Thangavel, A. Napoli and G. Sindona, *Dalton Trans.*, 2014, **43**, 1055–1062.
17 E. Furia, T. Marino and N. Russo, *Dalton Trans.*, 2014, **43**, 7269–7274.
18 A. Beneduci, E. Furia, N. Russo and T. Marino, *New J. Chem.*, 2017, **41**, 5182–5190.
19 E. Furia, *J. Solution Chem.*, 2017, **46**, 1596–1604.
20 E. Finotti and D. Di Majo, *Nahrung*, 2003, **47**, 186–187.
21 L. Zhang, L. Song, P. Zhang, T. Liu, L. Zhou, G. Yang, R. Lin and J. Zhang, *J. Chem. Eng. Data*, 2015, **60**, 932–940.
22 J. Zhang, P. Zhang, T. Liu, L. Zhou, L. Zhang, R. Lin, G. Yang, W. Wang and Y. Li, *J. Mol. Liq.*, 2015, **203**, 98–103.
23 C. Exley, *Environ. Sci.: Processes Impacts*, 2013, **15**, 1807–1816.
24 F. Crea, P. Crea, C. De Stefano, O. Giuffrè, A. Pettignano and S. Sammartano, *J. Chem. Eng. Data*, 2004, **49**, 658–663.
25 L. Di Donna, H. Benabdelkamel, D. Taverna, S. Indelicato, D. Aiello, A. Napoli, G. Sindona and F. Mazzotti, *Anal. Bioanal. Chem.*, 2015, **407**, 5835–5842.
26 F. Mazzotti, L. Di Donna, A. Napoli, D. Aiello, C. Siciliano, C. M. Athanassopoulos and G. Sindona, *J. Mass Spectrom.*, 2014, **49**, 802–810.
27 S. K. Singh, A. Kundu and N. Kishore, *J. Chem. Thermodyn.*, 2004, **36**, 7–16.
28 A. Soto, A. Arce and M. K. Khoshkbarchi, *J. Solution Chem.*, 2004, **33**, 11–21.
29 S. R. Poulson, R. R. Harrington and J. I. Drever, *Talanta*, 1998, **48**, 633–641.
30 A. J. Queimada, F. L. Mota, S. P. Pinho and E. A. Macedo, *J. Phys. Chem. B*, 2009, **113**, 3469–3476.
31 A. Osol and M. Kilkpatrick, *J. Am. Chem. Soc.*, 1933, **55**, 4430–4440.
32 E. Furia, M. Falvo and R. Porto, *J. Chem. Eng. Data*, 2009, **54**, 3037–3042.
33 P. Gans, A. Sabatini and A. Vacca, *J. Chem. Soc., Dalton Trans.*, 1985, **6**, 1195–1200.
34 C. F. Baes and R. E. Mesmer, *The Hydrolysis of Cations*, Wiley Interscience, New York, 1976.
35 D. Aiello, S. Materazzi, R. Risoluti, H. Thangavel, L. Di Donna, F. Mazzotti, F. Casadonte, C. Siciliano, G. Sindona and A. Napoli, *Mol. BioSyst.*, 2015, **11**, 2373–2381.
36 A. Napoli, D. Aiello, G. Aiello, M. S. Cappello, L. Di Donna, F. Mazzotti, S. Materazzi, M. Fiorillo and G. Sindona, *J. Proteome Res.*, 2014, **13**, 2856–2866.
37 S. Nafisi, M. Hashemi, M. Rajabi and H. A. Tajmir-Riahi, *DNA Cell Biol.*, 2008, **27**(8), 433–442.
38 H. Rimac, Ž. Debeljak, D. Šakić, T. Weitner, M. Gabričevič, V. Vrček, B. Zorc and M. Bojić, *RSC Adv.*, 2016, **6**, 75014–75022.
39 M. J. Hynes and M. O'Coinceanainn, *J. Inorg. Biochem.*, 2004, **98**, 1457–1464.

Anal Bioanal Chem (2016) 408:3783–3787
DOI 10.1007/s00216-016-9468-1

RESEARCH PAPER

Fast analysis of caffeine in beverages and drugs by paper spray tandem mass spectrometry

Domenico Taverna[1] · **Leonardo Di Donna**[1] · **Lucia Bartella**[1] · **Anna Napoli**[1] · **Giovanni Sindona**[1] · **Fabio Mazzotti**[1]

Received: 26 October 2015 / Revised: 9 February 2016 / Accepted: 4 March 2016 / Published online: 22 March 2016

Abstract A simple and fast method based on paper spray mass spectrometry for the determination of caffeine in commercial beverages and drugs has been developed; the analyses were carried out in MRM mode, monitoring the transitions *m/z* 195 → *m/z* 138 for caffeine and *m/z* 198 → *m/z* 140 for the labeled internal standard. To verify the reliability of the proposed approach, a spiked sample (soda drink and paracetamol tablet) with a known amount of caffeine has been prepared and analyzed by PS-MS, providing accuracy values about 100 %; the LOQ and LOD values were calculated at 1.2 and 1.6 μg/mL, respectively. Both beverages and drugs were also analyzed with the classic analytical method based on LC-UV measurements, showing consistent results between the two approaches, thus confirming the reliability of the developed ambient MS determination.

Keywords Caffeine · Paper spray · Mass spectrometry · Multiple reaction monitoring · Quantitative assay

Introduction

Caffeine is an alkaloid found in plant species predominantly growing in the tropic or subtropic regions of the world. Plants use caffeine as a natural pesticide since it is toxic to insects. Caffeine is naturally found in more than 60 plants, including tea leaves, coffee beans, kola nuts. Most of them are used to flavor soft drinks such as colas and cacao pods, and to prepare chocolate products [1]. Furthermore, caffeine is an ingredient of some energy drinks; it is often added in combination with synephrine in foods or food derivate usually used to induce weight loss or to increase sport performances. Moreover, some drugs as well as cosmetics contain caffeine [2]. Caffeine, like other natural compounds [3], shows pharmacologic effects in humans, such as central nervous system stimulation, diuresis, and stimulation of cardiac muscle. This alkaloid is able to cause insomnia and increases blood pressure [4–8]. Caffeine is metabolized within the liver: about 200 mg/dose of caffeine would take not less than 40 h to be completely excreted. However, the greatest perceived effects of caffeine consumption are experienced during the first 4–6 h. Recently, the European Food Safety Authority (EFSA) recommended the daily dose for an adult: for a safe intake, the suggested caffeine amount is 400 mg per day, corresponding to about four cups of coffee. Further, the maximum recommended dose for pregnant women is 200 mg [9]. Currently, several analytical methods describing the quantitative determination of caffeine within complex matrices are reported in literature. Different techniques and sample preparation protocols are used (e.g., HPLC, gas chromatography, electrochemical analysis, and mass spectrometry (MS) [10–18]. The latter is an analytical technique that employs ionization of compounds and their mass analysis in order to determine their formula, structure, and amount [19–25]. In particular, ESI-MS is one of the most versatile ion sources used in a wide range of analytical applications [26, 27]. Recently, a new family of MS ionization sources have been developed, allowing ions to be generated under ambient conditions and then collected and analyzed by MS [28–30]. Ambient mass spectrometry is a technique able to record mass spectra on ordinary samples, in their

✉ Fabio Mazzotti
fmazzotti@unical.it

[1] Dipartimento di Chimica e Tecnologie Chimiche, Università della Calabria, Via P. Bucci Cubo 12/C, 87036 Arcavacata di Rende, Cosenza, Italy

native environment, with minimum sample pretreatment by creating ions outside the instrument [31]. Many of these modern MS techniques are developed to work directly on the samples (e.g., biological tissue, fruits, leaves, or biological fluids) or on samples deposited on solid supports rather than on extracts obtained after several purification steps [32–34]. Paper spray mass spectrometry (PSMS) is a simple technique for introducing unprocessed samples of fluids to the mass spectrometer. Analyte ions are generated at room temperature and atmospheric pressure out of the spectrometer by applying a high voltage and a few microliters of spray solvent onto a porous substrate, such as a piece of paper; Fig. 1 schematically shows the operation of PS-MS.

Samples, depending on the experiments (qualitative, quantitative, derivatization chemistry), can be preloaded onto the paper or mixed into the spray solution. Paper spray ionization has been applied for the analysis of crude biological samples [35]. Application of PS MS was demonstrated with urine, blood, tissue samples, leaves (also called as leaf spray MS), and others [36, 37]. The geometry of the paper (usually a triangle) and the method of supplying the necessary internal standard for data normalization or perform an assay are important factors that affect the ionization efficiency as well as the sensitivity and accuracy of the spectrometric data. Moreover, changing the angle of the paper tip, the spray plume, the total spray current, and the electric field intensity at the tip all change accordingly, resulting in significant signal intensity differences. Furthermore, the sample loading procedure is important for obtaining stable ion current and, consequently, accurate analyses. Paper spray approach can be implemented for a high throughput analysis using an individual device [38, 39].

Furthermore, ambient mass spectrometry analysis is usually faster than the classic techniques: seconds to few minutes are usually needed to record MS and/or MS/MS spectra by the use of few microliters of a proper solvent or solvent mixture [40–43]. The use of labeled internal standards improves both precision and accuracy of the measurements by reducing drawbacks arising from the calibration procedure, sample preparation, and matrix effects; this approach is successfully adapted to the paper spray, where further problems may be due also to the paper triangle used as support for the sample handling [44]. The present study reports a paper spray mass spectrometry method for the rapid determination of caffeine in beverages and drugs based on multiple reaction monitoring (MRM) and isotope dilution method using as internal standard caffeine-(trimethyl-$^{13}C_3$) (Fig. 2).

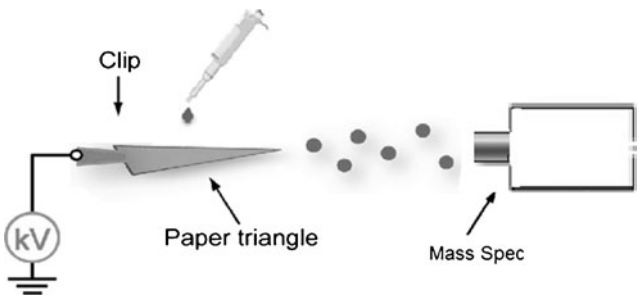

Fig. 1 Paper spray ionization mass spectrometry

Experimental

Sample preparation

Samples were purchased in a local store (beverages) and in a pharmacy (drugs). For PS-MS analysis, beverages (N = 8) were first centrifuged (3 min, 12,000 rpm); 30 μL of the internal standard solution at a concentration of 1000 μg/mL were added at 470 μL of each beverage sample, vortexed for 30 s, diluted 10 times with water, and then directly spotted onto the paper triangle for PS-MS analysis. Drugs (N = 2) were first ground and then extracted using 1 mL of methanol (7 mg and 3 mg, respectively); the internal standard solution was added (60 μL of a solution of 100 μg/mL). The same samples, properly diluted and without the internal standard, were submitted to LC-UV analysis.

Mass spectrometry

The MS analyses were carried out in positive ion mode with a LC 320 triple-stage quadrupole mass spectrometer (Varian Inc., Palo Alto, CA, USA), in-house implemented for PS-MS application. A volume of 15 μL of sample was spotted onto a triangular shaped paper matrix and, once dried (1 min), the same volume of methanol was added to allow the spray desorption every 30 s for a total run time of 2 min. The following working conditions were applied: needle voltage 5250 V; shield 800 V; capillary 60 V; housing temperature 35 °C, and the detector fixed at 1400 V. Collision gas was argon used at a pressure within the collision cell (Q2) of 2 mTorr, while the mass resolution at the first (Q1) and third (Q3) quadrupoles was set at 0.7 u at full width at half-maximum (FWHM). Scan time was set at 0.1 s. Collision energy (CE) was optimized and then set at 14 eV. MRM mode was used to quantify the analytes; in particular, the transition *m/z* 195 → *m/z* 138 for caffeine and *m/z* 198 → *m/z* 140 for the labeled internal standard were monitored. The ion current of each monitored transition, averaged over the total acquisition time, was used for the quantitative analyses.

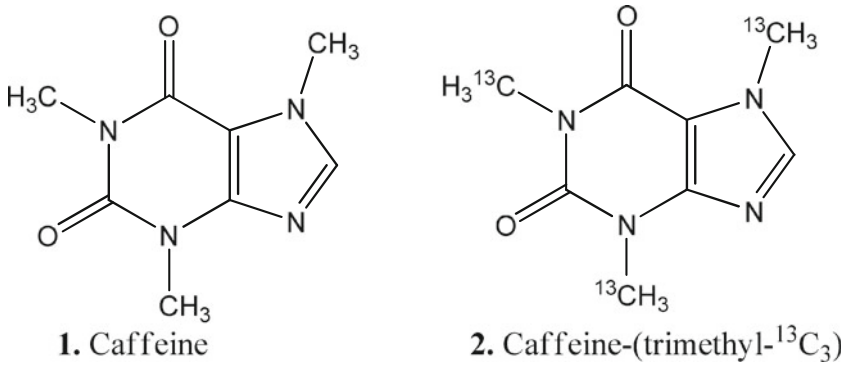

Fig. 2 Structure formulae of caffeine and caffeine-(trimethyl-$^{13}C_3$)

LC-UV analysis

LC analysis were carried out using an HPLC 1100 (Agilent Technologies, Waldbronn, Germany) equipped with a quaternary pump and a UV detector. Separation was achieved by using a reversed phase C_{18} column (Luna, Phenomenex, Torrance, CA, USA), using a flow rate of 1 mL/min and the detector set at 280 nm using a gradient water/methanol [45]. The reported analytical parameters of LOD and LOQ for caffeine are 4.2 and 14 μg/mL, respectively [14].

Analytical parameters

The limit of detection (LOD) and the limit of quantitation (LOQ) were calculated following the directives of IUPAC and the American Chemical Society's Committee on Environmental Analytical Chemistry, i.e., as follows:

$$S_{LOD} = S_{RB} + 3\sigma_{RB}$$
$$S_{LOQ} = S_{RB} + 10\sigma_{RB}$$

where S_{LOD} is the signal at the limit of detection, S_{LOQ} is the signal at the limit of quantitation, S_{RB} is the ratio of the signals given by the transitions of the analyte and of the internal standard from the blank sample, and σRB is its standard deviation. The concentrations were calculated by the standard curve.

Results and discussion

Paper spray is a simple and fast ambient MS technique for introducing unprocessed liquid samples within a mass spectrometer. Paper spray ionization incorporates adsorption chromatography and/or solid phase extraction steps directly into the ionization process, allowing direct analysis of analytes from different matrices. The MS/MS spectrum of caffeine is characterized by few diagnostic fragments; in particular, the ion at *m/z* 138, representing the base peak of the spectrum. The same fragment, showing a *m/z* value increased of 2 u was recorded within the MS/MS spectrum of the labeled standard, caffeine-(trimethyl-$^{13}C_3$); this ion more probably is generated by internal breakage of the six-membered of the molecule (Fig. 3).

The use of stable isotopes as internal standards for the MS analytes assay within complex mixtures represents an extremely accurate method of quantitative chemical analysis [46]. The quantitative method presented here is based on the coupling of the isotope dilution method and the paper spray mass spectrometry. Tandem mass spectrometry was chosen to ensure the greatest specificity, using MRM scanning mode with the paper spray to speed up both the sample pretreatment and the analysis total time. When the solvent is spotted onto the center of the paper triangle embedded with the beverage or the drug extract and high voltage is applied, a sort of spray of charged droplets is generated from the tip of the paper triangle. So, considering that the sample once deposited onto the triangle is allowed to dry for 1 min, and the acquisition time for the MRM experiment is 2 min, (spotting 15 μL of methanol each 30 s), the total time of the whole process is very short. The calibration curve, built by sampling in triplicate each of the five solutions at different concentrations, showed a good linearity ($y = 1.4449x - 0.1921$; $R^2 = 0.9952$). The concentrations of the analyte in the standard solutions ranged from 2 to 16 μg/mL (2, 4, 6, 8, 16, μg/mL), whereas that of the internal standard was fixed at 6 μg/mL. The beverage samples were analyzed without any treatment, whereas drug samples were quickly extracted with methanol; for all the samples, the internal standard solution was added before the dilution step (see Experimental). The PS-MS/MS method, described here, was applied to real samples (beverages and drugs) and spiked samples (soda drink and paracetamol tablet). The latter were used for the analytical parameters calculation. The accuracy of the method was determined from samples prepared by adding known quantities of the caffeine to blank samples. In the two spiked samples (Table 1), prepared at concentrations representing the limits of the calibration curve, the accuracy was higher than 97 %.

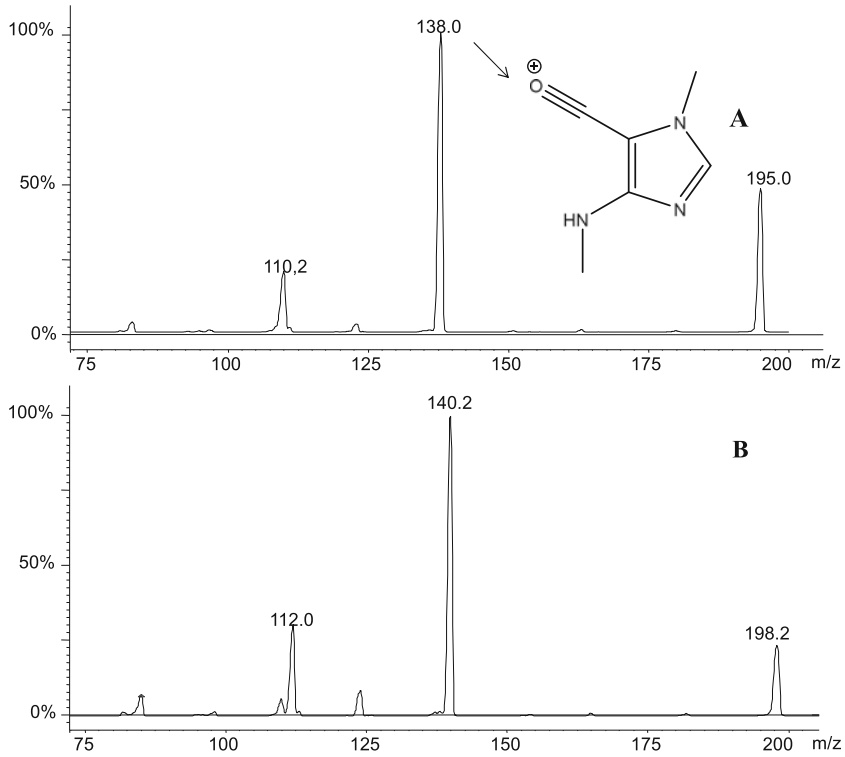

Fig. 3 MS/MS spectra of caffeine (**A**) and caffeine-(*trimethyl*-$^{13}C_3$) (**B**)

For all the analyzed samples, the RSD % values were calculated lower than 13 %, confirming the good repeatability of the PS-MS/MS measurements. Furthermore, the calculated analytical parameters of LOD, LOQ, as well as accuracy and reproducibility, confirmed the integrity of the proposed approach. The detection and the quantification limits ranged from 1.2 to 1.6 μg/ml, confirming the good sensitivity of the proposed. The recovery of the whole process related to the beverages was quantitative because no extraction step was involved within the beverages sample preparation. Since caffeine enriched drugs are on the market in a solid form (tablet or granulated powder), they were quickly solvent extracted. In any case, the recovery was quantitative. Caffeine amounts obtained from N = 8 commercially available beverages and N = 2 drugs are summarized in Table 2. Moreover, to further demonstrate the consistency of our presented PS-MS/MS methodology with the common methods reported within the literature, LC-UV analyses were carried out injecting the same samples, properly diluted [42]. Results were similar to the PS-MS/MS measured caffeine amounts. All the measured values are reported in Table 2.

Table 1 Analytical parameters of accuracy, LOQ, LOD, and reproducibility[a] (RSD %) of the proposed method

Spiked samples	Calculated amount μg/mL	RSD %	Accuracy %
Beverages			
S1 5 μg/mL	5.02 ± 0.69	13.7	100,4
S2 15 μg/mL	14.6 ± 0.43	2.94	97.0
Drugs			
S1 5 μg/mL	4.91 ± 0.61	12.4	101.3
S2 15 μg/mL	15.2 ± 0.51	3.36	97.0
	LOD μg/mL	LOQ μg/mL	Reproducibility RSD%[a]
Beverages	1.2	1.6	Cola 13.9
Drugs	1.2	1.5	Drug 1 12.3

[a] The reproducibility of the measurements was obtained by analyzing each sample three times over a period of 1 week

Table 2 Amount of caffeine found in real samples

Samples	Caffeine found (PS-MS) μg/mL	RSD %	HPLC analysis μg/mL
Cola	115.9 ± 8.2	4.14	123
Coffee espresso 1	6887.8 ± 203.9	3.38	6935
Coffee espresso 2	4921 ± 154.1	3.13	4650
Coffee espresso 3	4074 ± 201.5	4.94	4190
Coffee espresso 4	7864 ± 305.6	3.9	8177
Coffee espresso 5	6742 ± 287.2	4.2	6600
Energy drink	381.5 ± 12.0	3.15	378
Tea	119.7 ± 15.3	12.7	121
Drug 1	126.8 ± 8.9	7.03	122
Drug 2	164.3 ± 9.5	9.48	165

Conclusions

A reliable, fast, and "green" method for the assay of caffeine present in commercial beverages and drugs has been developed. The presented strategy appears as an alternative and faster method to the classic approaches for quantitative analysis commonly used and reported in literature, such as LC-UV methods. The analytical parameters and the direct comparison with the LC-UV measurements support the reliability of the PS-MS technique. The use of labeled internal standard is needed for quantitative analysis by PS-MS. Since ambient MS is quite adaptable to rapid and reproducible molecular screenings and semiquantitative and quantitative analyses, the method could be extended to the assay of caffeine metabolites within biological fluids, directly or after a simple step of sample preparation.

Acknowledgments Funds from Italian Regional Project, PSR Calabria 2007/2013 – Misura 1.2.4.– (SIAR n. 0279282) are gratefully acknowledged.

Compliance with ethical standards

Conflict of interest The authors declare that they have no conflict of interest.

References

1. Ashihara H, Crozier A. Trends Plant Sci. 2001;6:407–13.
2. James JE. In: Watson R, editor. Caffeine mental performance and mood. Cambridge: Woodhead Publishing Ltd. and CRC Press; 2003.
3. Mazziotti A, Mazzotti F, Pantusa M, Sportelli L, Sindona G. J Agric Food Chem. 2006;54:7444–9.
4. Buscemi S, Verga S, Batsis JA, Donatelli M, Tranchina MR, Belmonte S, et al. Eur J Clin Nutr. 2010;64:483–9.
5. Zhang Z, Hu G, Caballero B, Appel L. Am J Clin Nutr. 2011;93:1212–9.
6. Ding M, Bhupathiraju SN, Satija A, Van Dam RM, Hu FB. Circulation. 2014;129:643–59.
7. Solinas M, Ferré S, You ZB, Karcz-Kubicha M, Popoli P, Goldberg SR. J Neurosci. 2002;22:6321–24.
8. James JE. Psychosom Med. 2004;66:63–71.
9. Scientific opinion on the safety of caffeine. EFSA J. 2015;13:4102.
10. Svorc L. Int J Electrochem Sci. 2013;8:5755–73.
11. Shrivas K, Wu HF. J Chromatogr A. 2007;1170:9–14.
12. Horie H, Nesumi A, Ujihara T, Kohata K. J Chromatogr A. 2002;942:271–3.
13. Naik JP. J Agric Food Chem. 2001;49:3579–83.
14. Rostagno MA, Manchon N, D'Arrigo M, Guillamon E, Villares A, Garcıa-Lafuente A, et al. Anal Chim Acta. 2011;685:204–11.
15. Lee MS, Huong NL, Hoang NH, Shrestha A, Park JW. Anal Lett. 2014;47:1852–6.
16. Aranda M, Morlock G. Rapid Commun Mass Spectrom. 2007;21:1297–303.
17. Danhelova H, Hradecky J, Prinosilova S, Cajka T, Riddellova K, Vaclavik L, et al. Anal Bioanal Chem. 2012;403:2883–9.
18. Garrett R, Rezendeb CM, Ifa DR. Anal Methods. 2013;5:5944–8.
19. Benabdelkamel H, Di Donna L, Mazzotti F, Naccarato A, Sindona G, Tagarelli A, et al. J Agric Food Chem. 2012;60:3717–26.
20. Bongiorno D, Ceraulo L, Indelicato S, Turco Liveri V, Indelicato S. Charged supramolecular assemblies of surfactant molecules in gas phase. Mass Spectrom Rev. 2016;35:170–87.
21. Napoli A, Aiello D, Di Donna L, Sajjad A, Perri E, Sindona G. Anal Chem. 2006;78:3434–43.
22. Napoli A, Athanassopoulos CM, Moschidis P, Aiello D, Di Donna L, Mazzotti F, et al. Anal Chem. 2010;82:5552–60.
23. Bongiorno D, Indelicato S, Giorgi G, Scarpella S, Turco Liveri V, Ceraulo L. Eur J Mass Spectrom. 2014;20:169–75.
24. Furia E, Aiello D, Di Donna L, Mazzotti F, Tagarelli A, Thangavel H, et al. Dalton Trans. 2014;43:1055–62.
25. Napoli A, Aiello D, Aiello G, Cappello MS, Di Donna L, Mazzotti F, et al. J Proteome Res. 2014;13:2856–62.
26. Di Donna L, Mazzotti F, Salerno R, Tagarelli A, Taverna D, Sindona G. Rapid Commun Mass Spectrom. 2007;22:3653–7.
27. Di Donna L, Mazzotti F, Taverna D, Napoli A, Sindona G. Phytochem Anal. 2014;25:207–12.
28. Takáts Z, Wiseman JM, Gologan B, Cooks RG. Science. 2004;306:471–3.
29. Cody RB, Laramee JA, Durst HD. Anal Chem. 2005;77:2297–302.
30. Monge ME, Harris GA, Dwivedi P, Fernández FM. Chem Rev. 2013;113:2269–308.
31. Cooks RG, Ouyang Z, Takats Z, Wiseman JM. Science. 2006;311:1566–70.
32. Taverna D, Boraldi F, De Santis G, Caprioli RM, Quaglino D. Bone. 2015;74:83–94.
33. Taverna D, Pollins AC, Sindona G, Caprioli RM, Nanney LB. J Proteome Res. 2015;14:986–99.
34. Taverna D, Norris JL, Caprioli RM. Anal Chem. 2015;87:670–6.
35. Wang H, Liu J, Cooks RG, Ouyang Z. Angew Chem Int Ed Engl. 2010;49:877–80.
36. Yang Q, Manicke NE, Wang H, Petucci C, Cooks RG, Ouyang Z. Anal Bioanal Chem. 2012;404:1389–97.
37. Liu J, Wang H, Cooks RG, Ouyang Z. Anal Chem. 2011;83:7608–13.
38. Yang Q, Wang H, Maas JD, Chappell WJ, Manicke NE, Cooks RG, et al. Int J Mass Spectrom. 2012;312:201–7.
39. Shen L, Zhang J, Yang Q, Manicke NE, Ouyang Z. Clin Chim Acta. 2013;420:28–33.
40. Liu J, Wang H, Manicke NE, Lin J, Cooks RG, Ouyang Z. Anal Chem. 2010;82:2463–71.
41. Taverna D, Di Donna L, Mazzotti F, Policicchio B, Sindona G. J Mass Spectrom. 2013;48:544–7.
42. Espy RD, Manicke NE, Ouyang Z, Cooks RG. Analyst. 2012;137:2344–9.
43. Mazzotti F, Di Donna L, Taverna D, Nardi M, Aiello D, Napoli A, et al. Int J Mass Spectrom. 2013;352:87–91.
44. Di Donna L, Benabdelkamel H, Taverna D, Indelicato S, Aiello D, Napoli A, et al. Anal Bioanal Chem. 2015;407:5835–42.
45. Zuoa Y, Chena H, Dengb Y. Talanta. 2002;57:307–16.
46. Mazzotti F, Di Donna L, Benabdelkamel H, Gabriele B, Napoli A, Sindona G. J Mass Spectrom. 2010;45:358–63.